VOL.107 NO.TE6. NOV. 1981

TRANSPORTATION ENGINEERING JOURNAL OF ASCE

PROCEEDINGS OF
THE AMERICAN SOCIETY
OF CIVIL ENGINEERS

AEROSPACE
AIR TRANSPORT
HIGHWAY
PIPELINE
URBAN TRANSPORTATION

VOL.107 NO.TE6. NOV. 1981

TRANSPORTATION ENGINEERING JOURNAL OF ASCE

PROCEEDINGS OF
THE AMERICAN SOCIETY
OF CIVIL ENGINEERS

ISSN 0569-7891

AMERICAN SOCIETY OF CIVIL ENGINEERS

PARTICIPATING GROUPS

CONTENTS

The Transportation Engineering Journal of ASCE (ISSN 0569-7891) is published bimonthly by the American Society of Civil Engineers. Publications office is at 345 East 47th Street, New York, N.Y. 10017. Address all ASCE correspondence to the Editorial and General Offices at 345 East 47th Street, New York, N.Y. 10017. Allow six weeks for change of address to become effective. Subscription price to members is $12.50. Nonmember subscriptions available; prices obtainable on request. Second-class postage paid at New York, N.Y. and at additional mailing offices. TE.

POSTMASTER: Send address changes to American Society of Civil Engineers, 345 East 47th Street, New York, NY 10017.

DISCUSSION

Proc. Paper 16618

INFORMATION RETRIEVAL

The key words, abstract, and reference "cards" for each article in this Journal represent part of the ASCE participation in the EJC information retrieval plan. The retrieval data are placed herein so that each can be cut out, placed on a 3 × 5 card and given an accession number for the user's file. The accession number is then entered on key word cards so that the user can subsequently match key words to choose the articles he wishes. Details of this program were given in an August, 1962 article in CIVIL ENGINEERING, reprints of which are available on request to ASCE headquarters.

STATEMENT OF OWNERSHIP

The *Transportation Engineering Journal of ASCE* is edited and published by the American Society of Civil Engineers, with general business offices at 345 East 47th Street, New York, N.Y. 10017. The Manager of Technical and Professional Publications is Richard R. Torrens.

This Journal is owned wholly by the American Society of Civil Engineers, a nonprofit educational and professional organization with about 78,000 members. There are no individual owners or stockholders.

	Average No. Copies Each Issue During Preceding 12 Months	Single Issue Nearest To Filing Date
Total no. copies printed (net press run)	7,211	6,882
Paid mail circulation	5,233	5,486
Sales through dealers and counter sales	None	None
Free distribution	None	None
Total distribution	5,233	5,486
Left Over (extra for new orders, office use, etc.)	1,978	1,396
Total	7,211	6,882

I certify that the above statements made by me are correct and complete.—Richard R. Torrens, Manager of Technical and Professional Publications.

16624 PLANNING FOR DETROIT DOWNTOWN PEOPLE MOVER

KEY WORDS: Automation; **Central business districts;** Design criteria; **Detroit;** Guideway systems; **Mass transportation;** Performance characteristics; **Planning;** Systems engineering

ABSTRACT: Planning and preliminary engineering has been completed for automated mass transit system to be deployed in downtown Detroit, Michigan. Performance specifications and design criteria were developed for all system elements including vehicles, controls, guideway, stations, maintenance facility, and electric power. System requirements were defined including patronage, operating and failure management strategies, accommodations for the elderly and handicapped, and safety and security provisions. An Environmental impact analysis and other supporting studies were performed and documented. The costs of deploying operating, and maintaining the system were estimated. It is concluded that deployment of the system will contribute significantly to the redevelopment of downtown Detroit.

REFERENCE: McDonald, David J. (Downtown People Mover Project Mgr., Southeastern Michigan Transportation Authority, Detroit, Mich.), "Planning for Detroit Downtown People Mover," *Transportation Engineering Journal,* ASCE, Vol. 107, No. TE6, **Proc. Paper 16624,** November, 1981, pp. 597-606

16661 PRESSURE SCALE EFFECTS ON SHAPE DRAG IN CONDUIT

KEY WORDS: **Closed conduit flow; Cylinders; Drag;** Scale effect; Struts; **Testing**

ABSTRACT: While testing cylinders in closed conduit flow, it was found that the drag coefficient varied with pressure at a constant Reynolds number. The conditions at which this phenomenon occurs are presented along with a possible explanation of why it occurs. It is the purpose of the paper to present the problem and to generate ideas and discussion by the readers to help explain the phenomenon.

REFERENCE: Rahmeyer, William J. (Asst. Research Prof., Dept. of Civ. Engrg., Colorado State Univ., Fort Collins, Colo.), "Pressure Scale Effects on Shape Drag in Conduit," *Transportation Engineering Journal,* ASCE, Vol. 107, No. TE6, **Proc. Paper 16661,** November, 1981, pp. 607-612

16630 COFFERDAM AND COLUMBIA RIVER BRIDGE

KEY WORDS: **Bridge foundations; Bridges; Bridges (concrete); Cofferdams;** Columbia River; **Construction equipment; Construction procedure; Formwork (construction);** Interstate highway system; Pile driving; Underwater construction

ABSTRACT: The foundations for I-205 North Channel crossing of the Columbia River are two types, large spread footings with seals bearing directly on dense conglomerate and double bell shaped footings supported on bearing pile driven into the conglomerate. The methods used to construct these two types of foundations consist of two unique and separate cofferdam systems. The first system utilizes 100 feet long interlocking H-pile sections to form a cofferdam 145 feet by 59 feet by 100 feet deep. The use of these interlocking sections allows a designed dewatered depth of 62 feet with only two support points for the entire wall. The second system utilizes two bell shaped steel forms, stiffened to withstand a hydrostatic head of 54 feet. The larger of these two forms is 83 feet by 66 feet in plan by 62 feet high and weighs 450 tons. These forms, except for the top 14 feet, are one solid welded unit which was set and stripped in one piece.

REFERENCE: Bittner, Robert B. (Chief Engr., Construction Division, Riedel International, Inc., Portland, Oreg.), "Cofferdam Construction: I-205 Columbia River Bridge," *Transportation Engineering Journal,* ASCE, Vol. 107, No. TE6, **Proc. Paper 16630,** November, 1981, pp. 613-623

16666 COLUMBIA RIVER BRIDGE: DESIGN AND CONSTRUCTION

KEY WORDS: **Box girders; Bridge construction; Bridge design;** Bridges (concrete); Bridges (piers); Columbia River; **Concrete (post-tensioned);** Concrete (precast); **Concrete (prestressed)**

ABSTRACT: The I-205 Columbia River Bridge is the final link in a forty-mile circumferential highway east of Portland, Oregon and Vancouver, Washington. It is one of the largest single projects using prestressed post-tensioned concrete box girders in the United States today. Concepts for the structure were defined in a type study which compared construction cost, maintenance cost, constructability, and aesthetics of various alternatives. Continuously post-tensioned box girders constructed on falsework and precast segmental box girders (free cantilever erection) are used in the 7,500-ft-long (2286 m) dual structures. Each of the structures is 68 ft (20.7 m) wide. River piers of cofferdam, caisson, segmental precast-concrete shell construction techniques were developed for various applicable locations. Construction, presently underway, is expected to be completed in 1982.

REFERENCE: Blanchard, Fred P. (Project Mgr., Sverdrop & Parcel and Assoc., Inc., St. Louis, Mo. 63101), "I-205 Columbia River Bridge: Design and Construction," *Transportation Engineering Journal,* ASCE, Vol. 107, No. TE6, **Proc. Paper 16666,** November, 1981, pp. 625-633

16649 EQUIVALENT GRANULAR BASE MODULI: PREDICTION

KEY WORDS: **Aggregates;** Computer analysis; Elastic theory; **Flexible pavements; Forecasting; Granular materials;** Layers; Nomographs; **Pavement design;** Regression analysis

ABSTRACT: A simple, but accurate, technique to determine the equivalent one layer modulus for unbound aggregate material in a flexible highway pavement that accounts for the nonlinear behavior of the granular material has been developed. The solution is based upon predictive regression equations developed from an analysis of multi-layer elastic theory computer solutions. The equivalent granular moduli is a function of all pavement layer parameters influencing the bulk stress in the granular layer (surface and base thicknesses; surface and subgrade modulus and base course quality related to the K_1 value in the nonlinear modulus expression: $M_R = K_1 0^{0.5}$. Nomographic solutions are also presented. Comparison of this method shows relatively good agreement to methods developed by the U.S. Army Corps of Engineers, Kentucky Highway, and Shell Oil. Since the procedure accounts for significant factors affecting the nonlinear response of unbound granular materials, the technique is recommended for use in highway pavement design and analysis using theorectical layered approaches.

REFERENCE: Smith, Brian E. (Asst. Project Engr., Soil Testing Services, Fairfax, Va.), and Witczak, Matthew W., "Equivalent Granular Base Moduli: Prediction," *Transportation Engineering Journal,* ASCE, Vol. 107, No. TE6, **Proc. Paper 16649,** November, 1981, pp. 635-652

16648 DESIGN OF LIME-STABILIZED ROADS

KEY WORDS: Design; **Laterites; Lime soil stabilization; Pavement design;** Pavements; **Roads;** Stabilization; Subtropic; Triaxial tests; Tropic

ABSTRACT: In the tropical and subtropical regions of the world, where, due to lack of well processed aggregates, the main highway material is laterite soils, there has been virtually no shift from the empirical and semiempirical approach towards rational pavement design method. This may be due to the fact that there is no accumulation of knowledge on the resilient properties of laterite soils. A research program has been in progress at the Department of Civil Engineering, Leeds University to investigate the resilient properties of raw and stabilized laterite. The results obtained from one of the studies has been used in a rational design of lime-stabilized laterite for low cost roads. Using limiting stresses and strains associated with cracking, pavement thicknesses have been recommended. The recommended thicknesses compare favorably with existing design recommendations.

REFERENCE: Singh, Gurdev (Lect. in Civ. Engrg., Dept. of Civ. Engrg., Univ. of Leeds, Leeds LS2 9JT, United Kingdom), and Akoto, Baffour K.A., "Rational Design of Lime-Stabilized Laterite Roads," *Transportation Engineering Journal,* ASCE, Vol. 107, No. TE6, **Proc. Paper 16648,** November, 1981, pp. 653-665

16658 THE FLY-OVER: A VIEW FROM BOTH SIDES

KEY WORDS: Bridges; **Economic analysis;** Grade separation; **Intersections;** Traffic; **Traffic congestion;** Traffic safety

ABSTRACT: An examination of European and U.S. information available of fly-overs shows that they are not low-cost permanent solutions for congestion and safety problems at urban and rural intersections. Their main advantage is that they can be installed in less than 10 days and can be reused several times at different locations. Their main disadvantage is that they are often not esthetically pleasing, particularly in an urban environment where there is limited right-of-way. Some fly-overs being marketed today are constructed of weathering steel to reduce maintenance costs and can be used in a variety of geometric configurations to accommodate approach ramps, curves multi-level bridges, and different width lanes. Intersection accidents can be reduced by fly-overs if proper attention is given the structure's end treatment and good advance signing and roadway markings are used.

REFERENCE: Byington, Stanley R. (Chf., Traffic Systems Div., Office of Research, Federal Highway Administration, Washington, D.C.), "The Fly-Over: A View From Both Sides," *Transportation Engineering Journal,* ASCE, Vol. 107, No. TE6, **Proc. Paper 16658**, November, 1981, pp. 667-680

16677 SUBAREA FOCUSING WITH UTPS MODEL

KEY WORDS: Data reduction; Distribution patterns; **Forecasting;** Sensitivity analysis; Traffic; **Traffic distribution models;** Transportation models; **Transportation planning; Urban transportation**

ABSTRACT: The effect of a data reduction technique called subarea focusing on the accuracy of forecasts produced by the Urban Transportation Planning System (UTPS) distribution-split model is explored. The UTPS package is a product of the Urban Mass Transportation Administration and its distribution-split model is a default option of the UMODEL module of this system. The results of the sensitivity analysis of the UTPS distribution-split model to subarea focusing indicate that levels of zonal aggregationg of 75 percent or less are suitable for conventional subarea modeling. Even higher levels may be acceptable for sketch planning purposes.

REFERENCE: Nihan, Nancy L. (Assoc. Prof., Dept. of Civ. Engrg., Univ. of Washington, Seattle, Wash. 98195), "Subarea Focusing with UTPS Distribution-Split Model," *Transportation Engineering Journal,* ASCE, Vol. 107, No. TE6, **Proc. Paper 16677**, November, 1981, pp. 681-694

U.S. Customary-SI Conversion Factors

In accordance with the October, 1970 action of the ASCE Board of Direction, which stated that all publications of the Society should list all measurements in both U.S. Customary and SI (International System) units, the following list contains conversion factors to enable readers to compute the SI unit values of measurements. A complete guide to the SI system and its use has been published by the American Society for Testing and Materials. Copies of this publication (ASTM E-380) can be purchased from ASCE at a price of $3.00 each; orders must be prepaid.

All authors of *Journal* papers are being asked to prepare their papers in this dual-unit format. To provide preliminary assistance to authors, the following list of conversion factors and guides are recommended by the ASCE Committee on Metrication.

To convert	To	Multiply by
inches (in.)	millimeters (mm)	25.4
feet (ft)	meters (m)	0.305
yards (yd)	meters (m)	0.914
miles (miles)	kilometers (km)	1.61
square inches (sq in.)	square millimeters (mm^2)	645
square feet (sq ft)	square meters (m^2)	0.093
square yards (sq yd)	square meters (m^2)	0.836
square miles (sq miles)	square kilometers (km^2)	2.59
acres (acre)	hectares (ha)	0.405
cubic inches (cu in.)	cubic millimeters (mm^3)	16,400
cubic feet (cu ft)	cubic meters (m^3)	0.028
cubic yards (cu yd)	cubic meters (m^3)	0.765
pounds (lb) mass	kilograms (kg)	0.453
tons (ton) mass	kilograms (kg)	907
pound force (lbf)	newtons (N)	4.45
kilogram force (kgf)	newtons (N)	9.81
pounds per square foot (psf)	pascals (Pa)	47.9
pounds per square inch (psi)	kilopascals (kPa)	6.89
U.S. gallons (gal)	liters (L)	3.79
acre-feet (acre-ft)	cubic meters (m^3)	1,233

PLANNING FOR DETROIT DOWNTOWN PEOPLE MOVER[a]

By David J. McDonald[1]

(Reviewed by the Urban Transportation Division)

INTRODUCTION

Downtown Detroit, like the central business district (CBD) in many other older U.S. cities, has experienced a decline that has contributed greatly to disinvestment in the area. The existing Detroit CBD is also evidence of a concentrated major activity center the physical boundaries of which are limited by the mobility of its residents and day-time inhabitants. While the area generally referred to as the Detroit CBD is defined by a circumferential freeway system approximately 1.56 sq mile (4.0 km^2), development within this area is concentrated within a zone approximately 0.56 sq mile (1.5 km^2). Recent CBD developments outside of this concentrated area show a history of inability to attract choice tenants. These facilities function as separate self-sufficient activity nodes with little opportunity for interaction with the present core area. This impediment to convenient personal office-to-office and office-to-retail interaction is generally recognized as a major deterrent to the development of the CBD.

Clearly, an improved means of personal movement about the CBD is necessary to facilitate and promote those trips that fall outside the range of acceptable walking distance, since this currently defines the limits of core area development. This will contribute substantially to the viability of existing and proposed downtown developments by linking them. The resulting increases in their property values will stimulate development of nearby vacant land parcels, thereby further increasing real estate values. By permitting easier movement through the CBD, it will also lessen the demands on CBD land for parking, thus increasing the property available for more productive purposes. A program which increases such mobility should be designed to meet three primary needs:

[a]Presented at the October 27–31, 1980, ASCE Annual Convention and Exposition, held at Hollywood, Florida.

[1]Downtown People Mover Project Mgr., Southeastern Michigan Transportation Authority, Detroit, Mich.

Note.—Discussion open until April 1, 1982. To extend the closing date one month, a written request must be filed with the Manager of Technical and Professional Publications, ASCE. Manuscript was submitted for review for possible publication on January 23, 1981. This paper is part of the Transportation Engineering Journal of ASCE, Proceedings of the American Society of Civil Engineers, ©ASCE, Vol. 107, No. TE6, November, 1981. ISSN 0569-7891/81/0006-0597/$01.00.

1. Serve as an internal circulation system to facilitate travel about the CBD and thereby promote development and expansion.
2. Serve as a distributor for primary transit trips entering the CBD.
3. Serve as a distributor for primary auto trips entering the CBD.

Background.—In Detroit, studies dating back to 1968 have addressed these basic issues and concluded that an automated people mover system offers a solution to these local circulation problems by improving the efficiency of movement within the downtown area. In 1972, the Southeastern Michigan Transportation Authority (SEMTA) assumed responsibility for developing and refining the plans for the people mover system. Since the inception of this project, the city of Detroit, the Michigan Department of Transportation, key business and civic leaders, and the general community have participated in this planning. In 1974 and 1975, an extensive analysis, very similar to the preliminary engineering now required by UMTA's DPM demonstration program, was performed for Detroit. In fact, the results of that preliminary engineering study served as a basis for the proposal which SEMTA submitted to UMTA for participation in the latter's DPM demonstration program. That study had recommended a single lane loop system with eleven stations and a total length of 2.3 mile (3.7 km). The system was to utilize 30 vehicles, operating either individually or in trains, with each having a crush load capacity of 60 passengers. The maximum velocity would be 30 mph (48.3 kph), and the minimum headways would be 60 sec. The estimated capital cost of that Downtown People Mover System was $56 million.

In December, 1976, UMTA announced that four cities had been selected to receive DPM demonstration funds. Although not selected as a "first-tier" demonstration project, SEMTA was told it could proceed with the Detroit DPM provided they adhere to the following criteria:

1. The system would form a part of the total regional transit improvements being developed by an ongoing transit alternatives analysis.
2. It would be funded from the UMTA commitment of $600 million for those improvements.
3. The project would be conducted in accordance with UMTA's DPM demonstration guidelines.

In June, 1977, it was determined that all of the regional transit improvement alternatives still under consideration included a DPM system in Detroit's central business district and it was, therefore, concluded that the DPM project should proceed.

Preliminary Engineering.—In order to be certain that all aspects of any specific DPM system were thoroughly analyzed, UMTA guidelines require that the project be conducted in two phases: (1) Preliminary engineering; and (2) deployment. In October, 1977, SEMTA submitted a capital grant application for funds to accomplish the preliminary engineering phase of the Detroit DPM project. That preliminary engineering effort, which actually started in September, 1978, was divided into three work programs, and teams of consulting engineering firms were engaged to perform most of the work.

The first work program, "System Planning," included preparation of the

environmental impact statement as the major activity, plus conduct of cost/benefit analyses, preparation of a financial plan, investigation and analysis of joint development opportunities, and related matters.

The second work program, "System Engineering," was primarily devoted to the conceptual design of the system. This included the development of the guideway alignment and station locations, preparation of performance specifications for the system equipment, design criteria for the facilities, and an implementation plan for the deployment of the system. Estimates of the capital cost of the system and the subsequent cost of operating and maintaining the system were also prepared as part of this work program. The third work program, "System Safety," included preparation of the system safety plan and a safety overview of the other work programs.

Alignment Selection.—The first major effort of preliminary engineering was the selection of the DPM alignment. This began with the development of system objectives which were based on general community values and the city's overall social, economic, environmental, and transportation goals for the CBD. The relative weights of these objectives were provided by the members of a DPM steering committee, which consisted of representatives of the city, local governmental agencies, and downtown business and community interests. Measures of effectiveness were then identified to determine how well any alternative alignment would satisfy each system objective. The product of the objective weights and the measures of effectiveness, when summed, provided a weighted score for any given alignment.

A two-tier evaluation process was developed to better manage the selection of the preferred alignment from a large number of candidate alternatives. The first-tier preliminary evaluation reduced the numerous initial alternatives to a manageable number for detailed study. This was accomplished by applying only selected measures of effectiveness, to reduce data requirements, and limit the amount of information developed by the project staff and considered by the evaluators. The initial alternatives were ranked by weighted scores and then carefully scrutinized to establish a superior subset of alternatives. Five basic alternatives were found to meet the needs of the community. These were reviewed by the steering committee and the SEMTA Board of Directors, whose deliberations concluded that some variations of the basic alternatives should be subject to the second, detailed phase of the alignment selection process.

The detailed analysis, much of which utilized computer models, considered all of the parameters developed for the study, including ridership, cost, economic development potential, land use considerations, environmental impacts, and social impacts. Again, a weighted score yielded a ranking of alternatives which facilitated an interpretation of the merits of each alternative. To aid the steering committee and the SEMTA board in reviewing the final alternatives, various marginal cost effectiveness measures were also developed. Benefit and cost information also was provided for the various alignments. On May 15, 1979, the SEMTA board, after reviewing all of the pertinent data and recommendations of the steering committee, selected the alignment which was to be used for the remainder of the DPM preliminary engineering effort. That alignment is shown on Fig. 1.

Performance Specifications/Design Criteria.—After selection of the preferred alignment, the preliminary engineering effort focused on the development of specific features of the system. A topographic survey was conducted and soil

borings were made and analyzed. Utility locations were established and environmental impacts were identified and evaluated. Joint development opportunities were considered in more detail. On the basis of this work, the best location and orientation of the system facilities was specified.

Operations and failure management strategies were formulated and tested for the baseline design in order to develop the system and subsystem (primarily vehicle) service and performance characteristics to be incorporated in the system performance specifications. A parametric sizing analysis was performed to estimate station requirements such as corridor widths, queueing areas, and the number and type of service devices. Definitions were prepared for the climatic conditions under which normal and degraded operation of the DPM system would be required, and the related functional requirements (i.e., the necessary level, type, and extent of protection/treatment) were established. Federal, state,

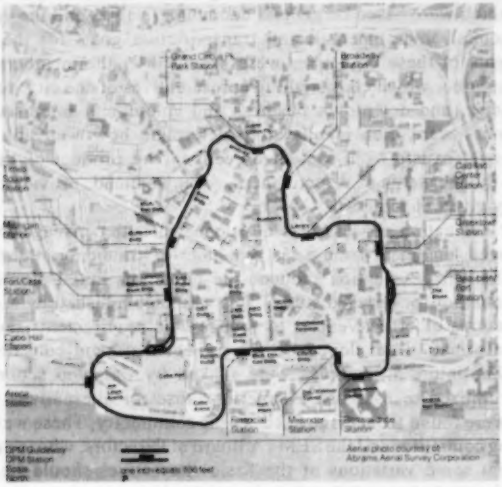

FIG. 1.—Detroit Downtown People Mover Alignment

and local requirements regarding public transportation accessibility for elderly and handicapped persons were reviewed to provide input for the specification of the DPM system, subsystem, and components.

Performance specifications were prepared for the system and for its major elements. Plan and profile drawings were generated for both bottom-supported and top-suspended vehicle technologies, and permissable guideway column locations were identified. The system requirements specified included patronage capabilities, levels of service (maximum wait times, passenger space allocations, etc.), operational requirements, system availability, and safety/security provisions. The environmental extremes in which the system must operate were defined. Performance requirements were established for operating equipment, including vehicles, controls, communications, fare collection equipment, and

the power distribution system. Design criteria were established for both the functional and architectural aspects of the system facilities, including the guideway, stations, and maintenance and control facility. These specifications and drawings became major components of a request for proposals that was developed as the means by which a system supplier would be acquired for the deployment phase of the project. The DPM system specifications also stipulated requirements for the maintenance of both facilities and equipment, and for verification of compliance with the operational and performance specifications.

Environmental Impact Statement.—A key task that was undertaken in earnest after selection of the preferred alignment was the preparation of the Environmental Impact Statement (EIS) for the DPM system. In accordance with applicable regulations, a description of the expected impacts was prepared for the DPM system and for a circulator loop bus system postulated to provide service comparable to that of the DPM. These impacts were compared with the environment which would exist if a "no build" alternative were pursued. A draft EIS was circulated for the review and comment of interested governmental agencies and the general public. The document was then finalized by the incorporation of all valid comments to enable federal and local officials to reach a decision regarding system deployment. The document completion process involved numerous meetings and other communications with federal and state authorities, especially those concerned with the project's impacts on parks, and features of historic or architectural significance, or both.

Other Tasks.—Other activities conducted during preliminary engineering included the following:

1. The development of system expansion criteria, based on consideration of alternative means to expand capacity and area coverage, and assessment of operational impacts, costs, and engineering requirements.
2. The formulation of a conceptual plan, in accordance with state and federal regulations, to relocate any residence or businesses, or both, to be displaced by construction of the DPM. In actuality, only two businesses and no residences will be displaced by the DPM.
3. The development of a plan to implement the deployment phase of the project, including management, scheduling, and budgetary aspects.
4. The preparation of a plan to evaluate several scenarios for financing the operation and maintenance of the system.

System Description.—The People Mover System in downtown Detroit is planned as a totally elevated, automated system providing circulation and distribution service along a 3 mile, single lane loop route around the core of the CBD (Fig. 1). The system will operate on a schedule frequency of not more than two minutes during peak periods, and three minutes during off peak periods. Vehicles will operate on the loop at speeds of up to 30 mph (48.3 kph) and, allowing a 20 sec stop at each station, the total time to traverse the loops will be less than 15 min. This translates into an average travel speed, including stops, of 12.6 mph (20.3 kph).

Stations will be unattended and vehicles will not have operators on board. Operations will be directed from a control center located at the maintenance

facility. There will be 13 on-line stations along the route. By-pass channels may be provided in two of these stations, located about half-way around the loop from each other, where vehicles can be stored when necessary, especially in response to failure situations. Patronage studies indicate that by 1990 as many as 71,000 passengers per day will ride the DPM, with the peak hourly use of 11,500 passengers occurring at noon. The maximum hourly link load will be approximately 5,500 passengers. The annual patronage of the system is forseen to be 22,000,000 passengers by 1990. To minimize land takings, street rights-of-way, curb lanes and medians, surface parking lots, and vacant land will be used for guideway and station facilities.

The maintenance facility, including the control center and system administrative offices, will be located on a parcel adjoining the Cobo Hall Station, on the north side of the Cobo Hall Convention Center. The station is directly connected to that facility by a pedestrian skywalk. The site of these DPM facilities is currently being considered as the location of a proposed major office and hotel development. The Fort/Cass Station will serve the western portion of the CBD's financial district. The Michigan Station is centrally located to serve the McNamara Federal Office Building, the headquarters office of the Michigan Bell Telephone Company, and the Book Cadillac Hotel. The Times Square Station will adjoin a new high-rise apartment building now under construction. The Grand Circus Park Station provides service to the office buildings in that area and is expected to stimulate the revitalization of the many old hotels around the park. This station will also provide a direct link to the light rail line being planned for Woodward Avenue.

The Broadway Station, on the site of a proposed eight story office building, will service the small shops in that area. The Cadillac Center Station will open directly into the mall of this proposed major shopping development for which ground is now being cleared, and is considered essential to its success. The Greektown Station is within the CBD's only concentration of ethnic restaurants and shops. The Fort/Beaubien Station will serve the Blue Cross/Blue Shield parking garage and office tower. The Renaissance Center Station will be linked by a skywalk directly to that seven-building office/hotel/retail complex, which has been the principal impetus for the revitalization of the CBC. This station will also provide service to the Pontiac Commuter Rail Station on the east side of the Renaissance Center.

The Millender Center Station will be located on a large, well located surface parking lot, in an effort to stimulate a major development on that site. The stop will also provide service, via a pedestrian skywalk, to the city-county office building. The Financial District Station is located in the heart of the CBD's largest concentration of office buildings, and on a site on which a twin-tower office structure is being planned. The Arena Station will serve the Joe Louis Arena, the site of the 1980 Republican Convention, and a large riverfront hotel and apartment complex. This station also connects with a large parking structure and the future Ann Arbor commuter rail terminal. Six of the DPM stations also serve as bus and auto intercepts along the major arteries leading downtown.

Guideway Requirements.—In assembling the specifications for the Detroit DPM, it was necessary to consider the UMTA requirement that a variety of technologies may compete for the implementation contract. Consequently, the preliminary

engineering drawings were developed to encompass all current technologies. Two profiles were prepared, one to apply to a bottom-supported system and the other for suspended vehicles. In the baseline system design, nominal span lengths of 80 ft (24.4 m) were assumed. The maximum span length required is approximately 130 ft (39.7 m). Beam depths on the order of 4.75 ft (1.45 m) are expected for top-supported vehicles operating on 100 ft (30.5 m) span guideway sections. The height above city streets varies from 15 ft (4.6 m) at some locations, to as high as 35 ft (10.7 m) at others. A 20 ft (6.1 m) clearance is maintained over the major arteries.

Station locations and pier placements were limited to minimize impacts on pedestrian or vehicle flows, or both, parking areas, and existing conditions in the CBD. In general, it was considered desirable to position the guideway within existing street rights-of-way or on other public property, thereby reducing the need for private property acquisition. Also, horizontal alignment decisions were aimed at minimizing side-to-side street crossings. The desirable maximum

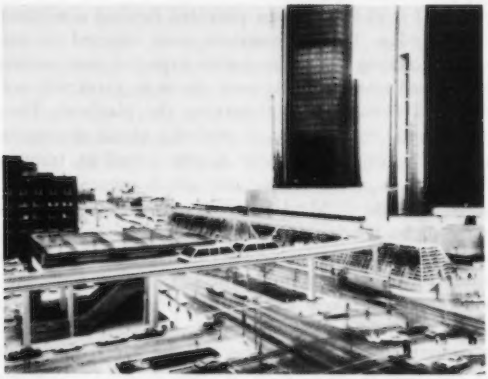

FIG. 2.—DPM Guideway at Renaissance Center

grade of 4% was established, with the maximum grade through station areas to be 0.2%. To facilitate drainage, this figure would also be the minimum grade maintained anywhere on the guideway. A minimum vertical curve length of 150 ft (45.7 m) was established, and the minimum horizontal curve radius considered was 100 ft (30.5 m). In addition to these criteria, urban design factors established specific guideway elevations compatible with major architectural elements along the route.

A DPM operated in the Detroit CBD must also be designed taking into consideration the requirements imposed on the system by civil codes and weather conditions. It is expected that the guideway running surface, if concrete, will be heated, probably by means of a circulating hot fluid system, and other vehicle and guideway components may be heated as necessary with electrical resistance wires. There are, however, certain technologies that may not require all of these weather protection features.

The safety of passengers and service personnel was a primary concern in

guideway design. Specifications require that no single vehicle failure or human error of omission or commision can cause serious personal injury or major property or environmental damage. Fail-safe features must be incorporated. Hazardous areas along the guideway will be clearly identified and protected as necessary. The guideway design also requires that all guideway elements be mounted within the structures such that they are safe and easily accessed but unobtrusive in appearance. The baseline system design assumes that 3-phase grounded a-c power will be utilized for propulsion.

Station Requirements.—The stations were sized to meet the projected 1990 level of patronage, based on the population employment forecast for that year. The stations were located to maximize convenient access for the largest number of people within the most prominent commercial and cultural activity centers. At least five of the stations will be integrated into existing or proposed developments. All stations will have access to and from the adjacent street. In specifying the station requirements, the minimum platform length was set at 80 ft (24.4 m). A minimum platform width of 10 ft (3.05 m) was established, with an additional 2 ft (0.61 m) to be provided beyond a windscreen installed along the platform edge. These dimensions were selected on the basis of the train lengths likely among the technologies expected and patronage levels at the most heavily used stations. Automatic doors or gates will not be provided at the boarding and deboarding positions on the platform. The stations will be constructed as metal frame cages, to minimize visual obstructions.

Requirements for safety and security dictate a well lit, transparent facility, with as few columns as possible, and one which incorporates a minimum of opaque elements. Since the DPM train arrivals will be frequent, patron occupancy of the stations will be relatively short-term. It was therefore concluded that a combination of natural convection ventilation and solar screening would provide reasonable comfort during the summer. The short patron wait-time also justifies the use of wind screening along the platform edge as an acceptable response to winter weather conditions, although some localized heating may be provided. The platform canopy will extend just beyond the center line of the guideway, to reduce the exposure of patrons to the elements, and to reduce the water running over the side of the car onto the platform. Also, because of the anticipated short-term patron occupancy, the stations will not be equipped with the amenities traditionally associated with the facilities of conventional transportation modes, i.e., there will be no vending machines, water fountains, public rest rooms, etc., in the stations.

Use of the system will be by means of tokens. At most stations, token dispensing and collection will be accomplished on a level other than that of the platform. One escalator, normally operating in the up direction, and two stairwells, one at each end of the platform, will be provided at each station, as will an elevator designed to accommodate the elderly and handicapped. Limited heating will be provided in the turnstile area. All stations will also be provided with closed-circuit TV surveillance and direct phone lines to the system's central control office.

An urban design treatment was identified for each station to illustrate how the proposed guideway, guideway columns, and stations would be configured. The principal goals of the urban design treatment were transparency, maintainability, and identity.

Maintenance and Control Facility Requirements.—The maintenance and control facility is located on a rectangular site adjacent to the Cobo Hall Station. This area is the best available location for the facility, which must provide the following functions:

1. Complete maintenance and parts storage for all necessary inspections and repairs except major vehicle body work and motor rebuilding.
2. Minor vehicle body repairs and replacement.
3. Storage space for the entire vehicle fleet, for climate protection and security purposes.
4. Office space for maintenance personnel and equipment.
5. Office space for administrative functions.
6. Command and control center for system operation and surveillance, with an adjacent public viewing area.

It was determined during preliminary engineering that such a maintenance facility would require approximately 70,000 sq ft (6,500 m^2) of space. The minimum acceptable length of the maintenance facility along the mainline guideway is 350 ft (100 m), and the minimum width of the maintenance facility is 100 ft (30.5 m). The selected site is approximately 580 ft (177 m) long and 130 ft (40 m) wide, with an area of approximately 75,000 sq ft (7,000 m^2). In this facility all maintenance will be performed at the guideway elevation. Some parts storage areas and offices will be located on the level below the maintenance floor. The ground level is available for parking or commercial uses. Major high-rise development over the site is also being considered.

Vehicle Requirements.—DPM vehicles will be constructed of aluminum, with their outer surfaces composed of either aluminum or fiber glass. Windows and doors will be located on both sides of the cars and door widths will be a minimum of 44 in. (1,118 mm), which will accommodate wheelchair passengers. Each car will provide perimeter seating for a minimum of 12 passengers. Maximum capacity, including standees, could be as high as 80. Exterior and interior vehicle noise will be lower than that of a diesel engine bus. The cars will also provide heating, ventilation, and air conditioning. These will adjust automatically to suit climatic conditions. Passengers will be linked to central control by "push-to-talk" radio equipment. To minimize system down time, each vehicle must also be capable of pushing another failed vehicle in emergency situations.

Benefits.—Studies indicate that a people mover system in downtown Detroit would have many beneficial effects on the area. By linking the various activity centers to each other and thereby stimulating travel about the CBD, the DPM would encourage the continued redevelopment of the downtown area. Presently identified development at various DPM station sites is estimated to involve investments of almost $600 million. It is forecasted that by 1990 the DPM would have stimulated the construction of 30,000 sq ft (2,790 m^2) of additional office space, 600 more hotel rooms, and 1,250 additional housing units. In addition, by that time, annual retail sales in the downtown are estimated to increase by at least $45 million as the result of the DPM. Finally, it is estimated that deployment of the DPM will result in 2,900 additional permanent jobs.

Cost.—The estimated cost of the final design, construction, and test of the DPM is $80.9 million in 1979 dollars. If escalation over the period of implementa-

tion is assumed to be 14% in 1979, 10% in 1980 and 1981, and 9% thereafter, when the system is placed in revenue service by the end of 1984 its deployment cost will have reached $127 million. The annual cost of operating and maintaining the system in 1985 is projected to be approximately $6.8 million. The SEMTA Board of Directors had adopted a policy that operation of the DPM system will not require a public subsidy. On this basis, it is forecasted that a fare of 30¢ will be charged to ride the system in 1985. In any case, fares and hours of operation will be adjusted as necessary to assure an economically self-sufficient operation.

Present Status.—The preliminary engineering phase of the project was completed in late 1980. The final environmental Impact Statement has been circulated, approved, and filed with the Environmental Protection Agency. Right-of-way property acquisition is underway. A request for proposals for the deployment of the system in the form of a major "total turnkey" contract has been advertised to the industry, and the responses received have been evaluated. The Urban Transportation Development Corporation of Toronto, Canada, has been selected as the system supplier. This firm will provide its Intermediate Capacity Transit System technology, which utilizes flanged steel wheeled vehicles which travel on conventional steel rails. The cars are propelled by linear induction motors and are controlled by a moving block, checked redundant system.

It is expected that the system supplier can be placed under contract by September, 1981. Allowing 40 months for deployment, the system will be operating for use by the public by the end of 1984. The application for a grant of 80% of the deployment cost was submitted to the federal government in July, 1980, and funds for the first year of work were approved in January, 1981. However, suspension of these funds is now being proposed by the administration, although initial funding has been approved by the state of Michigan and these funds were approved by the state legislature in September, 1980.

Conclusion

Considerable planning and preliminary engineering efforts have established that the deployment of a people mover system in downtown Detroit would contribute significantly to the redevelopment of that area. By providing a means for quick, convenient travel between the CBD's various activity centers, it is expected that each would become more productive and profitable, thereby stimulating their expansion and the construction of other facilities which would result in better utilization of the available land. A people mover system could be deployed in a manner which would meet these objectives at a cost which is considerably less than the resulting benefits.

Pressure Scale Effects on Shape Drag in Conduit

By William J. Rahmeyer,[1] A. M. ASCE

(Reviewed by the Pipeline Division)

Introduction

For the past two years testing has been conducted at Colorado State University (3,4) on the measurement of drag around cylinders and different shaped struts inserted across a section of pipe. In two separate series of tests with independent test setups and different pipe sizes, it was found that the drag coefficient calculated for the cylindrical shapes varied at a constant Reynolds number with different static wall pressures in the pipe. As shown in Fig. 1, the drag coefficient increased in value with an increase in static wall pressure at a constant Reynolds number. Some publications (1,5,6) state that the drag coefficient should only vary with the Reynolds number and not with pressure.

This phenomenon is important to industry because of the increasing use of cylindrical and shaped struts for flow measurement by inserting them through pipe sections to generate pressure differentials and fluctuations from the resulting drag forces. The purpose of this paper is to present the results of the testing and a possible explanation for the phenomenon and to generate interest and helpful discussion.

To study this phenomenon in detail, a test was constructed to examine different diameters and shapes of struts in various piping configurations. For this study, the drag coefficient (dimensionless) was defined

$$C_D = \frac{\Delta H}{\dfrac{V^2}{2g}} \quad \text{(1)}$$

in which ΔH = the head differential; V = the pipe velocity; g = the gravitational constant and the Reynolds number (dimensionless) was defined

[1] Asst. Research Prof., Dept. of Civ. Engrg., Colorado State Univ., Fort Collins, Colo.

Note.—Discussion open until April 1, 1982. To extend the closing date one month, a written request must be filed with the Manager of Technical and Professional Publications, ASCE. Manuscript was submitted for review for possible publication on March 12, 1981. This paper is part of the Transportation Engineering Journal of ASCE, Proceedings of the American Society of Civil Engineers, ©ASCE, Vol. 107, No. TE6, November, 1981. ISSN 0569-7891/81/0006-0607/$01.00.

$$R = \frac{V^* D}{\nu} \qquad (2)$$

in which D = the characteristic length of strut; and ν = the dynamic viscosity.

Experimental Program

The cylindrical struts or shapes tested had the diameters of 1 in. (2.54 cm), 0.75 in. (1.91 cm), and 0.5 in. (1.27 cm). The shaped struts had a cross-sectional diamond shape with a width of one inch. The drag coefficient (Eq. 1) was calculated from the pressure differential measured with manometers from pressure taps located in the upstream and downstream faces of the struts. The location of the taps and their sizes varied for different struts.

The struts were inserted perpendicular through the pipe walls of 6-in. (15.24-cm) schedule 40 standard steel pipe. One of the piping configurations (Fig. 1) used was a section of straight pipe with the struts installed with at least 100 pipe diameters in length of straight pipe upstream and downstream. The other piping configuration (Fig. 2) used was a short radius 90° elbow with straight pipe upstream and downstream. The struts were inserted perpendicular through the pipe walls in a section of pipe located 2 pipe diameters downstream of the center line of the elbow.

The static pipe pressure or the system pressure was measured with a precision dial gage from static pressure taps in the pipe walls placed upstream from

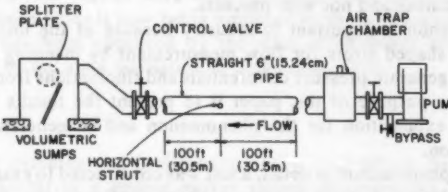

FIG. 1.—Test Setup for Straight Pipe Tests

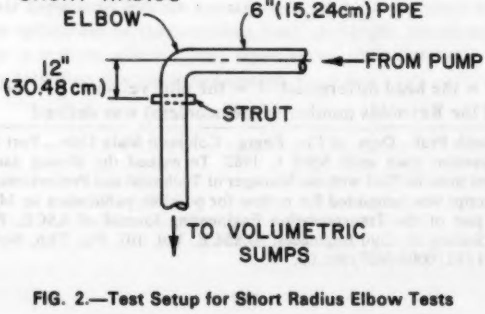

FIG. 2.—Test Setup for Short Radius Elbow Tests

the struts. Accuracy of pressure differentials and static pressures were within 0.5%. The flow media for the tests was water at a constant temperature of 70° F (21° C), and was supplied from a pump operated with a constant outlet pressure. An open type of flow system was used with the flow discharged into a large collection sump. The flow rate of the system was measured using a series of accurate volumetric sumps (±0.25% traceable by weight to N.B.S.).

Test data consisted of measured flow rate, measured pressure differential across the taps in the struts, and the static wall pressure of the pipe system. A series of 10–12 data points were measured for each test configuration for a flow range varying in Reynolds number from 1×10^4–2×10^5. All of these tests were conducted at constant pipe pressures.

Test Results

Both the cylindrical and diamond-shaped struts were tested in the straight pipe test configuration at constant pipe pressures of 10, 20, and 30 psi (68.9,

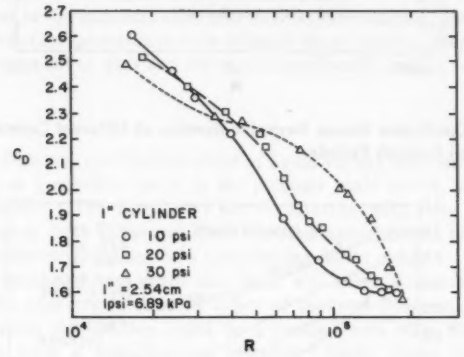

FIG. 3.—Drag Coefficient Versus Reynolds Number at Different Constant Pressures; 1 in. (2.54 cm) Smooth Cylinder

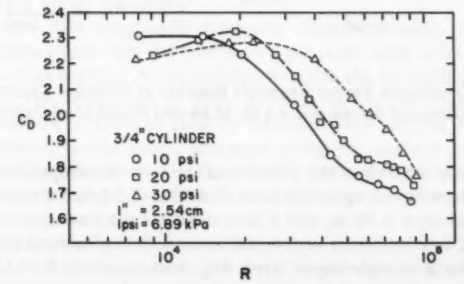

FIG. 4.—Drag Coefficient Versus Reynolds Number at Different Constant Pressures; 3/4-in. (1.91-cm) Smooth Cylinder

137.8, and 206.7 kPa). Plots of the test data are presented in Figs. 3, 4, 5, and 6. The variation in plots at different pressures shows the effect of the pressure dependence. The variations of plots are not due to the accuracy of test measurements that would result only in a deviation of 1%. However, for the test data (Fig. 6) from the shaped struts, there was no evident variation with pipe pressure. Tests results not presented, (4) in the elbow configuration found no effect on the drag coefficient from pipe pressure with either the cylindrical or diamond-shaped struts.

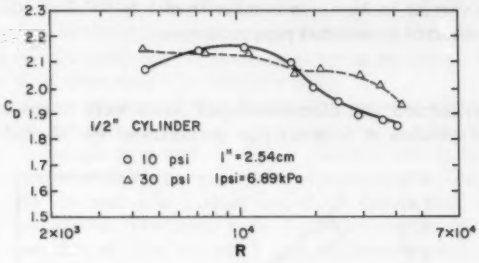

FIG. 5.—Drag Coefficient Versus Reynolds Number at Different Constant Pressures; 1/2-in. (1.27-cm) Smooth Cylinder

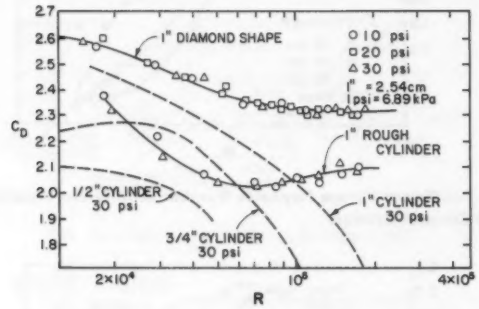

FIG. 6.—Drag Coefficient Versus Reynolds Number at Different Constant Pressures; 1-in. (2.54-cm) Diamond Shape and a 1-in. (2.54-cm) Roughened Cylinder

To help explain the lack of the pressure effect with the shaped strut, additional tests were made with the upstream face of a 1-in. (2.54-cm) diameter cylindrical strut roughened with 0.06 in. (15.9 cm) deep longitudinal grooves. The strut was roughened to control the separation around the cylindrical shape as would the edges of the diamond-shaped strut. Fig. 6 shows that, for tests in straight pipe with roughened strut, the pressure effect was absent.

Similar types of plots found in a text by Streeter and Wylie (6) show that the drag coefficient of a diamond shape is larger than for a circular shape,

and, while the drag coefficient of the diamond shape is fairly constant for certain ranges of Raynolds number, the coefficient for a circular shape will decrease with an increase in Reynolds number. The test data presented in Figs. 3–6 are in agreement with this.

Test results show that as the strut diameter decreases of the pipe diameter to strut diameter ratio (L/D) ratio increases, the drag coefficient decreases in the manner discussed in a text by Hunter Rouse (5). As the L/D ratio decreased in the test results, the effect of the pipe pressure or the pressure scale effect at a constant Reynolds number appeared to decrease.

The roughening of the 1-in. (2.54-cm) diameter cylindrical shape caused the drag coefficient to lessen (Fig. 6) in variation or slope with Reynolds number, and the drag coefficient of the roughened shape was less than the coefficient for the smooth cylindrical shape at low Reynolds number and greater for high Reynolds numbers. This can be explained by the premises that the roughened shape would have a smaller wake at low Reynolds numbers and a larger wake than the smooth shape at higher Reynolds numbers.

The variation in the number, size, and location of pressure taps of the struts had little influence on the pressure scale effect of the cylindrical shapes. However, only a limited amount of data and effort was involved in testing for this.

Conclusions

The results were analyzed for the effect of liquid density and viscosity variation with pressure as a possible factor in the pressure scale effect, but were ruled out as a possibility. The tests were also conducted with flow conditions to prevent cavitation from occurring from the separation around the struts, and, therefore, cavitation would not be a contributing factor either.

During the testing, it was noted that there was some air entrainment in the flow as can be expected with some types of pumped flow supply. Assuming that the entrained air bubbles could be a factor, tests were conducted with flow supplied from a high-pressure reservoir. Under these conditions, the cylindrical struts did not experience a pressure scale effect. It was then concluded that the size and number of entrained air bubbles would be less for higher pipe pressures and, therefore, a lesser pressure scale effect with less air entrainment from higher pressures.

However, tests with roughened cylinders, diamond shapes, and tests with short radius elbows upstream did not have a pressure scale effect even though air entrainment was present. An hypothesis was that the air entrainment affected the location of the separation of flow around the smooth cylindrical struts. As in the transition of laminar flow to turbulent flow around a cylinder, the point of separation would move upstream along the surface of the cylinder with transition. The turbulence generated by the entrained air bubbles increasing in size while accelerating around the cylinder and mixing into the separation zone, could then cause the transition to move the point of separation upstream. Higher pipe pressure would decrease the size of the accelerated air bubbles. The high level of turbulence generated by flow through an elbow would then cause the separation point to be upstream already and to not be affected by the amount of air entrainment or level of pipe pressure.

The hypothesis presented in this paper to explain the observed phenomenon

is highly subjective and based on a limited amount of data. There was no attempt to measure air entrainment or turbulence levels, to study boundary layer growth, or to account for the effect of the pipe walls on the phenomenon. While this effect is important under certain flow conditions for application in flow metering, it should not be used for evaluating industrial applications or products. The purpose of this paper is mainly for academic interest and possibly as the basis for additional detailed research into the causes and conditions for the phenomenon to occur.

Appendix I.—References

1. Doig, I. D., and Rose, D. W., "Transverse Tubes as Pitot Probes in Cylindrical Conduits," The Institution of Engineers, June, 1968, Australia.
2. Farell, C., Carrasquel, S., Guven, O., and Patel, V., "Effect of Wind Walls on the Flow Past Circular Cylinders and Cooling Tower Models," *Transactions* of American Society of Mechanical Engineers, Sept., 1977.
3. Rahmeyer, W., "Hydraulic Study and Analysis of Different Models of the Eight Inch Annubar Flow Meter," *Hydro-Machinery Lab Report, No. 101*, Colorado State University, Fort Collins, Colo., Apr., 1979.
4. Rahmeyer, W., "Hydraulic Tests of Pitot-Type Averaging Insertation Flow Meters with Different Cross-Sectional Areas and Shapes," *Hydro-Machinery Lab Report, No. 116*, Colorado State University, Fort Collins, Colo., Nov., 1980.
5. Rouse, H., *Elementary Mechanics of Fluids*, Dover Publications, Inc., New York, N.Y., 1978.
6. Streeter, V., and Wylie, E., *Fluid Mechanics*, Sixth Edition, McGraw Hill Book Co., Inc., New York, N.Y., 1975.

Appendix II.—Notation

The following symbols are used in this paper:

C_D = drag coefficient;
D = length of strut member;
g = gravitational constant;
R = Reynold's number based on length of strut;
V = pipe velocity;
ΔH = head (pressure) differential; and
ν = dynamic viscosity.

COFFERDAM CONSTRUCTION: I-205 COLUMBIA RIVER BRIDGE[a]

By Robert B. Bittner[1]

(Reviewed by the Highway Division)

INTRODUCTION

This paper describes the development of two unique and separate cofferdam systems used in the construction of the marine foundations for the I-205 Columbia River Bridge at Portland, Oregon. The first of these two systems utilized 24 in. (610 mm) deep interlocking H piles to form cofferdam walls, with a bending capacity five times greater than could be obtained using conventional Z sheet piles. These high strength walls allowed the construction of a cofferdam 100 ft (31 m) deep with only two levels of bracing.

The second cofferdam system used a single-piece bell-shaped form, which functioned as both cofferdam and form for the piers. The cofferdam form for the larger piers was 62 ft (19 m) high and was externally stiffened for a designed hydrostatic head of 54 ft (17 m). This 450-ton (408-Mg) cofferdam form was set and stripped in one piece, with the bottom 48 ft (15 m) welded into one solid unit.

The original substructure was designed by Sverdrup and Parcel for the Oregon State Department of Transportation. Contractor for this $30,300,000 substructure contract was a Joint Venture sponsored by Riedel International of Portland. The other partners were Alaska Constructors, Inc. of Anchorage, and General Construction Company of Seattle.

The supporting geological formation for the bridge foundations is the Troutdale, a cemented sand and gravel. This formation is at the ground surface on the Washington shore and slopes downward to a depth of 115 ft (35 m) below normal high water at about midchannel. In this area the Troutdale formation is covered with a layer of fine to medium sand 90–100 ft (27–30 m) thick.

[a]Presented at the April 14–18, 1980, ASCE Annual Convention and Exposition, held at Portland, Oreg.

[1]Chief Engr., Construction Div., Riedel International, Inc.; formerly, Willamette-Western Corp., Portland, Oreg.

Note.—Discussion open until April 1, 1982. To extend the closing date one month, a written request must be filed with the Manager of Technical and Professional Publications, ASCE. Manuscript was submitted for review for possible publication on October 29, 1980. This paper is part of the Transportation Engineering Journal of ASCE, Proceedings of the American Society of Civil Engineers, ©ASCE, Vol. 107, No. TE6, November, 1981. ISSN 0569-7891/81/0006-0613/$01.00.

It was the variable depth of the Troutdale which determined the two types of foundations and the corresponding two cofferdam systems.

Interlocking H Pile System

The first two piers off the Washington shore, Piers 12 and 13, flank the main 600 ft (183 m) navigation channel. Both of these piers were designed

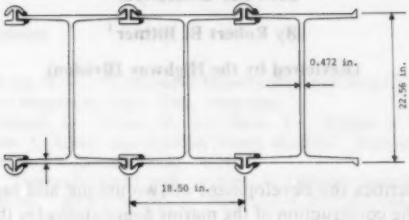

FIG. 1.—Interlocking H Pile System

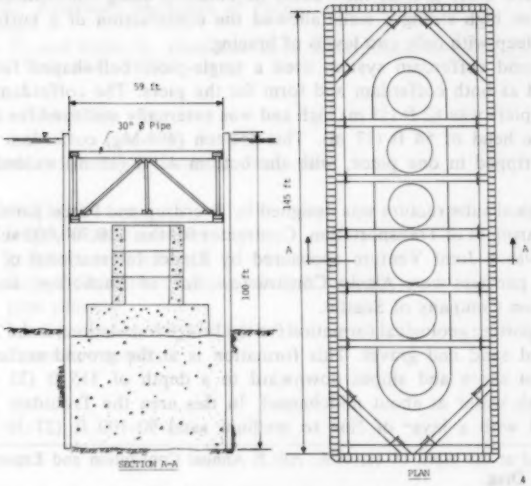

FIG. 2.—Cofferdam Bracing

to bear directly on the Troutdale. The design depth of the foundation at Pier 13 was 100 ft (31 m) below normal high water. Because of this extreme depth, it was originally designed as a concrete caisson. After the notice of contract award, a study was made to determine the feasibility of using a cofferdam approach. Again, due to the extreme depth, conventional sheet piling were ruled

out primarily because of the numerous levels of bracing which would have been required for the hydrostatic head of 62 ft (19 m) at Pier 13.

Two alternate sheeting systems were evaluated. The first of these was an interlocking pipe pile system offering a section modulus as high as 469 cu in./ft (252×10^5 mm^3/m) compared to the 46.3 cu in./ft (25×10^5 mm^3/m) for the highest capacity, Z, sheet pile manufactured. The second system was an interlocking H pile system which offered a section modulus as high as 555 cu in./ft (300×10^5 mm^3/m). Final selection was a H section with a section modulus of 243 cu in./ft (131×10^5 mm^3/m) (Fig. 1). These high strength sheets required only the seal and one wale support point. The final design used two wale frames (Fig. 2). The function of the top frame was to provide support during threading and driving of the sheet pile and to carry the wall loadings as struts were removed on the main frame for continuation of the pier shaft.

An additional advantage of the interlocking H pile over conventional Z pile was the closed pocket formed by the interlocking flanges. These pockets when filled with a silty sand mixture not only increased the water tightness of the cofferdam walls, but increased the total dead weight of the cofferdam by 2,450 tons (2,223 Mg). This increased weight allowed a corresponding decrease in the seal concrete volume by 1,250 cu yd (956 m^3). Two steps were taken to insure that this additional weight would be transferred into the seal. First, each pocket was cleaned out to the pile tip, and a concrete block was lowered to the bottom, where it wedged against the reinforced pile tip and sealed the bottom of each pocket. Second, a shear key was added to each pile. These keys were added prior to threading and were located below the top of seal on the inside face of the cell. The shear keys were designed to allow extraction of the H piles after completion of the pier.

The use of only one load carrying wale frame above the seal resulted in extremely high loadings on the frame members. The wales consisted of double W 36 × 230 beams stitch welded along both flanges to form a box section 36 in. × 32 in. (915 mm × 813 mm) and carried a design loading of 26 tons/ft (7.3 Mg/m) of wall. This section not only allowed utilization of conventional rolled shapes, but provided a stable section against any rolling tendency during the driving of the sheet piles. The struts consisted of 30 in. (762 mm) diameter pipe with a wall thickness of 0.750 in. (19 mm) and carried a maximum design loading on the diagonal struts of 700 tons (635 Mg) per strut. The entire bracing system when assembled weighed 350 tons (317 Mg) covered an area 145 × 59 ft (44 × 18 m) and stood 24 ft (7.3 m) high.

The initial step in the cofferdam construction after pre-assembly of the bracing frame, was to float the frame into position, and lift it clear of the barge using a 600-ton (550-Mg) capacity catamaran gantry barge as shown in Fig. 3. With the bracing frame suspended by four load blocks, four 36-in. (862-mm) diameter spud piles were driven, and the load of the bracing frame was transferred to the piles. Threading and driving of sheet piles followed, using a vibratory hammer with an eccentric moment of 4,331 lb-in. (5,000 kg-cm) and operating frequency of 1,100 cpm.

The double interlocking system with an interlock threaded on each flange of the H section was considerably more difficult to thread than conventional sheet piling. The primary cause of this difficulty was the ±1/4 in. (6 mm)

variation in the flange spacing at the interlocks. During the threading operation it was necessary to force the flanges of adjoining piles to match in order for threading to progress. The required force was provided by using the 7-ton (7-Mg) H pile being threaded as a drop hammer with the drop height at times approaching 40 ft (12 m).

After completion of threading and closing of the cell, the H piles were driven through 40 ft (12 m) of medium dense sand which became more dense as the driving progressed. The pile driving moved in a clockwise direction around the cell, driving each pile 8–10 ft (2–3 m) before progressing to the next. During the third driving cycle, the ground had become so compacted ahead of the piles that further attempts at driving resulted in melting of the interlocks. The piles were finally taken to the Troutdale by using a combination air and water jet down one of the pockets a few pockets ahead of the pile being driven. The jet was allowed to penetrate below the tips of the H piles and loosened the sand so effectively that while sections of wall began dropping as the vibratory hammer was turned on.

The remaining steps in the cofferdam construction were similar to conventional

FIG. 3.—Positioning Cofferdam Frame

cofferdams except for the size. The seal at Pier 13 as an example, was 38 ft (12 m) deep, required 11,500 cu yd (8,800 m^3) and took 72 hr to complete. Concrete for the seal pour was supplied by both a floating batch plant and a back up system of barge mounted concrete trucks. The floating batch plant was mounted on a barge 272-by-60-by-18 (84-by-18-by-6 m) deep and equipped with a concrete plant capable of producing 180 cu yd (138 m^3) per hour. Mounted on the bow of the barge were two 5-in. (130-mm) diameter concrete pumps equipped with 103 ft (32 m) articulating booms.

Upon completion of the seal and footing, the shaft was poured in lifts of 10 ft (3 m) up to the underside of the bottom struts. At that point, the bolts connecting the struts to the wale frame were removed and the cell was flooded to the surrounding river elevation. After allowing the disconnected struts to float to the surface, the cell was again dewatered to a point just below the last construction joint in the shaft, and the next lift on the shaft was completed. In this manner, the need for struts passing through the shaft was completely eliminated. This step was repeated on the top wale frame, as the shaft pour

was completed to the underside of the top struts. After removal of the struts on the top wale frame the top lift on the shaft was completed and the H piles were extracted (Fig. 4).

The final step in the cofferdam sequence was stripping of the 250-ton (227-Mg) double wale frame by using the floating gantry crane to lift the frame over the top of the completed shaft.

The transfer of the cofferdam frame from Pier 12–Pier 13 involved increasing the plan dimensions of the frame by 4 ft. This was accomplished by bolting 24 × 24 in. timbers to the outside of the wale frame. Another change made at Pier 13 was the method of pouring the seal. At Pier 12, the pour started in the middle of the cofferdam and worked towards each end. At Pier 13, the seal was started at one end and progressed to the other. This second method,

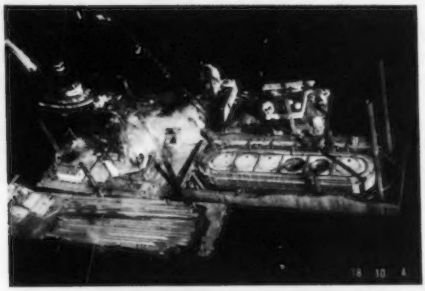

FIG. 4.—Extracting H Pile Wall

with only one direction of flow, resulted in a much more controllable seal pour and a more even surface on the completed seal.

Bell Pier System

The second cofferdam system was used on the remaining 26 piers, double piers 14–26. The Troutdale formation at these piers varies from 105–115 ft (32–35 m) below normal high water and is covered with a layer of dense to medium dense unconsolidated sands 90–110 ft (27–34 m) thick. These piers were originally designed as pile supported precast bells. The original design called for setting a bottom precast segment in a pre-excavated hole. The bottom slab of this segment was to be blocked out and used as a template for driving the 50–100 H piles at each pier. Once the piles were driven, cut off and the block outs grouted, three additional precast segments were to be stacked on top of the first. After sealing the joints between each segment, the interior of the bell was to be filled with tremie concrete.

The revised method of construction proposed by the joint venture, provided essentially the same pier but arrived at by a different means. The new concept consisted of the following basic stages of construction (Fig. 5). The stages are numbered consectively as follows.

1. Prepare pier site by pre-excavating, driving pile, and cutting plie off to grade under water.
2. Pre-assemble reinforcing cage and join reinforcing cage to bell pier form.
3. Position form over piling, set form to grade, and transfer form from floating gantry to spud piling.
4. Seal bottom of form by placing tremie concrete. After allowing seal to cure, dewater form, clean off top of seal, and place bottom reinforcing mat.
5. Place remaining concrete in the dewatered form, allow pier to cure, and strip form.

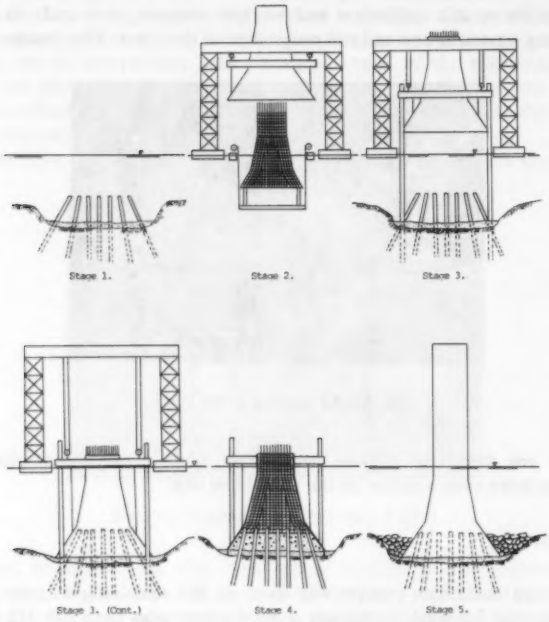

FIG. 5.—Bell Pier Construction Sequence

The remainder of the pier from the water line up was to be cast using conventional forming techniques. These steps were the general concepts developed prior to bid opening. After notice of contract award, work began on converting the concepts into the reality of functional systems and equipment.

The first pieces of equipment to be developed were the two bell pier forms. Due to scheduling requirements and the large variation in size for the required 26 piers, the decision was made to fabricate two forms. The dimensional and functional criteria for the forms were established by the joint venture personnel with the structural design and fabrication being performed by Ewing Records, Inc., of Converse, Texas. The forms were built as single piece cofferdams

designed for a hydrostatic head of 54 ft (17 m) without any internal bracing. The forms, unlike conventional cofferdams because of their sloping faces, were required to resist the hydrostatic loading in both the horizontal and vertical direction.

The form skin was 3/8 in. (10 mm) plate stiffened with 8 × 4 in. (200 × 100 mm) vertical angles. The angles were in turn supported by eleven horizontal trusses up to 7 ft (2 m) in depth, banked perpendicular to the sloping faces of the forms. These trusses formed rings circling the form and were stabilized by twelve vertical trusses along the form perimeter. The larger of the two assembled forms was 83 × 66 ft (25 × 20 m) in plan, stood 62 ft (19 m) high and weighed 450 tons (408 Mg) including support frame (Fig. 6). This weight plus the 100 tons (91 Mg) of reinforcing cage and spud piling brought the total required lift to 550 tons (500 Mg).

The heavy lift requirements of the bell pier construction were met by the design of a 600-ton (550-Mg) capacity catamaran gantry crane. Support of the straddle lift gantry was provided by two barges 104-by-30-by-10 ft (32-by-10-by-3 m) deep, one under each framed tower of the gantry. Vertical clearance under

FIG. 6.—Large Bell Pier Form and Support Frame

the cross beams was 80 ft (25 m) off the water, and horizontal clearance between the barges was 74 ft (23 m). The hoisting function of the gantry was performed by two double drum hydraulic winches rigged to four 12-part 1-1/4-in. (30-mm) diameter wire rope load blocks.

Prior to setting the form it was first necessary to install a 72-ft (22-m) high reinforcing cage inside the 62-ft (19-m) high form. In order to eliminate the two-week cage fabrication time from the pier construction cycle, it was necessary to pre-assemble the cage. This meant the bell-shaped cage had to be installed from the bottom side of the form. Rather than build a gantry crane with a head clearance of more than 130 ft (40 m), it was decided to sink the completed cage 40 ft (12 m) below the river surface, and allow the floating gantry to position the form over the reinforcing cage. Once over the cage the form was lowered and the reinforcing cage raised to meet the form.

The sinking of the cage was performed by building the cage on a steel deck suspended between two pontoons. The steel deck was supported by four cables running to hydraulic winches mounted on the pontoons. The deck was also

fitted with four vertical pipe columns that traveled through roller guides on the support pontoons. The purpose of the pipe and roller guides was to insure vertical alignment of the cage in the 3 ft/sec (1 m/s) river current.

After the cage was fitted up into the form, the reinforcing steel was secured to the face of the form with U-shaped clamps passing around the vertical bars and, in turn, bolted through the skin plate. The skin plate at these locations was backed with a water tight steel pocket to allow removal of the clamps during the pouring of the structural concrete.

Before joining the reinforcing cage and form, 50–100 H piles were driven into the pre-excavated pier site. The pile driving specifications required the piles to be positioned within a tolerance of ±6 in. (±150 mm) at a point approx 45 ft (12 m) below the river surface. This specification was met by installing an accurately placed template at a depth of 40 ft (12 m) and by providing a highly accurate and stable pile driver at the surface.

The template consisted of an adjustable pipe ring positioned 2 ft above the pile cut off point. The ring was supported by a trussed frame held in position by four 24-in. (610-mm) diameter spud piles. Fig. 7 shows the pile driving template

FIG. 7.—Pile Driving Template Prior to Sinking

at the surface prior to positioning on the bottom of the river. The template was positioned by triangulation from shore using two theodolites equipped with infra-red distance meters.

The requirement for an accurate and stable pile driver was met by the pile driving barge "Green Giant." The design of this pile driver insured accurate positioning capability by providing finite articulation of the leads without moving the barge. This was accomplished by using independent hydraulic drives and controls for each of the basic motions of the leads. The leads on this driver are supported on the top rail of a braced cross frame which batters both forward and back of vertical. The bottom of the leads are guided by a second rail which telescopes at the top deck level of the barge. The leads are connected to both of these rails by roller mounted carriages which allow the leads to travel along the rails from one side of the 52-ft (16-m) wide barge to the other in any compound batter configuration up to 4 on 12.

The next step consisted of positioning the form, reinforcing cage and support frame over the required pier location, lowering the entire load 58 ft (18 m)

to the river bottom over the top of the predriven piles and, finally, transferring the entire load from the floating gantry to the support frame and four 36-in. (920-mm) diameter spud piles. It was necessary to use the separate support frame to allow the floating gantry to work with both forms. The separate support frame and spud piles also provided a positive vertical control of the form, free from fluctuations in the river elevation.

The form was suspended from the support frame by four cables connected at midheight on the form, and was fixed into position by four arms jacketed to the support piles. These positioning arms were fitted with eight hydraulic rams, which allowed the entire form to be repositioned horizontally within a 1-ft (300-mm) radius of its initial set position. This feature allowed a precise positioning of the form once the form had been transferred from the floating gantry to the pile supported frame.

During the preliminary planning of the bell pier system, it was feared that as the form was lowered closer to the river bottom, the immense shape of the form would cause the river current to increase sharply at the lower edge of the form and progressively scour away the sand from below the form. To insure that this did not happen, the pier site was over excavated 2–3 ft (1 m) and a layer of 4 in. (100 mm) minus rock was placed. This rock layer also helped prevent contamination of the relatively thin tremie seal with the loose river bottom sand.

An additional precaution taken to insure the integrity of the seal was the installation of a 2-ft (600-mm) deep cutting edge attached to the bottom of the form. It was essential that the outer edges of the form be sealed tight against any water flow. The potential for this flow existed because of the possibility of scour under the edge of the form. The cutting edge eliminated both of these concerns.

After the form was in position, a single centrally located tremie pipe was used to place the 9-ft (3-m) deep 1,300 cu yd (1,000 m^3) seal. The rapid pour rate and on site batching capacity of the floating batch plant helped provide a free flowing tremie around the forest of H piles.

After a cure period of approx 60 hr, the interior of the form was dewatered and the top of the seal was cleaned off. The bottom reinforcing mat and interior void form were then placed. The next step was to place the remaining structural concrete from top of seal to a point 2 ft (600 mm) above normal high water. This 53-ft (16-m) vertical lift was poured in the dry.

The final stage in the sequence of pier construction was the removal of the bell pier form. The forms, except for their top 14 ft (4 m), were one solidly welded unit. The stripping step was the most critical of the entire bell pier operation. The bonded area of form to concrete was over 10,000 sq ft (930 m^2). To our knowledge, there had never been a form of this size stripped in one solid piece.

From a deflection analysis, it was expected that the form would move away from the face of the completed pier. During the dewatered stage of construction, the form was deflected inward under a maximum hydrostatic pressure of approx 21 psi (145 kPa), and the only outward pressure during the casting operation was that created by the fresh concrete which, under a pour rate of 3–5 ft (1–2 m) per hr, produced a maximum pressure of approx 5 psi (35 kPa). Once the pier was cast and water allowed to seep back between the steel skin and

the concrete, the form should have rebounded from the initial deflection.

There were four basic steps taken to insure that the form would come free of the pier. The first was to use a minimum sloping surface of 1 horizontal–6 vertical. In order to meet this criteria, it was necessary to isolate the top 14 ft (4 m) of vertical form and allow this bonded area to break free separately. The second step was to grease the entire surface of the form with a special grease used in the launching of ships. This grease was reapplied after every pier casting. The third step was to provide 140 hydraulic ports on 8-ft (2-m) centers over the interior face of the form. The purpose of these ports was to break the bond between the steel form surface and the face of the completed pier. This was accomplished by inducing water at a pressure of 80 psi (550 kPa) into a smaller cylinder which jacked the face of the form away from the pier in a small localized area. At the same time, the pressurized water was allowed to fill the localized void and progressively enlarge the bond free surface. The fourth and final precaution was to provide excess lifting capacity over that required to lift the dead weight of the form. The floating gantry was designed for a maximum lift of 600 tons (550 Mg). The jacking system on top of the spud piles used for final grade adjustments of the form had a designed lift capacity of 600 tons (550 Mg), and finally two 800-ton (725-Mg) jacks were available for setting on top of the completed pier for jacking against a reaction beam connected to the form. These three lifting systems had a combined capacity of 2,800 tons (2,550 Mg) to lift a form and frame which had a maximum dead weight of only 450 tons (408 Mg).

On the first pier to be stripped, it became evident the excess lifting capacity would not be required. The form lifted free of the pier with less than 10 tons (9 Mg) over the dead weight of the form. The following 25 piers in a like manner were stripped without the use of the excess lift capacity.

The 26 bell-shaped piers were cast over a period of 18.5 months utilizing two bell pier forms. The average cycle time for each pier was 37 calendar days including all weather and mechanical delays. This relatively fast cycle time per pier was attributable in part to three factors. First, the installation time for reinforcing was separated from the cycle time for each pier by prefabricating the reinforcing cage. Second, the multitude of construction steps associated with conventional sheet pile cofferdams were replaced with the single step of setting the form. And, finally, the steps of forming the footing and column were completely eliminated and the two concrete placing steps were combined into one.

In addition to the advantages of reduced construction time, the bell pier system offers the potential for substantial reductions in seal concrete volume. For the I-205 Columbia River Bridge, the bending strength of the seal determined the required seal thickness in the bell piers. For cofferdams with seals designed to provide dead weight against hydrostatic uplift of the whole cofferdam, the bell pier system can greatly reduce the required seal concrete by reducing the total uplift on the cofferdam. This can be accomplished because of the inward sloping faces of the bell pier cofferdam, which reduces the cofferdam's displaced volume in water without reducing the cofferdam's base area or height.

The bell pier system also offers the potential for adaptability to greater water depths. The bell pier system has performed at a depth of 62 ft (19 m) using a rectangular shaped form stiffened with heavy trusses. This same system could

be used to depths in excess of 100 ft (30 m) without the use of heavy stiffening trusses by designing the piers and cofferdam forms with circular cross sections allowing the cofferdam walls to carry all hydrostatic loads in compression.

Conclusions

Both the interlocking H pile cofferdam system and the bell pier cofferdam system proved to be sound methods of pier construction. All 28 marine piers were safely constructed to required specification within the scheduled 1,000 calendar days and within the owner's original estimate. Both systems offer the potential for savings on future marine foundation.

Acknowledgments

The author wishes to acknowledge Roger Brown, Scott Hanson, and Buck Woodward for their assistance in preparing this paper and Arthur Riedel for his encouragement and financial support of the innovative construction methods presented in this paper.

Appendix.—Bibliography

Etheridge, D., "Portland to Have a Second Columbia Bridge," Western Construction, Vol. 53, No. 7, July, 1978, pp. 22–26.

Gordon, C., "$175 Million Bridge Work Across the Columbia Begins," *Pacific Builder & Engineer*, Apr., 7, 1978, pp. 14–16.

Svensen, G., "Innovative Techniques Speed Columbia Bridge Construction," *Construction Contracting*, Oct., 1980, pp. 18–25.

"Giant Bridge Forms Get a Hefty Hydraulic Lift," *Construction Equipment*, Vol. 59, No. 7, pp. 68–73.

"Huge Piers Support Record Span," *Highway and Heavy Construction*, June, 1978, pp. 48–49.

"Innovative Equipment Aids U.S. Bridge Construction," *International Construction*, Apr., 1980, pp. 14–25.

"Special Forms, Equipment Cast River Piers," *Engineering News-Record*, June 22, 1978, pp. 58–59.

"Tight Bids Fall Low on Box Girder Bridge," *Engineering News-Record*, Jan. 18, 1979, p. 38

I-205 Columbia River Bridge: Design and Construction[a]

By Fred P. Blanchard,[1] M. ASCE

Introduction

One of the largest projects on the Interstate Highway System utilizing long-span post-tensioned concrete box girders is the I-205 crossing of the Columbia River (Fig. 1). The on-time, under-budget construction of the monumental structure was made possible by the joint efforts of the owners, the designer, and the contractors.

When type studies of the early 1970s indicated the desirability of constructing the crossing of concrete, based on first cost, maintenance, esthetics, and ease of construction, complete construction documents were prepared on that basis. However, it was realized that the long-span concrete bridge should be designed as it is to be built. Among the construction options were precast versus cast-in-place, high-strength posttensioning bars versus seven-wire strand, post-tensioned shear reinforcement versus nominal bars, and free-cantilever erection versus falsework-supported.

The following article traces the development of the project and the preparation of contract documents, including the now familiar "value engineering incentive clause," which invites the knowledge and expertise a contractor can provide. The article concludes with a description of the construction, which has resulted from the joint effort of the owners, the designers, and the contractors.

Planning and Site Constraints

A second vehicular crossing of the Columbia River near Portland and Vancouver has been planned by the Oregon State Highway Division and the Washington State Highway Commission. The decision to make the crossing a major link in Interstate 205, a circumferential route east of the two cities, was made in

[a]Presented at the April 14–18, 1980, ASCE Convention and Exposition, held at Portland, Oreg.

[1]Project Mgr., Sverdrup & Parcel and Assoc., Inc., St. Louis, Mo.

Note.—Discussion open until April 1, 1982. To extend the closing date one month, a written request must be filed with the Manager of Technical and Professional Publications, ASCE. Manuscript was submitted for review for possible publication on October 29, 1980. This paper is part of the Transportation Engineering Journal of ASCE, Proceedings of the American Society of Civil Engineers, ©ASCE, Vol. 107, No. TE6, November, 1981. ISSN 0569-7891/81/0006-0625/$01.00.

the late '60s after a highway location study was completed. The Oregon State Highway Division at that time commissioned Sverdrup & Parcel (S&P) to develop a type study and prepare construction documents for the crossing, and provide consultation during construction.

The 1960s location study predetermined several features for the crossing, (Fig. 2). First, to meet the selected corridor in Washington and also to clear expansion plans at the Portland International Airport, a curvilinear alignment (0°30′ curve, left, followed by a 1°00′ curve, right) was established. The bridge alignment would be about 7,500 ft (2,286 m) long from a major interchange 2,000 ft (609.6 m) north of the river to an embankment placed on Government Island south of the river's north channel. Second, the vertical alignment was established to provide vertical clearance for two highways and a railroad on the Washington escarpment, 150 ft (45.7 m) of clearance for a 500-ft-wide (152.4-m) ship channel on the north side of the river, and pass under the aircraft approach zone to the airport on the south. This required a north-south drop in elevation of approx 140 ft (42.7 m). And, last, a dual deck-type structure was to be

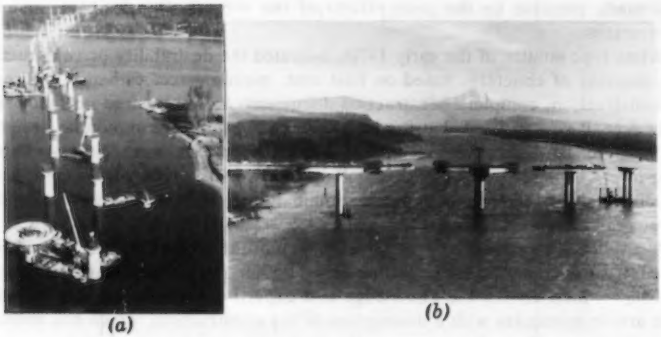

(a) (b)

FIG. 1.—Construction Photographs: (*a*) Bridge Site Looking North, Winter of 1979–1980, Foundation Contract Completed; (*b*) Bridge Site, December, 1980, 300-ft Cantilever, Completed from North Channel Pier

designed. Each 68-ft-wide (20.7-m) structure was to provide for four lanes of traffic with full shoulders. A later decision, after the study, added a 9-ft (2.7-m) recreation trail between the dual structures.

Pile and plate load tests made during S&P's type study showed the geology of the area provides excellent foundation conditions, with dense gravels and river bed sands overlying a dense conglomerate. The gravels or the conglomerate will support spread footings designed for 7 and 10 tons/sq ft (670 and 958 kPa), respectively, and the conglomerate will resist the penetration of 200-ton (1,780-kN) piles. With these design pressures and loads, differential settlements between piers will be of little or no concern.

Seismic activity in the aera was a major concern recognized in the crossing designs. A seismic event measuring about VII on the Modified Mercali scale

occurred in Portland as recently as 1962. Without proper design details, moderate-to-light damage might occur in structures under seismic loadings of this magnitude.

Design.—Using these predetermined design parameters, a number of superstructure and substructure concepts were studied and compared, along with a variety of span arrangements. This study resulted in the decision to develop construction documents for a three-cell post-tensioned concrete box-girder bridge. This section of the paper discusses S&P's designs, and how construction was envisaged.

Two different construction techniques were visualized for building the bridge. A cast-in-place-on-falsework procedure was considered feasible on the Washington shore, where access would be difficult for heavy equipment. A precast

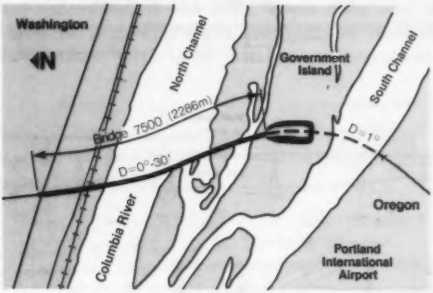

(a)

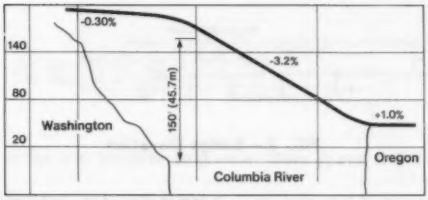

(b)

FIG. 2.—Vicinity Map and Profile

segmental (free cantilever erection) technique was accepted as a viable construction procedure for the remaining part of the bridge over the river, where heavy floating equipment could be mobilized and waterfront casting yard sites were available. Final design commenced on this basis.

The design details were completely developed. All materials were defined, dimensioned, and weighed. The geometry of final in-place concrete was given, tendon paths were completely contoured in three planes, jacking stresses were given, and bar lists were prepared. The design criteria were defined, including all assumed construction loads. A contractor could, therefore, construct the bridge from these designs with minimal engineering input.

The Washington approach spans were designed with three multispan rigid frames Fig. 3. The rigid frame, along with heavy neoprene bumpers and high-strength rod restrainers at the abutment and hinges, is the design answer to seismic activity. This scheme was used throughout the bridge.

The multicell box girders vary in depth from 7–17 ft (2.1–5.2 m) as the spans increase from 140–300 ft (42.7–9.14 m) and are posttensioned end-to-end of units with draped tendons in the webs. The deck is posttensioned in the transverse direction with high-strength rods. Hollow columns vary in diameter from 10–18 ft (3.0–5.5 m), and are supported on spread footings in the dense gravels.

The five-span rigid frame at the navigation channel, designed for precast

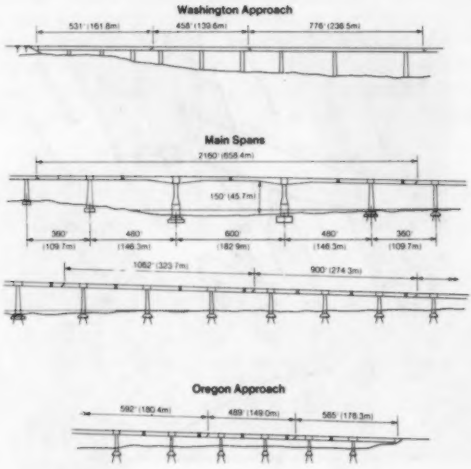

FIG. 3.—Bridge Elevation

segmental posttensioned box girders, is 2,160 ft (658.4 m) in length hinge-to-hinge (Fig. 3). The multicell box girder is 17 ft (5.2 m) deep, haunching parabolically to 32 ft (9.8 m) at the main channel piers. The main channel hollow columns are 22 ft (6.7 m) in diameter, with the foundations seated in the dense conglomerate by means of cofferdam and caisson construction. The solid, 18-ft (5.5-m) flanking columns are founded on a spread footing in the dense conglomerate for the overbank pier and on piling driven to the dense conglomerate for the river pier.

The Oregon approach spans over the river are articulated into five multispan rigid frames with spans varying from 240–360 ft (73.2–109.7 m) (Fig. 3). Box girder depths vary from 12–17 ft (3.7–5.2 m) and are supported by hollow columns varying in diameter from 12–18 ft (3.7–5.5 m). All foundations were to be constructed from nominally reinforced precast-concrete shells resting on piling driven to the dense conglomerate. The shells, after seating, were to be sealed with tremie concrete, and the remaining pier was to be completed in-the-dry.

The substructure contractor changed these plans in ways that will be discussed later.

Pier shapes for the river portion were configured to reduce river bed scour and lessen the increase in backwater from the restriction of the river by the structure. An oval base with its long axis parallel to stream flow was, therefore, used, and the shape was reduced parabolically to a circular section part way up the column.

The superstructure segments, designed with 5,000 psi (34.5 MPa) concrete, vary from 6–16 ft (1.8–4.9 m) in length because of a 250-ton (2,225 kN) weight restriction imposed by the erection equipment available for the work. In addition to nominal reinforcement for temperature, shrinkage, and shear stresses, ducts were installed in the top slab and webs for cantilever erection and final loadings. For segments near the center of the span, ducts were also installed in the bottom slab for tendons to complete the continuity of the rigid frames. The transverse top slab tendons were to be installed and tensioned in the casting

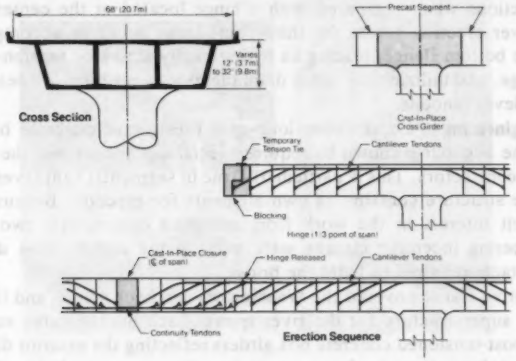

FIG. 4.—Cross-Section and Erection Sequence: Main Spans and Oregon Approach

yard. Posttensioning was to be done with 270 ksi (1,800 MPa) strand and 160 ksi (1,102 MPa) bars.

For design purposes, the precast superstructure was visualized as being matched to the cast-in-place column by erecting the first two segments in position on falsework. The cross girder at the pier could then be formed, reinforced, and cast using the first two segments as end dams. The top slab and web cantilever tendons could then be placed and tensioned after the cross girder concrete had cured. Erection could then continue (Fig. 4).

Since each pier was designed to support one full segment out of balance, the erection sequence then was to continue by raising one segment at a time, epoxy coating the matching surfaces, clamping with a positive force evenly over the contact surfaces, and alternating each side of the column. After each pair of segments was raised, the top slab and web cantilever tendons were to be placed and tensioned before proceeding to the next units. With this

procedure, an experienced erection crew could comfortably average four segments per shift, two on each side of the pier.

The position of the end of the cantilever to be checked at each step against a predetermined position of the segment as the structure increases in length. Corrective measures, including consideration of a cast-in-place section, were to be made if a divergence from that predetermined position was evident. Closure at the center of span was the desired end point of the erection and the checking.

The final segment to complete a span was a cast-in-place section. This was to be done by clamping the ends of two cantilevers into alinement, forming the box, placing reinforcement and ducts, and casting the concrete in place. Continuity tendons were then to be placed in the bottom slab and tensioned. These tendons were designed for positive movement from superimposed dead-loads, live loads, impact, and redistribution of dead load from creep and shrinkage.

The design provided for articulating the structure, using hinges at the approx one-third point of span for the continuous rigid frames. The third-point was selected since it minimized any future discontinuity of the riding surface from creep deflections when compared with a hinge located at the center of span. The cantilever erection across the third-point hinge could be accomplished by blocking the bottom flange, placing an hydraulically activated tension-tie across the top flange, and utilizing the hinge diaphragms as a position for dead anchors of the cantilever tendons.

Value Engineering.—Constructing long-span prestressed-concrete box-girders was from the beginning known to require special equipment and the expertise of qualified contractors. This is particularly true in segmental cantilever erection, in which the structure contains its own elements for erection. Because of this, and to solicit interest in the work from qualified contractors, two different value-engineering incentive clauses were used in the construction documents for the contracts required to build the bridge.

One incentive clause covered the Washington approach spans, and the second covered the superstructure for the river spans. Each limited value engineering redesign to post-tensioned concrete box girders reflecting the exterior dimensions of the box girders given in the construction documents, and the river-spans clause also fixed the span arrangement.

A contractor bidding on the Washington approach had the option of proposing to construct the bridge as designed or constructing a bridge of his choice limited in scope by the value engineering clause. The cost for state review of any alternate proposal was to be included in the contractor's bid prices.

River span proposals, however, had to be based on the contract documents, with value engineering then accepted in a two-step procedure. The contractor could submit a written description of the value engineering revisions he wished to make along with any anticipated cost savings. After review, if the revisions were determined to be acceptable by the State and its consultant, S&P, the contractor could develop and submit the revised designs for review. The cost of the review was to be reimbursed from the construction cost savings, and any remaining funds were to be divided equally between the state and the contractor.

Construction

Three prime contracts have been let for constructing the bridge. These covered

the Washington approach spans; the river spans substructure, and the river spans superstructure. The Washington approach spans contractor submitted an alternative to the design plans. The alternative was accepted. That part of the bridge was cast in place on falsework, span by span, using slip forms. The span arrangement was revised, and a corresponding adjustment was made in the box girder depth. The State of Washington through its Highway Commission took over the administration of that contract after final design.

The river spans substructure contractor made several revisions in the design plans. The caisson for the south main channel pier was replaced by cofferdam and seal-course construction. This was made possible by using Arbed piles, which are an H-Section with interlocks on the flange tips and can withstand higher pressures for greater depths than standard sheet-pile sections. The extensive base, a seal course in lieu of the caisson, required mobilizing sufficient concrete plant and equipment to pour about 14,000 cu yds (10,719 m^3) of tremie

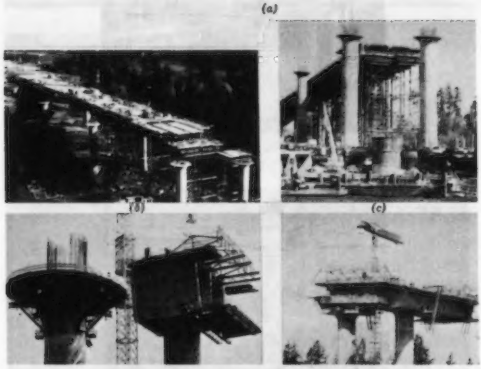

FIG. 5.—Main-Span Construction: Cast-in-Place Free-Cantilever Construction: (*a*) Washington Approach Spans Cast-in-Place on False Work; (*b*) Erection of Form Traveler; (*c*) Cantilever at North Pier

concrete at an average rate of 207 cu yds (158.3 m^3) per hr for over 60 hr (a major construction feat in itself). In addition, when the river spans design was divided into substructure and superstructure contracts (a benefit in funding), the advantage of the precast-shell construction technique was lost for the remaining pier bases. The contractor instead used a segmental-steel form which reflected the exterior shape of the precast shells and was adjustable in size for the various pier bases.

Shortly after the contract for the river spans was awarded, the contractor requested two design revisions under the value engineering incentive clause. These were to eliminate one web from the cross section and to move the hinges to the center from the third-point of span. A third revision, not included under the value engineering clause but which was considered a permissible alternative, was to use cast-in-place segmental free cantilever erection for the navigation span rather than precast techniques. These revisions were accepted, and S&P

acted as the reviewing agency under its agreement with the Oregon State Highway Division.

Construction of the rigid frame for the navigation spans began on the north end with the casting of the cross girder at the northbound roadway flanking pier, (Figs. 5 and 6). When this was completed, the moveable forms were erected for the cantilevering sequence. To be competitive in this phase, the contractor has to realize a 24- to 48-hour turnaround on each segment, and this requires partially prestressing concrete which was in various stages of curing. Particular attention to the location of the ends of each section to ensure closure at the center of span had to be made in this technique, since the shrinkage deflections are much greater than in the precast method.

Construction of the Oregon approach spans began almost simultaneously in

(a)

(b)

FIG. 6.—Main-Span Construction: (*a*) Northbound 300 Ft, Cantilever Complete Southbound under Construction, Washington Approach in Background; (*b*) River Traffic Unimpeded

the casting yard and on the southernmost pier, (Fig. 7). The circular section of the southernmost pier column was cast in place, after which the cross girder was constructed. The pier was then made ready to receive the precast segments from the casting yard by installing the erection equipment.

A short-line match-cast technique was used in the casting yard. Each segment as it was cast was moved forward onto a platform that could be rotated horizontally and vertically to duplicate the alinement of the structure. The next segment was then cast against it to achieve a workable interface. After removal from the casting bed, the segments were cured in a storage yard while awaiting erection in the bridge.

The contractor chose to interface the cast-in-place cross girders and the precast elements by using the completed cross girder and the first precast segment

as end dams in a 1.5-ft (46 cm) cast-in-place segment.

The construction was generally on schedule and under budget. Monthly on-site meetings were held to discuss and anticipate any problems that might affect on-time completion of the project in mid-1982.

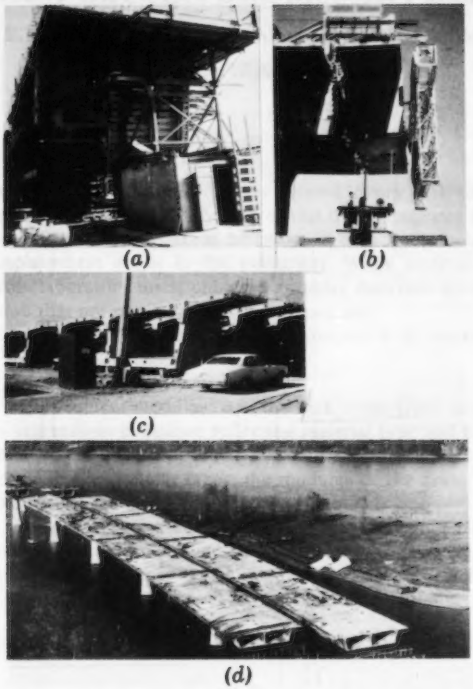

FIG. 7.—Oregon Approach: Precast Segmental Free-Cantilever Erection: (*a*) Short-Line Casting Bed; (*b*) Segment Erection; (*c*) Storage Yard; (*d*) Three Spans Prepared for Continuity Segment

S&P's experience with the design and construction of this bridge, and with others now in the design phase, indicates that long-span concrete bridges are a viable alternative when considering the selection of a bridge concept for the solution of a particular problem.

Equivalent Granular Base Moduli: Prediction

By Brian E. Smith,[1] A. M. ASCE and Matthew W. Witczak,[2] M. ASCE

(Reviewed by the Highway Division)

Introduction

In the past several years, the use of elastic layered theory in flexible pavement design has significantly increased. The use of this theory requires that the layer moduli, Poisson's Ratio, and thickness be known in order to compute the stress, strain, and displacement states in the pavement. While material moduli can be obtained from laboratory tests, unbound granular materials have been found to exhibit moduli that are nonlinear or stress dependent.

One widely used form of expressing this nonlinearity is by use of

$$M_R = K_1 \theta^{K_2} \quad (1)$$

in which M_R = the resilient modulus; θ = the bulk stress (first stress invariant) and K_1, K_2 = regressions constants reflecting material type and physical state. Because the modulus is related to the stress state and the state of stress varies in all directions within a granular layer; the modulus of the granular base must likewise change with these directions.

As a result, various agencies and researchers have developed techniques to incorporate some aspect of this nonlinearity directly into elastic layered solutions. In general, these procedures can be grouped into: (1) Empirical Relationships; (2) iterative Layered Approach; and (3) finite Element Solutions.

Review of Existing Approaches

At present, there are several simplified approaches available for estimating the modulus of an unbound granular material within a flexible highway pavement. They have been developed by the Shell Oil Company, Kentucky Highway Department and the U.S. Army Corps of Engineers. Each of these procedures use the subgrade modulus as a basis for the granular material estimation.

The Shell Oil Company procedure for predicting the modulus of an unbound granular layer was developed by Dorman and Metcalf (8), based upon the

[1] Asst. Project Engr., Soil Testing Services, Fairfax, Va.
[2] Prof., Dept. of Civ. Engrg., Univ. of Maryland, College Park, Md.

Note.—Discussion open until April 1, 1982. To extend the closing date one month, a written request must be filed with the Manager of Technical and Professional Publications, ASCE. Manuscript was submitted for review for possible publication on October 9, 1980. This paper is part of the Transportation Engineering Journal of ASCE, Proceedings of the American Society of Civil Engineers, ©ASCE, Vol. 107, No. TE6, November, 1981. ISSN 0569-7891/81/0006-0635/$01.00.

investigations of Heukelom and Klomp (12). Dorman and Metcalf assumed that the effective modulus of the combined thickness of base and subbase course was in the range of 2–4 times that of the subgrade modulus. Edwards and Valkering (9) later confirmed this assumption with the results of vibratory tests. They found that the modulus of the unbound layer (E_2) was dependent on the modulus of the subgrade (E_3), and the modular ratio (E_2/E_3) was approximately equal to 2. Only when thick granular layers were placed on weak subgrades did the modular ratio tend to be higher and reach values near 5. A practical design modular ratio of 3 to 4 was suggested to account for the difficulty of achieving high compaction states in the field over weak subgrades. Using this information and correlating results to give reasonable agreement to CBR (California Bearing Ratio) design curves, an expression relating to unbound base thickness (h_2) to the modular ratio ($R = E_2/E_3$) was developed as:

$$R = 0.58\,(h_2)^{0.45} \quad (2)$$

In this equation, h_2 is expressed in millimeters.

Deen, Southgate, and Havens (7) have presented an approach for estimating unbound granular moduli for the Kentucky Highway Department. In this technique, the 1,500 CBR relationship for the subgrade modulus, developed by Heukelom and Foster (11), was used along with the Shell Oil concept that the modular ratio (E_2/E_3) was a function of granular base thickness. By use of the Chevron elastic layered program, the effect of the asphalt layer modulus was incorporated into the prediction of the modular ratio. Because Heukelom and Klomp had found that the ratio had a range between 2 and 4, Deen and Southgate selected a modular ratio of 2.8 to occur at a CBR = 7 for all E_1 values. It was further assumed that the modular ratio would equal one under the conditions of $E_1 = E_2 = E_3$. Using these assumptions, along with a linear log-log relationship between subgrade CBR and modular ratio, the Kentucky procedure is shown in Fig. 1.

The U.S. Army Corps of Engineers have developed and utilized two general estimation techniques to predict the equivalent modulus of a granular layer. One of these procedures was developed for airfield loading conditions by Barker and Brabston (2). For highways, Brabston, Barker, and Harvey (3) modified the airfield analysis to account for typical highway loads. Based on a nonlinear analysis of sublayers within a granular layer, it was concluded that the modular ratio could be related to material quality and the sublayer thickness. The suggested modular ratio relationship applicable for highway loading conditions is shown in Fig. 2.

One direct way for incorporating nonlinear material behaving directly into linear layered models is through use of an iterative stress-modulus approach. Sublayers within the nonlinear layer are developed and assumed moduli values initially assigned to each. Layered solutions are then performed and states of stress within each sublayer are computed. These stress results are then substituted into the modulus expression to obtain predicted moduli values. Comparisons are then formulated between the assumed and predicted sublayer moduli. Iteration is pursued until a tolerable error difference between these moduli are reached. The development of a computerized solution to this process is relatively straight forward. One such available program utilizing this approach is PDMAP, developed for NCHRP 1-10B (10).

The only disadvantage associated with this approach is the fact that stress dependency can only be accounted for in a vertical direction. That is, the linear

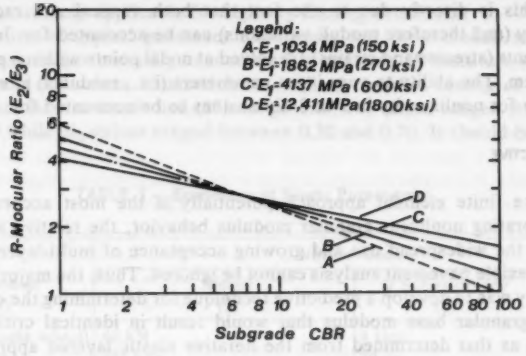

FIG. 1.—Modular Ratio Versus Subgrade CBR (Kentucky Highway Procedure)

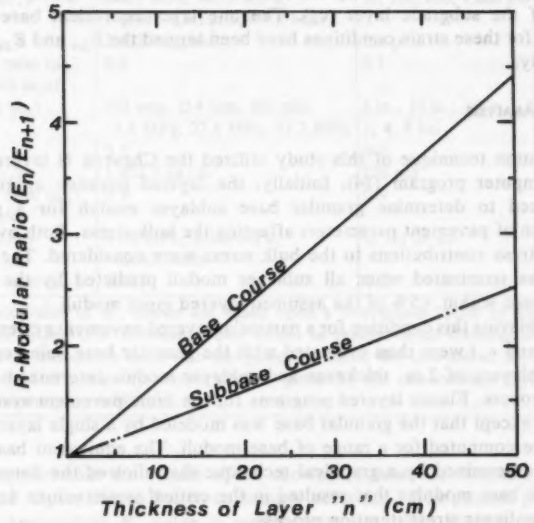

FIG. 2.—Modular Ratio Versus Thickness of Layer "*n*" (USACE Highway Procedure)

layered assumption of homogeneity and isotropy within the *i*th layer must be satisfied. While this approach may tend to agree with peak stresses, strains and displacements, one cannot expect to complete agreement with stress, strain

or displacement basins because of the radial nonlinearity within a given layer.

From a theoretical viewpoint, the use of finite element solutions affords the greatest probability of precisely defining states of stress within a pavement system. This is directly due to the fact that both vertical and radial stress dependency (and therefore moduli variations) can be accounted for. In essence, displacements (stresses and strains) are solved at nodal points within a predefined mesh system. The ability to vary input parameters (i.e., modulus) at each nodal point allow for nonlinearity in 2 or 3 dimensions to be accounted for.

Study Objective

While the finite element approach potentially is the most accurate model for incorporating nonlinear granular modulus behavior, the relative simplicity, along with the widespread use and growing acceptance of multi-layered elastic theory in flexible pavement analysis cannot be ignored. Thus, the major objective of this study was to develop a predictive technique for determining the equivalent one layer granular base modulus that would result in identical critical strain parameters as that determined from the iterative elastic layered approach that directly accounts for the nonlinear granular base behavior. Two critical strain parameters were selected. They were the maximum principal tensile strain at the bottom of the asphaltic layer (ϵ_t) and the vertical compressive strain at the top of the subgrade layer (ϵ_v). The one layer equivalent base modulus developed for these strain conditions have been termed the E_{2et} and E_{2ev} moduli, respectively.

Method of Analysis

The solution technique of this study utilized the Chevron N layered elastic theory computer program (14). Initially, the layered iteration approach was accomplished to determine granular base sublayer moduli for a particular combination of pavement parameters affecting the bulk stress. Both overburden and load stress contributions to the bulk stress were considered. The iteration process was terminated when all sublayer moduli predicted by the modulus equation were within ±5% of the assumed layered input moduli.

Upon achieving this condition for a particular layered pavement system, critical strains (ϵ_t and ϵ_v) were then evaluated with the granular base being comprised of "n" sublayers of 2 in. thickness and sublayer moduli determined from the iteration process. Elastic layered programs for the same pavement system were then rerun except that the granular base was modeled by a single layer. Critical strains were computed for a range of base moduli. The equivalent base moduli were then determined by a graphical technique that allowed the determination of a unique base modulus that resulted in the critical strain values determined from the nonlinear stress iteration process.

As a result of this procedure, unique E_{2ev} and E_{2et} values were determined for a particular function of h_1, h_2, E_1, E_3, K_1, and K_2 where h_1 is the thickness of the asphalt concrete layer. Multiple regression techniques were then utilized to obtain predictive equations for the equivalent base moduli as functions of the variables considered in the study.

In the computer analysis, the load parameters were held constant. A 40-kN

(9-kip) single wheel load with 483 kPa (70 psi) pressure was assumed to approximate the effects of an 80-kN (18-kip) single axle load. Because the results are directly dependent upon the load conditions assumed, it should be noted that the results of this study are only applicable for highway loading conditions.

The selection of typical pavement thicknesses and layer moduli was based upon common ranges normally encountered in practice. A literature review of typical K_1 and K_2 values obtained from resilient modulus testing of unbound granular material was conducted (17). In general, K_1 values ranged from about 1,500–8,000 while K_2 values ranged between 0.30 and 0.70. It should be pointed

TABLE 1.—Summary of Study Parameters

Parameter (1)	Values Used: Metric (2)	Values Used: U.S. customary (3)	Levels (4)
Tire load (single wheel)	40 kN	9 kips	1
Tire pressure	483 kPa	70 psi	1
Asphalt layer			
Thickness (h_1)	102 mm; 203 mm; 305 mm	4 in.; 8 in.; 12 in.	3
Modulus (E_1)	344.7 MPa; 689.5 MPa; 3,447.4 MPa; 6,894.8 MPa	50; 100; 500; 1,000 ksi	4
Density (γ_1)	2,402.8 kg/m^3	150 pcf	1
Poisson's ratio (μ_1)	0.3	0.3	1
Granular base layer			
Thickness (h_2)	102 mm; 254 mm; 402 mm	4 in.; 10 in.; 16 in.	3
K_1[a]	13.8 MPa; 27.6 MPa; 55.2 MPa	2; 4; 8 ksi	3
K_2	0.5	0.5	1
Density (γ_2)	1,922.2 kg/m^3	120 pcf	1
Poisson's ratio (μ_2)	0.4	0.4	1
Subgrade layer			
Modulus (E_3)	41.4 MPa; 103.4 MPa; 206.8 MPa	6; 15; 30 ksi	3
Poisson's ratio (μ_3)	0.45	0.45	1

[a]The metric value of K_1 shown are based upon a conversion factor of 6.89 MPa = 1 ksi applied to the U.S. customary unit value. In reality, since the original research work used U.S. customary units with the power equation, the true metric K_1 equivalent is a function of the slope (power) value K_2 given by the relationship: K_1(metric) = K_1(U.S. Customary) $\times$ $6.89^{(1-K_2)}$.

out to the reader that the values of K_1 shown are those developed for power equations of M_R in United States customary units (i.e., 0 in pounds per square inch). The appropriate K_1 value in metric units (i.e., 0 in kilopascals) cannot be obtained unless a specific value of the K_2 constant (power) is known.

Because of the rather small range in K_2 values plus the necessity to keep the problem parameter matrix as manageable as possible, only one value of K_2 (K_2 = 0.50) was used in the study. Table 1 summarizes the factors, levels and values used in the equivalent base modulus study. A total of 324 E_{2et} and 324 E_{2ev} values were determined.

Results

Comparison of Equivalent Base Modulus Types.—For each of the 324 problems analyzed, both E_{2ev} and E_{2et} base modulus values were found. This allowed for a general comparison to be conducted between the two equivalent base modulus types. From this study, the following conclusions were obtained:

1. In general, the E_{2et} was always greater than or equal to the E_{2ev} value.
2. The ratio of the equivalent base modulus for tensile strain (E_{2et}) to the equivalent base modulus for vertical strain (E_{2ev}) increased as the K_1 (base quality) and h_2 (granular base thickness) increased and the h_1 (asphaltic surface thickness) and E_1 (asphaltic layer modulus) decreased.

Thus, as a general overall conclusion, it can be noted that the greatest differences in equivalent base moduli will occur for typical flexible pavement cross sections (i.e., flexible pavements with relatively thin wearing surfaces but high quality thick granular base layers).

This conclusion can be logically supported by understanding the general distribution of granular base sublayer moduli with depth throughout the entire granular layer. For the "classical" flexible pavement structure, the modulus of the granular sublayer at the top of the base is much higher than at the bottom of the base course because of the rapid attenuation of the bulk stress with depth. Because it is a known fact that the tensile strain in the asphaltic layer is extremely sensitive to the modular ratio of the asphalt layer to the layer below, it appears that the asphalt strain is controlled by an equivalent modular ratio reflecting a granular sublayer near the top of the granular layer itself. In contrast, the criteria for the equivalent vertical modulus (E_{2ev}) is based on the strain at the top of the subgrade. Since the strain is dependent on the stress at this location and the stress is distributed throughout the entire granular layer, the equivalent modulus more nearly reflects the average modulus of the entire base layer.

To illustrate the general range of ratios found between the E_{2et} and E_{2ev} values for the study; ratio magnitudes of 2.74, 1.92, and 1.47 are noted for subgrade moduli of E_3 = 41.4 MPa, 103.4 MPa, and 206.8 MPa (6 ksi, 15 ksi, and 30 ksi), respectively for a classical flexible pavement structure: h_1 = 100 mm (4 in.); E_1 = 344.7 MPa (50 ksi); h_2 = 402 mm (16 in.); and K_1 = 8,000 psi (U.S. units only). In contrast to these ratios, values of E_{2et}–E_{2ev} of 1.01, 1.00, and 0.98 were found for similar subgrade moduli and pavement layer conditions of h_1 = 305 mm (12 in.); E_1 = 6,894.8 MPa (1,000 ksi), h_2 = 102 mm (4 in.) and K_1 = 2,000 psi (U.S. units only).

Development of Predictive Equations.—As previously noted, the previous portion of this study allowed for both E_{2et} and E_{2ev} values to be obtained for a particular combination of h_1; E_1, h_2, E_3, and K_1. Such results allowed for the development of predictive mathematical equations for the E_{2e} values in terms of the parameters noted by multiple regression techniques. The details of this study may be found in Ref. 17.

From this analysis, it was found that the highest correlation coefficients were obtained with full logarithmic models. In addition, the use of partial regression models, holding the least significant variable constant, greatly increased correla-

tion and at the same time greatly reduced the residual error (predicted minus actual modulus) of all regressions.

In this study, the least significant variable in the total log model was found to be h_2 (granular base thickness). Thus, partial regression models were developed with this value constant. In general, this allowed the relative residual error to be decreased from about 69% of the data points being less than a ±10% error (total model) to about 82% of the data points being less than ±10% relative error.

The regression coefficients for both the total and partial models, along with

TABLE 2.—Summary of Regression Models—Total Model (h_2 Included)

$$\text{Log } E_{2e} = A_0 + A_1 \text{ Log } h_1 + A_2 \text{ Log } h_2 + A_3 \text{ Log } E_1 + A_4 \text{ Log } E_3 + A_5 \text{ Log } K_1$$

Variable (1)		Value of Coefficients	
		E_{2et} analysis (2)	E_{2ev} analysis (3)
Constant	A_0	1.079	0.959
h_1	A_1	−0.511	−0.430
h_2	A_2	−0.008	−0.073
E_1	A_3	−0.155	−0.122
E_3	A_4	+0.279	+0.294
K_1	A_5	+0.888	+0.848
		($R^2 = 0.958$)	($R^2 = 0.942$)

TABLE 3.—Summary of Regression Models—Partial Model (Separate h_2)

$$\text{Log } E_{2e} = B_0 + B_1 \text{ Log } h_1 + B_2 \text{ Log } E_1 + B_3 \text{ Log } E_3 + B_4 \text{ Log } K_1$$

	Value of Coefficients					
	E_{2et} analysis			E_{2ev} analysis		
(*a*) Variable	$h_2 = 4.0$	$h_2 = 10$	$h_2 = 16$	$h_2 = 4$	$h_2 = 10$	$h_2 = 16$
Constant	0.912	1.111	1.194	0.884	0.900	0.877
h_1	−0.481	−0.525	−0.527	−0.436	−0.417	−0.426
E_1	−0.131	−0.157	−0.176	−0.116	−0.128	−0.121
E_3	+0.400	+0.265	+0.172	+0.373	+0.298	+0.216
K_1	+0.751	+0.900	+1.013	+0.755	+0.844	+0.933
	($R^2 = 0.961$)	($R^2 = 0.983$)	($R^2 = 0.987$)	($R^2 = 0.955$)	($R^2 = 0.944$)	($R_2 = 0.958$)

correlation coefficients, are shown in Table 2 and Table 3 for each type of equivalent granular base modulus. The resulting high R^2 values shown, along with the low residuals from the predictive equations, result in an extremely accurate but simple technique for evaluating the E_{2e} values. When the partial model is used, it is obvious that the final value (for any particular h_2) must be found by interpolation (or extrapolation of results) found by the h_2 = 102 mm, 254 mm, and 402 mm (4 in., 10 in., and 16 in.) models.

Nomographic Solutions.—Figs. 3–8 present the nomographic solutions for the partial model regression equations shown in Table 2. Figs. 3–5 are for the E_{2et} value while Figs. 6–8 are to be used for the E_{2ev} modulus. Fig. 9 presents

a set of instructions for the use of the nomographs. Details leading to the development and construction of these nomographs may be found in Ref. 17.

Significance of Variables.—In the multiple regression analysis conducted, correlation matrices between the predictor variables were determined. Since a complete factorial analysis was conducted, there was no intercorrelation between the predictor variables. This leads to the fact that the percentage of the variation

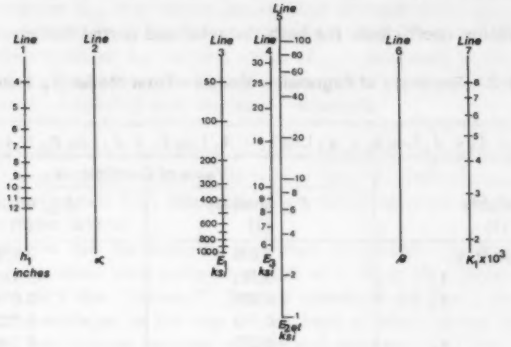

FIG. 3.—Equivalent Tangential Modulus Nomograph (h_2 = 4 in.)

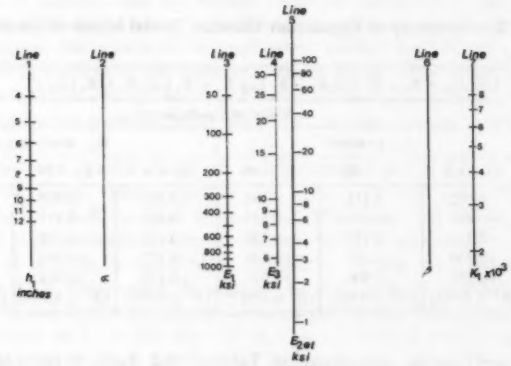

FIG. 4.—Equivalent Tangential Modulus Nomograph (h_2 = 10 in.)

explained by each of the variables is simply the square of the correlation. Table 4 is a summary of the significance of each variable for the E_{2e} moduli computed by the partial models.

As can be observed, the most significant variable affecting the E_{2e} value is the K_1 parameter (quality of base course material). This is quite logical as this parameter plays a significant role in determining the nonlinear sublayer

modulus for any given bulk stress value. It can be also seen that as the thickness of the granular layer increases, the significance of the subgrade modulus decreases substantially. In contrast, the effect of the thickness and moduli of the upper pavement layer remain relatively constant.

Example Problem Solution.—To illustrate the use of the study results, an example problem is presented. In this problem, it is described to determine the equivalent one layer base modulus resulting in an equal vertical subgrade

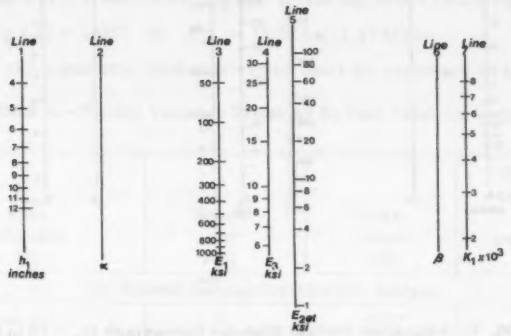

FIG. 5.—Equivalent Tangential Modulus Nomograph (h_2 = 16 in.)

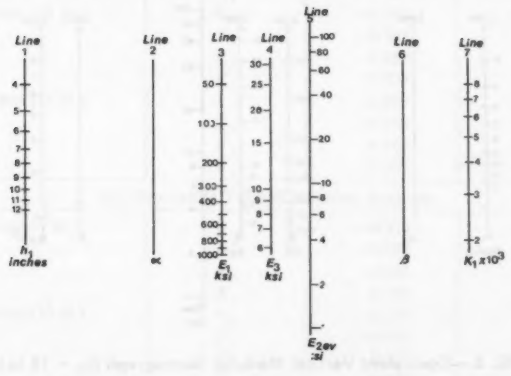

FIG. 6.—Equivalent Vertical Modulus Nomograph (h_2 = 4 in.)

strain for a layered pavement system comprised of the following:

Layer	Material	Thickness	Modulus
1	Ash. Concrete	6″ (150 mm)	300 ksi (43.4 MPa)
2	Gran. Base	10″ (250 mm)	* $M_R = 4500\ \theta^{0.5}$
3	Subgrade	—	7 ksi (1.01 MPa)

•Non-Linear modulus relationship obtained from the Resilient modulus lab test.

If the total model is selected for use, the solution is obtained using the

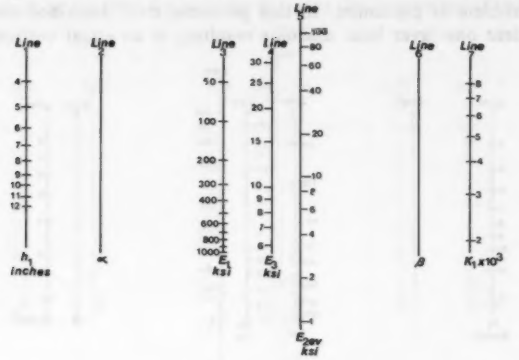

FIG. 7.—Equivalent Vertical Modulus Nomograph (h_2 = 10 in.)

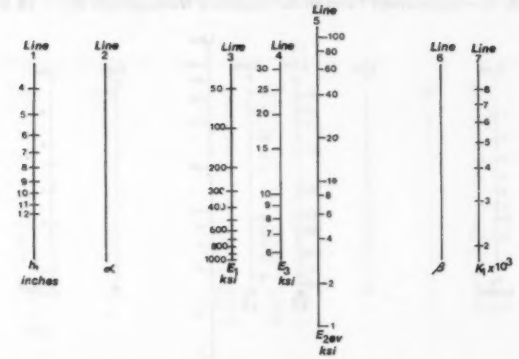

FIG. 8.—Equivalent Vertical Modulus Nomograph (h_2 = 16 in.)

appropriate equation coefficients from Table 2 (Total Model; E_{2ev}).

Therefore:

$$\text{Log } E_{2ev} = 0.959 - (0.430 \log h_1) - 0.073 \log h_2 - (0.122 \log E_1$$
$$+ (0.294 \log E_3 + (0.848 \log K_1)$$
$$= 0.959 - 0.430 \log 6) - (0.073 \log 10) - (0.122 \log 300) + (0.294 \log 7)$$
$$+ (0.848 \log 4.5) = 1.052 \quad \text{or} \quad E_{2ev} = 11.27 \text{ ksi (1.63 MPa)}$$

If the partial model (Table 2) was selected for use, the solution normally would have to be interpolated for the base thickness (h_2) value. However, since the given $h_2 = 10$ in. layer is one of the three h_2 levels used in the partial model, the interpolation is not required for this solution. The E_{2ev} value is:

$$\log E_{2ev} = +0.900 - (4.17 \log h_1) - (0.128 \log E_1) + (0.298 \log E_3)$$

$$+ (0.844 \log K_1) = 0.900 - (4.17 \log 6) - (0.128 \log 300) + (0.298 \log 7)$$

$$+ (0.844 \log 4.5) = 1.062 \quad \text{or} \quad E_{2ev} = 11.52 \text{ ksi (1.67 MPa)}$$

In using the equations, thickness values must be expressed in inches while

TABLE 4.—Percent Variation Explained By Each Predictor Variable

Base thickness (1)	Parameter (2)	Correlation (3)	Variation explained, as a percentage (4)
(*a*) Equivalent Tangential Modulus Analysis			
102 mm (4 in.)	h_1	−0.377	14.2
	E_1	−0.271	7.3
	E_3	0.455	20.7
	K_1	0.733	53.7
254 mm (10 in.)	h_1	−0.382	14.6
	E_1	−0.303	9.2
	E_3	0.280	7.8
	K_1	0.817	66.7
402 mm (16 in.)	h_1	−0.357	12.7
	E_1	−0.316	10.0
	E_3	0.169	2.9
	K_1	0.855	73.1
(*b*) Equivalent Vertical Modulus Analysis			
102 mm (4 in.)	h_1	−0.328	10.6
	E_1	−0.289	8.1
	E_3	0.481	23.1
	K_1	0.760	57.8
254 mm (10 in.)	h_1	−0.319	10.2
	E_1	−0.283	8.0
	E_3	0.320	10.2
	K_1	0.822	67.6
402 mm (16 in.)	h_1	−0.341	11.6
	E_1	−0.239	5.7
	E_3	0.221	4.9
	K_1	0.875	76.6

all moduli and K_1 factor for the granular material are expressed in kips per square inch units.

The nomograph shown in Fig. 7 for the partial model can also be used to

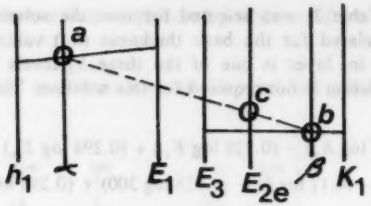

FIG. 9.—Instructions for Nomograph Use

obtain the approximate modulus (allowing for normal nomographic inaccuracies). This solution would correspond to the $E_{2ev} = 11.52$ ksi solution obtained by the equation.

Application of Results

The significance of the study conclusions (equations) have several important applications. First, the procedure presented can offer a significant savings in computer time and cost by not having to conduct detailed non-linear computerized solutions for normal elastic layered stress-strain-displacement problems. This approach has already been employed by the senior author within a flexible pavement design computer program (DAMA) for The Asphalt Institute used in the development of their forthcoming revised highway design manual MS-1. It is estimated that computer cost savings (with little, if any, loss in accuracy) were in the thousands of dollars for the number of computer solutions required for this study.

The analytical solution also provides a rapid solution capability for engineers to determine critical layer stress and strain values in three layer systems without the necessity of a computerized solution but yet incorporating the nonlinear behavior of granular material directly into the solution. This can be accomplished, for example, by using the results of this study directly with tabular/graphical stress and strain solutions currently available (e.g., Three Layer Solution of Jones/Peattie and Acum/Fox).

Finally, the solution technique can be utilized by the engineer to obtain important information relative to the influence of all pavement variables (layer thickness, environmental effects of temperature and moisture upon moduli, granular material quality as measured by the laboratory resilient moduli test) upon the probable performance of flexible pavement systems throughout various periods of the year.

Comparison to Existing Prediction Methods

Table 5 is a summary of the variables considered by three existing procedures noted as well as the technique developed by this study. It can be seen that none of the existing methods incorporates all of the variables considered by

TABLE 5.—Comparison of Predictor Variables Used by Agency

	Factors Influencing Modular Ratio (R)				
Agency (1)	h_1-asphalt thickness (2)	E_1-asphalt modulus (3)	h_2-granular base thickness (4)	K_1- or Q_b-base quality (5)	E_3-subgrade modulus (6)
U.S.A. Corps of Engineers	NA	NA	(x)	(x)	(x)
Kentucky Highway	NA	(x)	NA	NA	(x)
Shell Oil	NA	NA	(x)	NA	NA
University of Maryland	(x)	(x)	(x)	(x)	(x)

Note: Modular Ratio (R) = E(Base)/E(Subgrade).

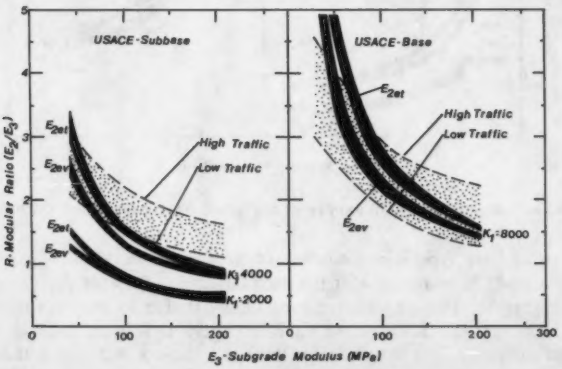

FIG. 10.—Comparison of University of Maryland Results to USACE Procedure

the study presented. It can also be observed that there is a broad lack of agreement between the existing methods as to what variables are indeed significant and also how they affect the modular ratio value, R. For example, in the USACE procedure, an *increase* in aggregate quality results in an *increase* in the R value. The R value, however, is *independent* of quality (base type) in the Kentucky

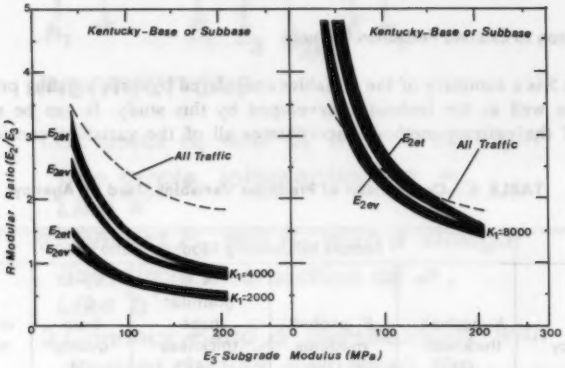

FIG. 11.—Comparison of University of Maryland Results to Kentucky Procedure

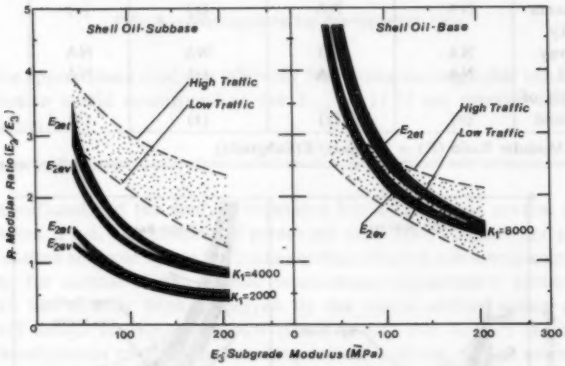

FIG. 12.—Comparison of University of Maryland Results to Shell Oil Procedure

procedure as base type is not considered as a variable. Finally, the Shell Oil procedure leads to a *decrease* in the modular ratio, R, with the use of higher quality aggregate. This apparent inconsistency is due to the fact that as base quality is increased, the required base thickness is less to achieve the same structural adequacy. It is this decrease in base thickness that causes the decrease in the modular ratio.

Because of the multitude of factors considered by the study developed in

this report relative to the variables considered and differences between existing procedures, it is quite difficult to truly assess and compare computed ratio values by the proposed technique to the other methods for all variables. However, in order to obtain a general idea of how these ratios compare to the existing methods, an analysis was conducted using a typical spectrum of highway pavement design cross sections as a standard. The pavement sections were developed using The Asphalt Institute's MS-1 design procedure as the structural guide (19). In this analysis, designs were generated for: three levels of subgrade support (see Table 1); two levels of traffic (50 and 5000 DTN-design traffic number); one level of asphalt surface thickness h_1 = 102 mm (4 in.) and two levels of granular base quality (TAI "High Quality" and TAI "Low Quality" base with recommended substitution ratios of 2.0 and 2.7, respectively).

For each pavement cross section (combination of above variables), the modular ratio was determined with each existing procedure. In addition, the modular ratio from the study procedure was calculated using the following considerations: (1) Total Regression Model; (2) E_1 = 1,034.1 MPa (150 ksi); (3) K_1 = 2,000 and 4,000—low quality base; and (4) K_1 = 8,000—high quality base. The results of this study are shown graphically in Figs. 10, 11, and 12 comparing the modular ratios generated by the study procedure to the USACE, Kentucky, and Shell Oil methods.

An examination of these figures reveals that all of the procedures show very similar trends as to the significant influence of R with subgrade modulus, E_3. The plots also clearly demonstrate the general magnitude of difference in base modulus between the equivalent tangential and vertical modulus values (E_{2et} and E_{2ev}) generated from the results of this study. In general, the difference is not large and is increased as the base quality (K_1 factor) is increased.

In general, threre appears to be a very excellent agreement between the procedure developed in this report to all existing procedures for the high quality base (K_1 = 8,000) conditions. In practice, one would probably obtain even better correlations at low subgrade modulus values due to the difficulty in actually obtaining high densities on weak subgrade supports. This phenomena would tend to decrease the effective K_1 value over the soft soil condition.

The comparison of results is not as agreeable for poorer quality base materials. In general, the existing procedures yield R values in excess of those determined by the procedure developed in this study. Another significant difference that can be observed between the method of this report and the USACE and Shell Oil procedures is the relative influence of traffic (in reality, base thickness) upon the modular ratio. For the proposed procedure, the influence of traffic on base thickness is very minor as evidenced by the narrow band widths on each figure. This is in agreement with the fact that the base thickness was one of the least significant variables found by the statistical analysis of the multiple regression equations. In contrast, the two existing procedures show a significant change in R due to traffic levels. This is directly due to the primary influence of base thickness upon the modular ratio value.

Conclusions

In this study, a simple, practical, and accurate technique has been developed to predict the equivalent granular layer modulus from nonlinear material charac-

terization parameters. The results indicate that two different equivalent granular moduli exist, depending upon whether the tensile strain at the bottom of the upper layer is important or the vertical strain at the bottom of the upper layer is important or the vertical strain at the top of the subgrade layer is the variable of interest. In general, the equivalent tangential modulus (E_{2et}) was found to be greater than or equal to the equivalent vertical modulus (E_{2ev}). Although the difference may not be significant from a practical viewpoint for many problems, the difference between moduli increases when the pavement structure is more "flexible" (i.e., thin surface layer with thick high quality granular material).

Multiple regression techniques, using partial models to reduce the residual error, were developed to predict the equivalent modulus in terms of pavement variables (h_1, E_1, h_2, E_3, and K_1). Nomographic solutions were also developed as a practical solution technique.

The predictive technique developed demonstrated relatively good agreement with several existing procedures to establish granular layer modulus. The existing procedures examined were those developed by the U.S.A. Corps of Engineers, Kentucky Highway Department and Shell Oil Company. The agreement with the predictive technique for high quality base material was considered very excellent while for lower quality base materials the existing methods yielded higher equivalent granular moduli than the predictive method. Because of greater versatility of the method developed in this report to incorporate all of the significant factors affecting the nonlinear response of unbound granular materials, the technique is highly recommended for use in highway design and analysis using theoretical layered approaches.

Acknowledgments

The writers are indebted to The Asphalt Institute for the Bernard Gray Grant which made this research study possible. Gratitude is also expressed to the University of Maryland Computer Science Center for their financial support of the computer phase of the work presented.

Appendix I.—References

1. Allen, J. J., and Thompson, M. R., "Resilient Response of Granular Materials Subjected to Time-Dependent Lateral Stress," *Transportation Research Record No. 510*, Jan., 1974.
2. Barker, W. R., and Brabston, W. N., "Development of a Structural Design Procedure for Flexible Airport Pavements," *Report No. FAA-RD-74-199*, U.S. Army Engineer Waterways Experiment Station, Vicksburg, Miss., Nov., 1974.
3. Brabston, W. N., Barker, W. R., and Harvey, G. G., "Development of a Structural Design Procedure for All-Bituminous Concrete Pavements for Military Roads," *Technical Report S-75-10*, U.S. Army Engineer Waterways Experiment Station, Vicksburg, Miss., July, 1975.
4. Brown, S. F., "Repeated Load Testing of a Granular Material," *Journal of the Geotechnical Engineering Division*, ASCE, Vol. 100, No. GT7, Proc. Paper 10684, July, 1974, pp. 825–841.
5. Cleasen, A. I. M., Valkering, C. P., and Ditmarsch, R., "Pavement Evaluation with the Falling Weight Deflectometer," presented at the Febraury 16–18, 1976, AAPT Annual Meeting, held at New Orleans, La.

6. David, D. S., *Nomography and Empirical Equations,* Reinhold Publishing Corp., New York, N.Y., 1955.
7. Deen, R. C., Southgate, H. F., and Havens, J. H., "Structural Analysis of Bituminous Concrete Pavements," *Research Report 305,* Division of Research, Kentucky Department of Highways, May, 1971.
8. Dorman, G. M., and Metcalf, D. T., "Design Curves for Flexible Pavements Based on Layered System Theory," *Highway Research Record No. 71,* Jan., 1965.
9. Edwards, J. M., and Valkering, C. P., "Structural Design of Asphalt Pavements for Heavy Aircraft," Koninklijke/Shell Laboratorium, Amsterdam, Holland.
10. Finn, F., Saraf, C. L., Kulkarni, R., Nair, K., Smith, W., and Abdullah, A., "The Use of Distress Prediction Subsystems for the Design of Pavement Structures," *Proceedings, Fourth International Conference on the Structural Design of Asphalt Pavements,* 1977.
11. Heukelom, W. and Foster, C. R., "Dynamic Testing of Pavements," *Journal of the Structural Division,* ASCE, Vol. 86, No. SM1, Proc. Paper 2368, Feb., 1960, pp. 1–28.
12. Heukelom, W., and Klomp, A. J. G., "Dynamic Testing as a Means of Controlling Pavements During and After Construction," *Proceedings, International Conference, Structural Design of Asphalt Pavements,* 1962.
13. Jones, M. P., and Witczak, M. W., "Subgrade Modulus on the San Diego Test Road," *Transportation Research Board Record 641,* Washington, D.C., 1977.
14. Michelow, J., "Analysis of Stresses and Displacements in an N-Layered Elastic System Under a Load Uniformly Distributed on a Circular Area," Chevron Research Corporation, Richmond, Calif., 1963.
15. Monismith, C. L., Hicks, R. G., and Salam, Y. M., "Basic Properties of Pavement Components," *Report No. FHWA-RD-72-19,* Sept., 1976.
16. Seed, H. B., Mitry, F. G., Monismith, C. L., and Chan, C. L., "Factors Influencing the Resilient Deformation of Untreated Aggregate Base in Two-Layered Pavements Subjected to Repeated Loading," *Highway Research Record No. 190,* Jan., 1967.
17. Smith, B. E., "Prediction of Equivalent Granular Base Moduli Incorporating Stress Dependent Behavior in Flexible Pavements," thesis, presented to the University of Maryland, at College Park, Md., in partial fulfillment of the requirements for the degree of Master of Science.
18. Smith, W. S., and Nair, K., "Development of Procedures for Characterization of Untreated Granular Base Course and Asphalt-Treated Base Course Materials," *Report No. FHWA-RD-74-61,* Oct., 1973.
19. Thickness Design-Full Depth Asphalt Pavement Structures, *MS-1,* The Asphalt Institute.

Appendix II.—Notation

The following symbols are used in this paper:

CBR = California Bearing Ratio;
E_1 = asphalt concrete layer modulus;
E_2 = unbound granular layer modulus;
E_3 = subgrade modulus;
E_{2et} = equivalent tangential modulus of unbound granular layer;
E_{2ev} = equivalent vertical modulus of unbound granular layer;
h_1 = thickness of asphalt concrete layer;
h_2 = thickness of unbound granular layer;
k_1 = regression derived intercept—constant used in nonlinear modulus—bulk stress relationship for unbound granular material;
k_2 = regression derived slope constant used in nonlinear modulus bulk stress relationship for unbound granular material;
M_R = Resilient Modulus of unbound and granular material;

R = modular ratio of unbound granular layer modulus to subgrade modulus;
R^2 = correlation coefficient squared of multiple linear regression;
TAI = The Asphalt Institute;
α = reference line (turning point) on nomograph;
β = reference line (turning point) on nomograph;
γ_1 = mass density of Asphalt Concrete layer;
γ_2 = mass density of granular base layer;
ϵ_t = maximum principal tensile strain at bottom of asphalt concrete layer;
ϵ_v = maximum principal vertical strain at top of subgrade;
θ = bulk stress (first stress invariant);
μ_1 = Poisson's ratio of asphalt concrete layer;
μ_2 = Poisson's ratio of granular base layer; and
μ_3 = Poisson's ratio of subgrade layer.

RATIONAL DESIGN OF LIME-STABILIZED LATERITE ROADS

By Gurdev Singh,[1] M. ASCE and Baffour K. A. Akoto[2]

(Reviewed by Highway Division)

INTRODUCTION

Good road network is essential for the development of every nation. However, the construction and maintenance of roads involves substantial expenditure with the road pavement itself constituting about one-third of this expenditure. Any means devised to reduce this expenditure will go a long way in helping the distribution of a nation's scarce resources.

A low cost road is a road constructed at low capital cost and capable of being maintained at low recurring cost; it does not imply inferiority. This therefore calls for a stringent use of the pavement materials. In the tropics and subtropics, the common material for road construction is laterites and lateritic gravel. Although there are some laterites which do not require treatment to give them sufficient load bearing capacity, most laterites require some sort of stabilization for their use in road construction.

Lack of information on the elastic properties of natural laterites or stabilized laterite has resulted in the use of empirical or semiempirical tests like the California Bearing Ratio (CBR) and the Unconfined Compression tests for pavement design in the tropical and subtropical regions of the world. Even though such simple static tests are easier to perform, there is an overwhelming evidence that the correlation between such tests and field performance is poor. If roads are to be constructed at low cost in the tropics, a mechanistic approach to pavement design must be adopted. This mechanistic approach requires the knowledge of the elastic and nonelastic parameters of the highway materials.

FACTORS INFLUENCING RESILIENT PROPERTIES OF LIME-STABILIZED LATERITE

A detailed study has been undertaken to determine the factors which influence

[1]Lect. in Civ. Engrg., Dept. of Civ. Engrg., Univ. of Leeds, Leeds LS2 9JT, United Kingdom.

[2]Formerly Research Student, Dept. of Civ. Engrg., Univ. of Leeds, Leeds LS2 9JT, United Kingdom.

Note.—Discussion open until April 1, 1982. To extend the closing date one month, a written request must be filed with the Manager of Technical and Professional Publications, ASCE. Manuscript was submitted for review for possible publication on October 9, 1980. This paper is part of the Transportation Engineering Journal of ASCE, Proceedings of the American Society of Civil Engineers, ©ASCE, Vol. 107, No. TE6, November, 1981. ISSN 0569-7891/81/0006-0653/$01.00.

the resilient properties of a lime stabilized laterite (1,10). The laterite used for the study was obtained from Kenya. The results of the physical and chemical tests run on the natural soil are shown in Tables 1 and 2. The main minerals in this soil were feldspar, quartz, gibbsite, and kaolinite. The presence of kaolinite indicates that the soil was highly weathered.

Results obtained from the dynamic triaxial loading tests confirm, in general, the findings of Thompson (11) and Robnett and Thompson (8) that the resilient properties of lime stabilized laterite are influenced by such factors as stress

TABLE 1.—Some Engineering Properties of Kenya Laterite

Physical properties (1)	Amount of content (2)
Liquid limit, as a percentage	49.2
Plastic limit, as a percentage	29.7
Plasticity index	19.5
Mod. AASHO max. dry density, in kilograms per cubic meter	1,760
(pounds per cubic feet)	109.6
Optimum moisture content, as a percentage	19.7
Specific gravity < 2 mm	2.62
< 5 mm	2.71
pH	5.3

TABLE 2.—Chemical Analysis by X-ray Fluorescence of Fraction < 5 mm

Elements (1)	Percentage by weight (2)
SiO_2	31.22
Al_2O_3	26.83
Fe_2O_3	22.42
TiO_2	2.21
MnO	1.16
MgO	0.38
CaO	0.55
K_2O	0.30
P_2O_5	0.24
NaO	0.54
Water loss in fusion	15.06
	Total = 100.33

intensity, lime content, moisture content, age of curing and the number of load repetitions.

The variations of resilient modulus and vertical resilient strain with stress intensity and number of load application are shown in Figs. 1 and 2. The resilient deformation increases with number of load applications until it reaches a certain maximum, thereafter it decreases with increase in the number of load application. The resilient modulus decreases with increase in load applications until it reaches

a certain minimum, and then increases with increase in number of load applications. The resilient modulus decreased with increase in stress intensity. Shen (2) and Robnett and Thompson (8) working on cement-stabilized clay also observed that the resilient modulus decreased with an increase in stress intensity. Under triaxial conditions, the resilient moduli varied primarily with vertical stress and deviator stress. The general qualitative relationships between resilient moduli, vertical and deviator stresses are shown in Fig. 3. Increase in vertical stress increases the resilient Poisson's ratio.

Under the same stress intensity, increase in lime content increases the resilient modulus (Fig. 4), however the increase in resilient modulus is not proportional

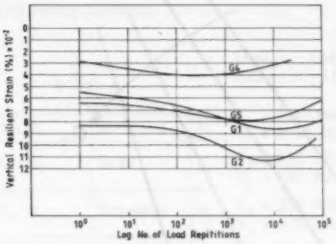

Test Group	Stress (kN/m²) σ_V	σ_H	σ_D
G1	500	400	100
G2	500	200	300
G4	300	0	300
G5	400	0	400

FIG. 1.—Effects of Stress Intensity and No. of Load Applications on Resilient Strain

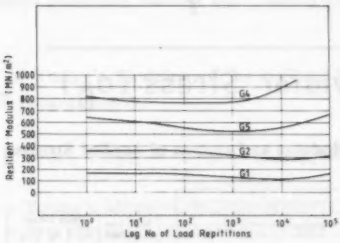

Test Group	Stress (kN/m²) σ_V	σ_H	σ_D
G1	500	100	100
G2	500	200	300
G4	300	0	300
G5	400	0	400

FIG. 2.—Effect of Stress Intensity and No. of Load Applications on Resilient Modulus

to the increase in lime content. Increase in lime content decreases Poisson's ratio.

It was also observed from the study that increase in age increases the resilient modulus and an increase in moisture content generally decreases the resilient modulus.

Application of Experimental Results to Pavement Thickness Design

Several design procedures, for example that of McDowell (3), are available for mechanistic methods of incorporating lime treated layers. In this paper the range of resilient moduli and the resilient Poisson's ratios obtained from the study (1) were used to determine the critical stresses and strains in pavements

incorporating lime-stabilised base. Using limiting stresses and strains associated with two design criteria, that of 'cracking' and that of 'no-cracking,' pavement thicknesses have been recommended for a set of conditions relating traffic loading and material properties. Due to lack of information on thermal stresses induced

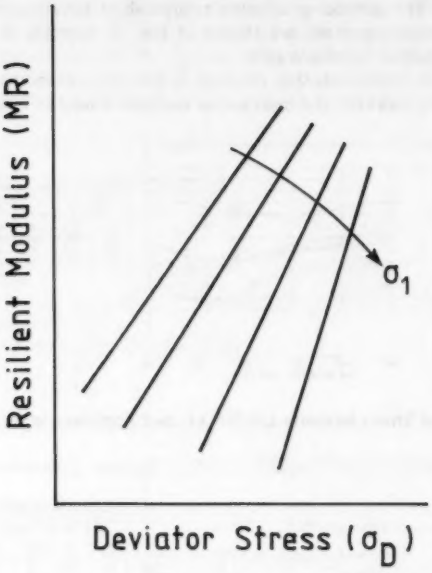

FIG. 3.—Resilient Modulus as Function of Applied Stresses

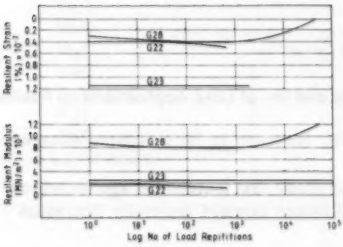

Test Group	Lime Cont	Stress (kN/m²) σ_V	σ_H	σ_D
G22	5%	-75	0	-75
G23	7%	-150	125	-275
G28	10%	-150	125	-275

FIG. 4.—Effect of Lime Content on Resilient Properties

in the lime-stabilized laterite, the stresses used in determining the thicknesses were based solely on those exerted by traffic loading.

Calculation of Stresses and Strains.—For the calculation of the stresses and strains, (using the BISAR computer program) a four-layer pavement structure

(Fig. 5) incorporating layers of varying thicknesses of h_1 and h_2 was used. Two conditions of the top layer were assumed; in one the top layer was made up of only surface dressing, and in the other it was made up of Bituminous layer of 50 mm, 100 mm, and 200 mm thickness. Taking into account the ambient temperature experienced in the tropics, a Young's modulus of 2,000 mN/m^2 was adopted. Four values of Young's moduli of the stabilized layer (500 mN/m^2, 1,000 mN/m^3, 3,000 mN/m^3, and 8,000 mN/m^2) of five different thicknesses (100 mm, 200 mm, 300 mm, 450 mm, and 600 mm) were used. One value of subbase modulus and two values of subgrade moduli were used. The range of the stabilized layer moduli (E_2) used were calculated from the tensile resilient moduli and the Poisson's ratio (determined during laboratory repeated loading tests) in the following manner.

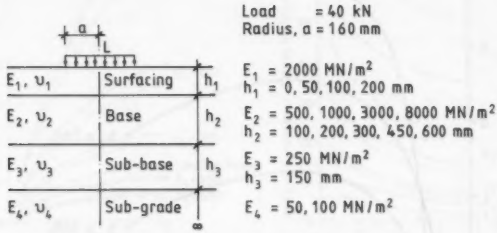

FIG. 5.—Assumed Pavement Section and Loading Condition for Stress and Strain Calculations

The value of Young's Modulus, E, as defined by elastic theory and as used in the BISAR programme is

$$E_y = \frac{1}{\epsilon y}[\sigma_y - \nu(\sigma_x + \sigma_z)] = \frac{1}{\epsilon y}[\sigma_y - 2\nu\sigma_x] \text{(when } \sigma_x = \sigma_z) \quad \ldots\ldots (1)$$

in which E_y = Young's Modulus (in y direction); ϵ_y = Strain (in the y direction); σ_y, σ_x, σ_z = are the octahedral stresses; and ν = Poisson's ratio. On the other hand, the Resilient Modulus, M_R, as defined in literature is

$$M_R = \frac{\sigma_D}{\epsilon_y} \quad \ldots\ldots\ldots\ldots\ldots\ldots\ldots\ldots\ldots\ldots\ldots\ldots\ldots\ldots\ldots\ldots (2)$$

in which σ_D = deviator stress; and = $(\sigma_y - \sigma_x)$. Contrary to general misconception that "under these simple test conditions the resilient modulus is identical to Young's modulus" (5), it is important to state that this equality is valid only when ν is equal to 0.5.

At other values of Poisson's ratio, Young's Modulus is not equal to Resilient Modulus. To illustrate the importance of the foregoing, an example is shown in the following:

$\sigma_y = -100\ kN/m^2$; $\sigma_x = 250\ kN/m^2$

$\epsilon = 0.7\% \times 10^{-2}$; and $\nu = 0.25$ (average).

From Eq. 1:

$$E = 1/7 \times 10^5 [-100 - 2 \times 0.25 \times 250] \text{ kN/m}^2$$
$$= 3{,}200 \text{ mN/m}^2$$
$$M_R = 1/7 \times 10^5 [-100 - 250]$$
$$= 5{,}000 \text{ mN/m}^2$$

This difference between E and M_R is obviously very significant and should

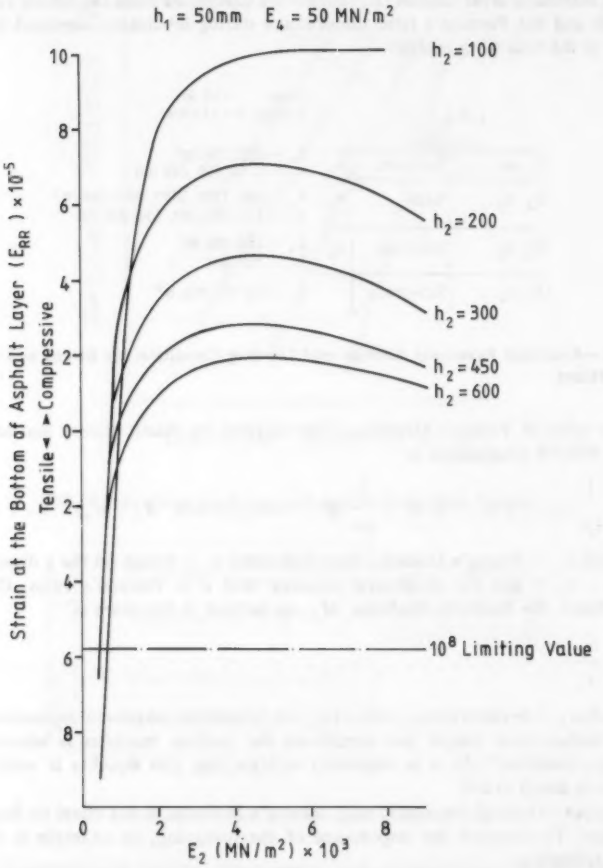

FIG. 6.—Effect of Base Thickness on Strain at Bottom of Asphalt Layer with Respect to E_2 and E_4

not be ignored because the horizontal stresses in the stabilized layer are dramatically influenced by E of the material.

Although the measured values of Poisson's ratio from experimental work ranged from 0.1–0.35, but for simplicity and because of its minor direct effect on stresses and strains, a single value of 0.25 has been adopted. The design load and other parameters used in calculating the stresses and strains are shown in Fig. 5.

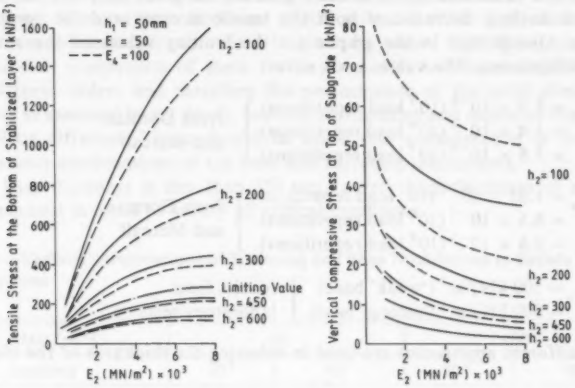

FIG. 7.—Effect of Base Thickness of Stresses in Base and Subgrade Sections of Pavement for Different Values of E_2 and E_4

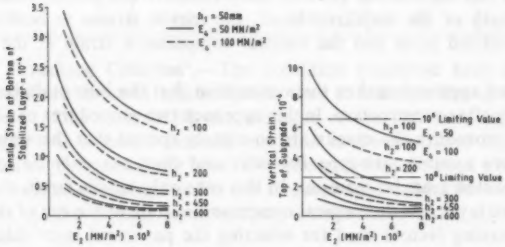

FIG. 8.—Effect of Base Thickness on Tensile Strain in Base and Compressive Strain at Top of Subgrade Sections of Pavement for Different Values of E_2 and E_4

By assuming a low value of E_1 and E_4 with relatively strong base course, the most severe stress-strain would be obtained in the stabilized base course. The stresses and strains which were of interest were the following: (1) The tensile strain (ϵ_{RR_1}) at the bottom of the asphalt layer; (2) the horizontal stress (σ_{RR_2}) and strain (ϵ_{RR_2}) occurring at the bottom of the stabilized layer; (3) the vertical compressive stress (σ_{ZZ_4}); and (4) strain (ϵ_{ZZ_4}) at the top of the subgrade. These calculated values were then compared with the permissible

strain values as proposed by Dormon and Metcalf (2) and Mitchell and Shen (9) and stress values from the laboratory tests.

The solutions from the computer program showing the relationships between the resilient modulus of the base (E_2) and the tensile stresses, strains, and compressive strains, for $h_1 = 50$ mm are presented in Fig. 6–8. Similar relationships were obtained for the other values of h_1. As expected with an increase in E_2, the tensile stresses at the bottom of the stabilized layer increase and the compressive strain and stress at the top of the subgrade decrease; an increase in h_2 results in a decrease of both the tensile stresses and the compressive stresses. Also plotted in the graphs are the limiting values of the strain and stress components. The values used were:

$$(a)\ \left.\begin{aligned}\epsilon_{RR_1} &= 2.3 \times 10^{-4}\ (10^5 \text{ load repetitions})\\ &= 1.4 \times 10^{-4}\ (10^6 \text{ load repetitions})\\ &= 5.8 \times 10^{-5}\ (10^8 \text{ load repetitions})\end{aligned}\right\} \text{ from Dorman and Metcalf} \quad \ldots\ldots\ldots (3)$$

$$(b)\ \left.\begin{aligned}\epsilon_{ZZ_4} &= 1.05 \times 10^{-3}\ (10^5 \text{ load repetitions})\\ &= 6.5 \times 10^{-4}\ (10^6 \text{ load repetitions})\\ &= 2.6 \times 10^{-4}\ (10^6 \text{ load repetitions})\end{aligned}\right\} \text{ from Dorman and Metcalf} \quad \ldots\ldots\ldots (4)$$

$$(c)\ \left.\begin{aligned}\sigma_{RR_2} &= 100 \text{ kN/m}^2 \text{ ('weak' base)}\\ &= 300 \text{ kN/m}^2 \text{ ('strong' base)}\end{aligned}\right\} \text{ results from laboratory tests} \quad \ldots\ldots\ldots (5)$$

Two different approaches are used in selecting the thickness of the stabilized base.

The first approach makes an assumption that the pavement possesses slab-type behavior (and thus the layers are assumed to be infinite in longitudinal and transverse direction). For this approach selection of the base thickness is made on the basis that the induced stresses and strains are not greater than the fatigue tensile strength of the stabilized layer, the tensile strains in both the asphalt and the stabilized layer and the vertical compressive strain at the top of the subgrade.

The second approach makes the assumption that the lime-stabilized base will crack shortly after construction. In this approach two procedures can be adopted. In the first procedure the cracks are so closely spaced that the stabilized layer does no more assume slab-type behavior and thus can only be looked at as a well-compacted granular material. In this case only tensile strain at the bottom of the asphalt layer and the vertical compressive strain at the top of the subgrade are the governing factors used for selecting the pavement layer thickness. The second procedure makes provision for cracking but the crack spacings are assumed to be wide; and because of the finite dimensions of the slabs, 'edge'-loading conditions are assumed. In this case the induced stresses are higher than those calculated assuming a slab infinite in extent ('interior'-loading).

Three loading conditions were assumed—a low trafficked road (10^5 repetitions), medium-trafficked road (10^6 repetitions) and heavily-trafficked road (10^8 repetitions).

Design for 'No-Cracking' Criterion.—When initiation of cracking is used as the criterion, the critical factor is the tensile strength of the stabilized layer, and to some extend the induced tensile strain at the bottom of the asphalt layer. Fig. 9(*a*) shows the relationship between the thickness of the asphalt

layer and the thickness of the base layer to satisfy all criteria for the various values of $E_2 \geq 1{,}250\ \mathrm{mN/m^2}$.

From Fig. 9(*a*) it will be observed that for surfacing thickness up to 100 mm, there is a 1:1 relationship between the thickness of the base and that of the surfacing. Any combination of the thicknesses of surfacing and base which add up to 450 mm will satisfy all the criteria examined. That is by decreasing the surfacing by, say 10 mm, the base thickness should be increased by the same amount (10 mm). For the loading conditions examined, it will appear to be cheaper to use a base thickness of 450 mm and either surface dressing or thin layer of asphaltic concrete. It must be stated that the permanent deformation or compaction of these two layers under subsequent traffic may be of different orders and therefore the performance of the total alternative structures, as assessed by rut depth, resilient deformation and radius of curvature may well be different. These should be taken into consideration in deciding on the various combinations of the base and surfacing thicknesses.

If the base thickness is less than 350 mm, a very high thickness of asphalt will be required in order to satisfy all critical conditions.

TABLE 3.—Various Combinations of Surfacing and Base Thicknesses to Satisfy Design Considerations

E_4 (MN/m^2)	50		100	
Loading	10^5	10^6	10^5	10^6
h_1 (mm)	h_2 (mm)			
0	175	250	100	200
50	100	275	100	100
100	100	100	100	100
200	100	100	100	100

Design for 'Cracking Criterion'.—The condition examined here is the one where the stabilized layer is cracked such that it behaves like a compacted granular material. Due to cracking the modulus of the stabilized layer will be highly reduced. It is assumed that the modulus of the stabilized layer will be four times that of the underlying layer (5). The value of E_2 used here is 1,000 $\mathrm{mN/m^2}$. The critical conditions under this circumstance will be the tensile strain at the bottom of the asphalt layer and the compressive strain at the top of the subgrade.

The various thicknesses, loading conditions and subgrade stiffnesses to satisfy the strain criteria are shown in Table 2 and Fig. 9(*b*).

From Table 3 it will be observed that for a 'strong' subgrade and low loading condition, a minimum practicable base thickness of 100 mm will satisfy the strain conditions, irrespective of the surfacing thickness. For a 'weak' subgrade and low loading condition, a minimum base thickness of 175 mm (with surface dressing) is required. When the surface thickness is increased to 50 mm, the base thickness reduces to 100 mm (i.e., total base plus surfacing thickness of 150 mm).

For higher loading conditions, when the subgrade is 'weak,' the minimum base thickness of 250 mm is required when only surface dressing is used. When

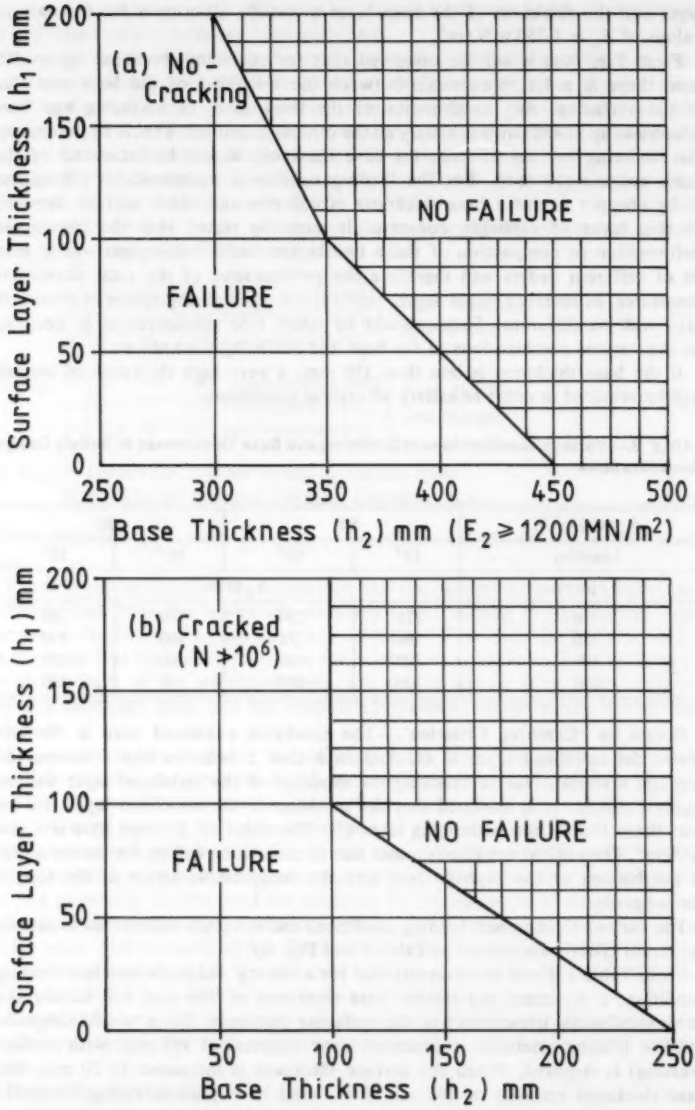

FIG. 9.—Relationship Between Asphalt Layer and Base Thickness to Satisfy all Design Criteria

the surfacing thickness is increased to 50 mm, the base thickness reduces to 175 mm (i.e., total base plus surfacing thickness of 225 mm). With surfacing thickness of 100 mm, the base thickness reduces to 100 mm (i.e., total base plus surfacing thickness of 200 mm). With a 'strong' subgrade, a minimum base thickness of 200 mm (with surface dressing) will be required. When the surfacing thickness is increased to 50 mm, the minimum practicable base thickness reduces to 100 mm (i.e., a total base plus surfacing thickness of 150 mm).

The stiffness of the subgrade plays an important part in the selection of the pavement thicknesses. Increasing the stiffness of the subgrade from 50 mN/m^2 to 100 mN/m^2 could lead to a reduction of up to 75 mm in the base

TABLE 4.—Comparison of Pavement Thicknesses by Three Design Procedures

Pavement, layer (1)	THICKNESSES, in millimeters						
	Road note 31 (2)		Proposed				
			'No-cracking' (3)		'Cracked' (4)		
(*a*) $N = 10^5$							
Surfacing	0		0	50	0	50	
Base	150		450	400	175	100	
Sub-base	200		150	150	150	150	
Total	350		600	600	325	300	
(*b*) $N = 10^6$							
	0	50	0	50	0	50	100
	200	150	450	400	250	175	100
	225	225	150	150	150	150	150
	425	425	600	600	400	375	350
(*c*) $N = 10^8$							
	Road Note 29						
	210		0	50	100	200	0	50
	210		450	400	350	350	450	400
	300		150	150	150	150	150	150
	720		600	600	600	650	600	600

thickness. This is quite different from the first design consideration (assuming no cracking) where the subgrade modulus of 50 mN/m^2 or 100 mN/m^2 did not make any significant difference in the selection of the base thickness.

The choice of the combination of the base and surfacing thicknesses to satisfy the design criterion must be based on the respective costs of the asphalt and the stabilized layers. Increasing the surfacing layer from 0 mm–50 mm could result in the reduction of the base thickness of between 75 mm and 100 mm.

Comparison of Proposed Thickness Design Methods with Some Existing Methods

To assess the reasonableness of the proposed procedures, thicknesses selected

for various highway loading conditions have been compared with Road Notes 29 (6) and 31 (7). Since the maximum number of standard axle load used in Road Note 31 is 2.5×10^6, lower loading conditions were compared with Road Note 31 and the higher loading conditions compared with Road Note 29.

One value of subgrade stiffness (C.B.R. = 5%, $E = 50\ mN/m^2$) and three loading conditions (number of standard axle $N = 10^5$, 10^6, and 10^8), were examined. Table 4 shows the proposed thicknesses and those recommended by Road Note 29 and 31.

For the lightly trafficked road ($N = 10^5$ and 10^6) the proposed procedure based on 'cracking' agrees very well with Road Note 31, though compared with the proposed procedure, Road Note 31 appears to be over-designed. The thicknesses obtained by using 'no-cracking' procedure are far higher than both Road Note 31 and the 'cracked' procedure.

For the heavily trafficked road ($N = 10^8$), both the 'cracked' and 'no-cracking' procedures give about the same thicknesses; which are lower than those obtained from Road Note 29.

Conclusions

'No-Cracking' Procedure.—(1) The most critical parameter is the tensile strength of the stabilized layer and, to a lesser extent, the tensile strain at the bottom of the asphalt layer; (2) up to 100 mm thick surfacing, increasing the surface thickness results in the decrease of the base thickness by the same amount; and (3) the procedure appears to be more appropriate to high volume roads where the thickness obtained compares favorably with other design procedures.

'Cracked' Procedure.—(1) The procedure results in thicknesses which compare favorably with those proposed in Road Note 31 for low to medium volume roads; and (2) the effect of having thick asphaltic layers (up to 100 mm) results in a reduction in the overall pavement thickness.

Acknowledgment

The help rendered by the following is acknowledged: A. R. Cusens for making available the facilities at his Department; the Director of the Transport and Road Research Laboratory, United Kingdom and the Staff in the Overseas Unit for providing the laterite used in the study and the Ghana Government for sponsoring the second writer for the study.

Appendix.—References

1. Akoto, B. K. A., "The Characterization of a Lime Stabilized Laterite," thesis presented to the University of Leeds, at Leeds, England, in 1980, in partial fulfillment of the requirements for the degree of Doctor of Philosophy.
2. Dormon, G. M., and Metcalf, C. T., "Design Curves for Flexible Pavements Based on Layered System Theory," *Highway Res. Rec. No. 71*, 1965, pp. 69–84.
3. McDowell, C., "Flexible Pavement Design Guide," *Bulletin 327*, National Lime Association, 1972.
4. Mitchell, J. K., and Shen, C. K., "Soil-Cement Properties Determined by Repeated Loading in Relation for Flexible Pavements," *Proceedings 2nd Conference on the Structural Design of Asphalt Pavements*, Vol. 1, 1967, pp. 427–451.
5. Pell, P. S., ed., "Developments in Highway Pavement Engineering—1," Pub., Applied

Science Pub., Ltd., London, England, 1978.
6. "A Guide to the Structural Design of Pavements for New Roads," *Road Note 29,* Her Majesty's Stationary Office, London, England, 1970.
7. "A Guide to the Structural Design of Bitumen-Surfaced Roads in Tropical and Sub-tropical Countries," *Road Note 31,* Her Majesty's Stationary Office, London, England, 1977.
8. Robnett, Q. L., and Thompson, M. R., "Effect of Lime Treatment on the Resilient Behaviour of Fine-grained Soils," *Transp. Res. Rec. No. 560,* 1976, pp. 11–20.
9. Shen, C. K., "Behaviour of Cement Stabilized Soil Under Repeated Loading," thesis presented to the University of California, at Berkeley, California, in 1965, in partial fulfillment of the requirements for the degree of Doctor of Philosophy.
10. Singh, G., and Akoto, B. K. A., "Factors Influencing Resilient Properties of Lime-stabilized Laterite," presented at the 1981 Second Australian Conference on Engineering Materials, U.N.S.W. Sydney, Australia, 1981.
11. Thompson, M. R., "Soil-lime Mixtures for Construction of Low-volume Roads," *Transp. Res. Board Special Report 160,* 1975, pp. 149–165.

THE FLY-OVER: A VIEW FROM BOTH SIDES

By Stanley R. Byington[1]

(Reviewed by the Urban Transportation Division)

INTRODUCTION

Fly-overs, marketed in Europe and elsewhere, are lightweight, prefabricated, structural steel grade separation structures. They can typically be erected over a weekend, and are reusable after dismantling. They do not include the typical separation structures routinely used for interchanges and individual ramps in the United States. Compagnie Francaise d'Enterprises Metalliques, a French company, has built 190 fly-overs in eight countries in Europe, Asia, Africa, and South America (12).

Because fly-overs can potentially unclog traffic at overloaded urban and rural intersections, this article presents both their positive and negative aspects by examining the following questions:

1. Should a fly-over be considered a permanent fix to an existing intersection traffic congestion problem?
2. How much traffic can a fly-over handle, and what is the existing and expected future traffic demand for use of the fly-over and for the intersection as a whole?
3. Will a fly-over satisfy existing safety, esthetic, and environmental goals and policies?
4. Will the existing right-of-way and intersection layout permit the installation of a fly-over, i.e., can the design characteristics of a fly-over accommodate the traffic that must use the fly-over and still leave sufficient room for surface traffic to make safe directional movements at the intersection?
5. Can the fly-over and its related foundations be erected in a short period of time that will not adversely affect existing traffic conditions?
6. How much will a fly-over cost?
7. How cost effective will the fly-over be in relation to other traffic control measures?

[1]Chief, Traffic Systems Div., Office of Research, Federal Highway Administration, Washington, D.C.

Note.—Discussion open until April 1, 1982. To extend the closing date one month, a written request must be filed with the Manager of Technical and Professional Publications, ASCE. Manuscript was submitted for review for possible publication on December 12, 1980. This paper is part of the Transportation Engineering Journal of ASCE, Proceedings of the American Society of Civil Engineers, ©ASCE, Vol. 107, No. TE6, November, 1981. ISSN 0569-7891/81/0006-0667/$01.00.

This article includes information from reports and correspondence on the design aspects and costs of fly-overs installed in Europe, their effect on safety, and their cost-effectiveness. Also presented are the costs and effectiveness of conventional highway structures and alternative traffic-control measures typically used in the United States to alleviate congested intersections.

This information should aid decision-makers in economic analyses on the possible use of a fly-over. Some nonmarket factors—esthetics, the environment, and societal goals—are also briefly discussed so decision-makers can properly weigh them before deciding whether or not to use a fly-over.

Fly-Overs: Temporary or Permanent.—Should fly-overs be considered as temporary or permanent structures? G. D. Cochrane of Braithwaite and Co. Structural Ltd. in England claims that fly-overs should not be considered temporary structures because the marketed fly-over system called "Fliway" is designed for a life of 120 yr (12). However, R. Lapierre of the German Ministry of Transportation states in a letter to the Federal Highway Administration

TABLE 1.—Maximum Traffic Volumes Observed on Fly-Overs within Urban Areas of France[a]

Fly-over type (1)	Number of fly-overs (2)	Total traffic (all lanes) during the peak hour, in passenger car units (3)
One-lane, one way	3	850
One-lane, two way (traffic alternate)	1	660
Two-lane, one way	3	2,200
Two-lane, two way	9	3,000[b]
Four-lane, two-way	2	2,600

[a]Ref. 4.
[b]All but one of the fly-overs carried 2,500 or fewer vehicles per hour.

that, in practice, "Fly-overs have always been regarded as a temporary and urgent measure for a period of 5 years until a complete and permanent reconstruction or improvement of an intersection could be realized." He also states, "Experience has shown that 'temporary' fly-overs, once installed, tend to last much longer, which in turn is not a very satisfactory situation from the esthetic point of view."

Although, structurally, fly-overs can be used for a considerable time period, this does not appear to be the governing factor. The extent and time of fly-over usage is probably more dependent upon existing and expected growth in traffic demand, safety considerations, environmental and esthetic policies, and the fly-over's design load.

Traffic Capacity on Fly-overs.—A study of 9 two-lane, two-way fly-overs built in France in 1970 and 1971 revealed that the traffic volume carried during peak hours was generally at most 2,500 passenger cars per hr. The maximum traffic on 9 other multiple type fly-overs is shown in Table 1. Of the combined 18

fly-overs, 14 had surface street reserve capacities equal to or in excess of 30% (4). Surface street reserve capacity, as used here, is the difference between one and the following percentage: the number of vehicles using the surface streets at the intersection immediately after opening of the fly-over divided by the maximum number of vehicles that such surface streets can reasonably accommodate.

In considering traffic demand and available capacity, attention must be paid to both fly-over traffic and traffic remaining at ground level. The latter is basically traffic that desires to change directions at the intersection and heavy or long vehicles trucks and buses, or both, that cannot travel on the fly-over because of too low a design load or inadequate geometrics. The study in France suggests that a fly-over should not be considered as a permanent solution to intersection congestion unless there is a capacity reserve of at least 30% on the surface streets at the intersection (4). Otherwise, traffic demand at the intersection will exceed capacity within a short time frame, and the intersection will again become a problem. In the U.S., a capacity reserve of 30% would accommodate traffic growth for about 6 yr because, historically, traffic has grown at the rate of about 5% per year (10). The time would be shorter if nearby land development for commercial, industrial, or residential use, or all three of the above, is an important trip generator.

Safety Considerations.—A fly-over's safeness depends on the quality of signing at the entrance of the structure. One-half of all accidents at fly-overs occurs at the ends of the access ramps. To reduce such accidents, the choice of direction must be clear to road users so they do not hesitate as they approach the fly-overs (4).

In urban areas with good visibility, Europeans typically place an overhead sign 330 ft (100 m) in advance of the structure. If sight distance is restricted, another overhead sign is placed 500 ft (150 m) upstream of the advance sign. In rural areas, they locate the additional sign 1,650 ft (500 m) upstream of the advance sign (4).

Where fly-overs are used, Europeans also enhance road markings by including a continuous yellow line for 330 ft (100 m) ahead of the front end of the structure to separate opposing traffic streams. In addition, they may provide the following protective devices on both sides of the fly-over at the fly-over approaches: an illuminated sign, divisional island, or rigid divider, or all the above, rising gradually and shielding the ends of the fly-over guardrails. These devices prevent most fly-over entrance accidents (4). In the United States, the road marking would have to be two solid yellow lines to be in conformance with the Manual on Uniform Traffic Control Devices (9). In addition, the rigid divider used by the Europeans should probably be replaced with one of several types of crash cushions now used in the United States as protective systems to shield rigid objects or hazardous conditions that cannot be removed, relocated, or made breakaway (5).

Fly-over supports must also be adequately protected by guardrails to protect surface street traffic. Also, the supports must be located carefully to provide adequate sight-distance on the surface streets.

User familiarity also strongly affects safety. The French have generally found that fly-over associated accidents decrease four-fold three months after opening of a fly-over to traffic (4).

FIG. 1.—An Old Fly-Over in Operation in Europe

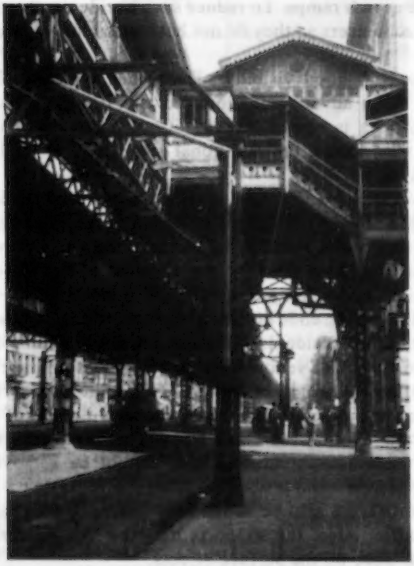

FIG. 2.—An Old Elevated Transit Structure in the United States

Esthetic and Environmental Issues

Both R. Lapierre and B. Horn, the latter from the Paris-based Organization for Economic Cooperation and Development, conclude in letters to the Federal Highway Administration that because of esthetic and environmental reasons fly-overs are used less and less in Europe as a remedy for congested intersecting roadways.

The fly-over concept has been utilized in the United States, particularly in Chicago in the 1960's, though most such structures were not lightweight. Many environmental complaints showed that such structures were not well received by the public. Some concerns expressed were

1. Roadway is "up in the windows."
2. Property values are reduced resulting in boarded up buildings.
3. The area under the structure is dark, moist, dirty and becomes esthetically a slum.

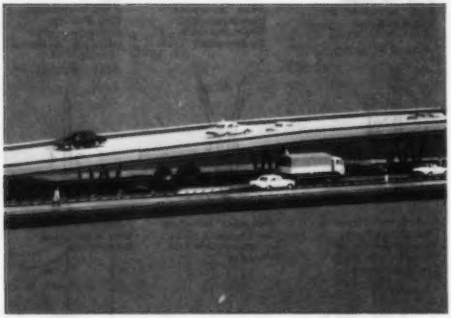

FIG. 3.—New Fly-Over Type Now Being Marketed in the United States

Fly-overs, particularly older designs and those most often used in urban areas, typically resemble some of the unsightly elevated transit structures built many years ago in the United States. Figs. 1 and 2 show an older fly-over design and an elevated transit facility respectively. Such structures are unacceptable today. In 1969, the Congress passed legislation setting forth policies dealing with the environment, one of which assures all Americans of esthetically and culturally pleasing surroundings (3).

As shown in Fig. 3, modern fly-overs can be attractive. This fly-over is being marketed and built world-wide by Nobels-Kline, Ltd. They claim that ". . . enamelled decorative panels harmonizing with the color of the steel are available" and that "the firm, clear-cut lines give the bridge an attractive appearance that blends well with contemporary urban environments (11)."

Because of existing environmental and esthetic policies, fly-over use in the U.S. may be restricted to temporary structures in work zones or as more permanent structures in rural areas or within urban industrial sections. More attractive fly-overs may also be viable alternatives for accommodating major directional

traffic movements at sports stadiums and large shopping center complexes.

Design Characteristics.—France appears to be the principal country to make use of fly-overs at critical road locations in both urban and rural areas. One of the French fly-over structures—"Autoponts"—was originally developed in the late 1960's through a competitive contract process. The original structure was designed for a truck of 33.1 tons (36,000 kg)—roughly equivalent to HS–20 designed structures in the United States (1). The heaviest, legally loaded trucks on highways in the United States are approx 40 tons; the exact weight limit varies slightly among the states.

The "Autopont" is a system of prefabricated, standard, modular elements

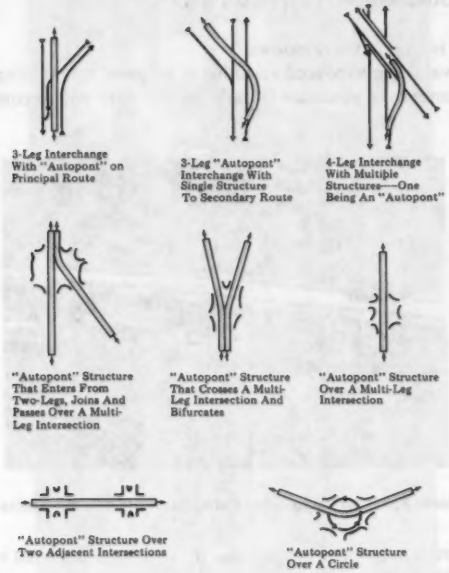

FIG. 4.—Examples of One-Lane Fly-Overs

that can be assembled in a few days to build a temporary fly-over and later dismantled and reused in another structure. The deck elements provide 11.5 ft (3.50 m) lanes and a turning radius of 250 ft (75 m)–1,000 ft (300 m). Slopes of 6–7% can be handled by the "Autoponts," but for comfort the slopes are usually restricted to 3% (4). The portable "Autoponts" have been used to carry one and two lanes of traffic, both in rural and urban situations. Examples of their applications are shown schematically in Figs. 4 and 5. In each figure, the shaded area depicts the "Autopont" fly-over.

Other developed fly-overs include the "Toboggan," "Jacgmain," and the Nobels-Kline Bridge. The first was developed and patented by the French firm, Creusot-Loire. Its function and characteristics are similar to those of the "Autopont (1)."

The "Jacgmain" fly-over was developed in Belgium, and first used in 1970. It is extremely light and portable,being primarily designed for passenger cars. The design load is 82 psf (3,928 Pa) with an impact coefficient of 1.25. It is designed to be erected and dismantled ten times (8).

The Nobles-Kline structure was developed jointly by Nobels Peelman n.v. and Kline Iron and Steel Company; the former is in Belgium, and the latter is in Columbia, South Carolina. Their design and fabrication accommodate a design live loading of HS-20. Spans ranging from 50 ft (15 m)–110 ft (33 m)

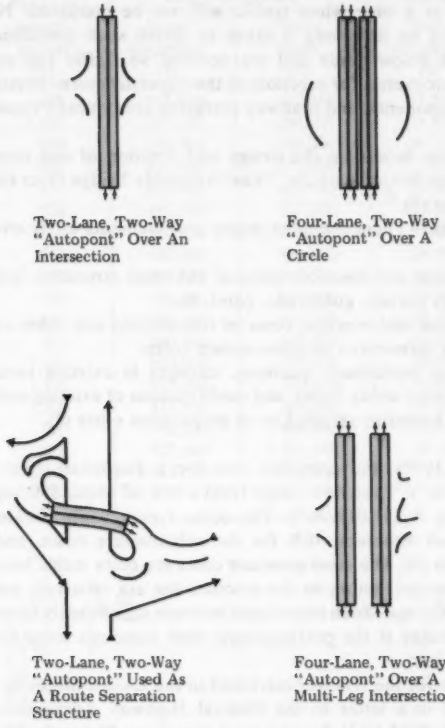

FIG. 5.—Examples of Multilane Two-Way Fly-Overs

can be constructed from their modular construction units. Their deck components are 6 ft (1.83 m) wide and are identical and interchangeable. Therefore, various numbers of lanes and widths are possible; e.g., two 9-ft (2.8-m) lanes, two 12-ft (3.6-m) lanes, and three 10-ft (3.0-m) lanes (12).

Although traditional fly-over prefabricated units have been constructed of structural steel, prestressed concrete units could be developed and marketed as alternatives.

Erection Factors.—One major advantage cited for the use of fly-overs is that the superstructure can be erected within a short time frame, for example, over a weekend. The erection of a 660 ft (200 m) long two-lane "Autopont" superstructure takes about six days (1). It is claimed that it has never taken more than four nights to erect a "Toboggan" superstructure (6), and Nobels-Kline, Ltd. states that its structure ". . . provides instant relief from congested traffic in less than 20% of the time it normally takes to construct a bridge (11)."

Fly-over foundations—which may be precast or cast in place concrete footings, depending on soil conditions—are usually installed before the superstructure is erected and at a time when traffic will not be disrupted. No information could be located on how long it takes to install such foundations. They are typically placed below grade and are covered so traffic can pass over them until they are uncovered for erection of the superstructure. Portal frames, deck and parapet components, and roadway surfacing are typically constructed offsite (11).

More extensive details on the design and erection of one type fly-over can be found in Elmar Koger's article, "Fast Assembly Bridge Over the Aegidientorplatz in Hanover (7)."

Fly-Over Costs.—There are three major cost elements of fly-overs:

1. The purchase and erection costs of the steel structure, including related elements such as portals, guardrails, paint, etc.
2. The purchase and erection costs of foundations and other concrete items, hereafter jointly referred to as substructure costs.
3. The cost of preliminary planning, changes in existing installations (e.g., removal of overhead utility lines), and modifications of existing surface roadways and signing; all hereafter referred to as preparation costs (4).

In the early 1970s, the complete cost for a European fly-over was about \$45/sq ft (484/m^2). They now range from a low of about \$50/sq ft (\$538/m^2) to over \$100/sq ft (\$1,075/m^2). The costs typically are divided as follows: 54% for the steel structure, 10% for the substructure costs, and 36% for the preparation costs (4). The steel structure costs are quite stable because transportation costs from the factory to the erection site are relatively unimportant—at least in western Europe. Such costs could increase significantly for use of fly-overs in the United States if the prefabricated steel structure were purchased from a European concern.

Current prices for the fly-over marketed in the United States by Nobels-Kline Ltd., as quoted in a letter to the Federal Highway Administration, are now about \$64/sq ft (\$688/m^2) for the steel structure, \$2/sq ft (\$21/m^2) for the foundations and \$7/sq ft (\$75/m^2) for erection of the fly-over. These costs are based upon the following conditions:

1. The steel structure is prefabricated in Belgium and shipped 200 miles (322 km) inland in the United States. Additional transportation would increase the steel structure cost.
2. The foundation cost is based on a soil with a bearing capacity of 4,000 lb/sq ft (191,600 N/m^2). Any soil not this firm or that requires piles or other foundation treatment will increase the cost.

3. The erection cost is based upon average area labor rates for iron workers in Dallas, Texas.

The sum of the three cost values supplied by Nobles-Kline does not compare

TABLE 2.—Costs of Fly-Over Installed within Urban Areas of France During 1970–1971[a]

Fly-over width, in feet (1)	Fly-over length, in feet (2)	Costs, in dollars		Costs, in dollars per square foot	
		Steel structure (3)	Other costs (4)	Steel structure (5)	Other costs (6)
11.5	695	267,950	82,050	33.50	10.25
11.5	1,191	437,500	250,000	31.95	18.25
11.5	899	270,000	180,000	26.10	17.40
23.0	663	425,000	175,000	27.85	11.50
23.0	971	625,000	625,000	28.00	28.00
23.0	774	482,500	217,500	27.10	12.20
23.0	640	400,000	675,000	27.15	48.85
23.0	663	440,000	395,000	28.85	25.90
23.0	836	580,250	1,585,500	30.20	82.45
23.0	754	525,000	287,500	30.25	16.60
23.0	653	429,000	182,500	28.55	12.15
23.0	571	390,500	147,000	29.75	11.20
23.0	1,164	800,000	475,000	29.90	17.75
23.0	1,305	925,000	700,000	30.80	23.30
11.5	1,309	475,000	250,000	31.55	16.60
23.0	207	152,500	400,000	32.05	84.00
46.0	636	825,000	1,100,000	28.20	37.60
23.0	1,509	1,013,000	324,500	29.20	9.35

[a]Ref. 4.

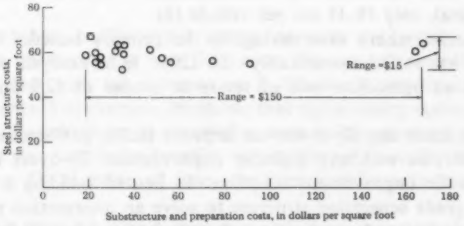

FIG. 6.—Comparison of Steel Structure Costs Versus Other Fly-Over Costs

favorably with a composite of bid prices for conventional structures currently being built in the United States. Such prices, as furnished by the Federal Highway Administration's Bridge Division, now run around \$28/sq ft (\$301/m^2) to \$45/sq ft (\$484/m^2) depending on the HS loading and span arrangement.

The substructure costs are typically 15–20% of the steel structure costs minus

any transportation costs. The former costs are typical for a concrete foundation—special foundations are rare—and for any necessary piles. The columns, bays, steel structure and concrete slab flooring are not typically included in these costs (4).

The preparation costs for building a fly-over are extremely variable and important because, in a number of cases, these costs are more than 50% of the total fly-over cost (Table 2). Data in the table are for the 18 fly-overs in France discussed earlier. The cost figures shown are 1970 and 1971 prices. These costs would double if inflated to 1980 dollars assuming 8% inflation (4).

Fig. 6, which is a plot of costs per square foot for the steel structure versus other fly-over costs (using inflated 1980 prices), shows just how variable the preparation costs are when compared to the relatively stable steel structure costs. The preparation costs have a range of about $150 while the steel structure costs have a range of only $15.

When structure, substructure, and preparation costs are all considered, fly-overs are not low-cost structures. Three rural fly-overs averaging 450 ft (140 m) long built in France in the 1970's cost an average of $350,000 each ($700,000 in 1980 dollars). Urban fly-overs are even more costly; the various length fly-overs listed in Table 2 cost an average of $1,000,000 each ($2,000,000 in 1980 dollars) (4). Part of these high initial costs are recoverable, however, because fly-overs are designed to be portable and the superstructures can be relocated as traffic patterns change.

Cost Effectiveness.—The following cost effectiveness analysis is based on data from France. Time and accident savings are included in the analysis, but fuel savings are not. Note that research in the United States has shown that fuel savings, expressed in dollars, typically range from being the same to one-third the dollar value of time saved by drivers and passengers through reductions in delay (12).

The French have found that in rural areas, where safety benefits are predominant, the immediate rate of return (one-year time and safety benefits divided by total cost) is around 50%. Time savings are important in rural areas only on high traffic volume routes (e.g., a recreational route). Otherwise, time savings may be marginal, only 10–15 sec per vehicle (4).

In urban areas, where time savings is the primary benefit, the immediate rate of return has varied considerably—20–120%. In an analysis of 18 fly-overs, only one had an immediate rate of return in excess of 82% and 13 had less than 46% (4).

There is no doubt that fly-overs can improve traffic performance at intersections. However, as with any highway improvement, fly-overs must compete with other traffic improvement solutions. In lieu of building a fly-over or a conventional grade separation structure to solve an intersection problem, engineers might improve performance through optimization of signal timing (if signals are currently used at the intersection), coordination of traffic signals along the travel route, addition of lanes if space permits, use of intersection channelization, or some other type or combination, or both, of traffic control improvement.

Assuming that traffic signal system improvements have a negligible effect on vehicle miles of travel, F. Wagner calculates that the energy conserved from such improvements is 0.60 gal (0.228 m^3) for each vehicle hour of travel time reduction (12). Using this relationship, it has been shown that if signal

optimization results in one less vehicle being stopped per approach per cycle during a 12-hr working day, 5,500 gal (20,845 L) of fuel will be saved per intersection per year (2,14). A properly coordinated, pretimed signal system typically yields 30% or greater improvement—reduced delays, fewer stops, better transit performance, reduced accidents and reduced fuel consumption—over noncoordinated signals (14).

Table 3 presents typical immediate rates of return and initial construction costs for the two discussed traffic signal control measures and similar data for rural and urban fly-overs. Annual costs were used for the signal timing optimization improvement; it was assumed that the optimization would be good for only one year because of changing volume conditions. Time savings only, valued at \$3/hr, were considered as benefits of the two signal alternatives while both time and safety benefits are included in the two fly-over improvements. The fly-over data is from France (4) and the signal data from the United States (12).

TABLE 3.—Construction Costs and Immediate Rates of Return for Various Intersection Traffic Control Improvements

Traffic control improvement (1)	Range of construction costs in dollars per intersection or signal (2)	Range of immediate rates of return, as a percentage (3)
Rural fly-over	400,000–850,000[a]	50–60[a]
Urban fly-over	700,000–2,800,000[b]	20–120[b]
Signal timing optimization	300–400[c]	10,800–14,000[d]
Signal coordination	2,000–10,000[c]	900–4,500[d]

[a]Ref. 4.
[b]Ref. 4.
[c]Ref. 14.
[d]Ref. 14.

Table 3 shows how traffic signal system projects can greatly improve the efficiency of an intersection at very little cost. The rate of return for the signal alternatives appears high but is based on F. Wagner's projected benefits for such improvements. For example, he shows that signal timing optimization saves a minimum of 36 vehicle-hr of travel for each dollar spent to provide such benefits. When the vehicle-hr benefits are converted to dollar savings using the conservative \$3/hr value of time, the cost/benefit ratio becomes 1/108 (14).

Traffic signals that are timed correctly and interconnected also contribute to energy conservation, air pollution reduction, and accident reduction. For example, F. Wagner states, "Every project dollar spent for systematic improvement of the areawide traffic signal system will return an estimated conservation of 12 gal (45 L) of motor vehicle fuel (14)." H. Strate also shows that safety improvement projects involving only intersection signalization result in annual safety benefits (expressed in dollars) that are more than double the annual construction cost of the improvement (13).

TABLE 4.—Advantages and Disadvantages of Fly-overs

Factors (1)	Advantages (2)	Disadvantages (3)
Are flow-overs a permanent solution?	Structurally, they can be built to handle a HS-20 design load. They can be built of different widths and lengths and with curved roadways.	Primarily intended to be used for genuinely temporary (weeks or months) trouble spots because of esthetic reasons; particularly in urban areas where right-of-way is very restrictive.
How much traffic can fly-overs carry?	Maximum observed traffic volumes (all lanes) on different type fly-overs are as follows: one-lane, one way: 850 cars/hr; two-lane, one-way: 2,200 cars/hr; two-lane, two-way: 2,500 cars/hr	Many large trucks and buses will reduce the capacity and cannot always be handled because of the design load.
Are fly-overs esthetically pleasing?	New designs provide sharp, clean lines suitable for use in an urban environment provided there is sufficient right-of-way.	Older designs look like old elevated transit structures.
How do fly-overs affect accidents?	They can reduce the number of accidents because the number of conflict points at an intersection are typically cut in half.	Good advance signing, roadway markings, and end treatments are needed to prevent accidents at ends of the fly-overs. Sight-distance may also be decreased for surface traffic making a directional movement change at the intersection.
Are fly-overs costly?	Minimum maintenance is required on new designed fly-overs that are constructed of weathering steel.	They are not low-cost as some claim. Urban fly-overs now typically cost $2,000,000. Rural fly-overs cost about $700,000.
Are fly-overs easy to erect?	This is the major advantage of fly-overs. The superstructure can normally be erected in 10 days or less. The foundations are erected ahead of time and buried. Another major advantage is that fly-over structures are reusable after dismantling.	Planning and preparation of site may be time consuming, but certainly no more, and probably less, than for a conventional structure. Some design features have to be ordered specially; e.g., superelevation.

TABLE 4.—*Continued*

(1)	(2)	(3)
Are fly-overs cost effective?	Time and safety benefits over a two-year span typically equal fly-over costs. Fly-overs are good temporary solutions to very congested intersections.	Cheaper traffic control improvements, such as improved signal timing, have much higher benefit/cost ratios and are probably a better permanent solution for less severely congested intersections.

Although the data in Table 3 is general, it shows the potentially large differences in costs and rates of return between fly-overs and other intersection improvements. Decisionmakers should have their staffs make detailed analyses of both planned fly-overs and other alternative traffic improvement schemes before a final decision is made on how to solve an intersection congestion or safety problem, or both.

Summary and Conclusions

During the past decade, there has been renewed interest in the use of prefabricated, portable type bridges called fly-overs. They have been used frequently, especially in France, to alleviate bottlenecks at major urban intersections and have been proposed for greater use in the United States (12). Fly-overs, like other traffic control improvements, certainly have their advantages. They also have some disadvantages. This article was prepared to provide decisionmakers with both the positive and negative aspects of fly-overs. Table 4 itemizes the advantages and disadvantages of fly-overs. In summary, there are situations where fly-overs should be used to correct a traffic control problem but, as in any decision-making process, they must compete with other candidate traffic control schemes on the basis of economic and other factors (e.g., esthetics, safety, traffic performance, etc).

Acknowledgment

The preparation of this article was made possible through the translation of portions of several foreign language reports by Guido Radelat, a Highway Research Engineer with the Office of Research in the Federal Highway Administration.

Appendix.—References

1. "Autoponts et Toboggans, Les passages Superieurs," *Chantiers Magazines*, No. 52, Apr., 1974, pp. 99–104.
2. "Energy Fact Sheets Nos. 6 and 7," Federal Highway Administration, Washington, D.C., Mar., 1980.
3. "Federal Laws and Material Relating to the Federal Highway Administration," Federal Highway Administration, Washington, D.C., Jan., 1980, p. II-239.
4. Franc, M., Le Poulit, J., and Ciolina, F., "Les Differents Aspects de L'emploi des Viaducs Metalliques Demontables," *Travaux*, No. 440, Nov., 1971, pp. 39–49.

5. "Guide for Selecting, Locating, and Designing Traffic Barriers," American Association of State Highway and Transportation Officials, Washington, D.C., 1977, pp. 128–155.
6. Jolliot, R., "Toboggan et Minitob," *Bulletin de liaison du Groupe D'Etude des 'Ponts Metalliques,'* No. 4, July, 1972, pp. 51–59.
7. Kroger, E., "Fast-Assembly Bridge over the Aegidientorplatz in Hanover," *Highway Research Record,* No. 372, 1971, pp. 47–54.
8. Liber, J., Mas, E., and Vloeberghs, G., "Viaducs Amovibles a Bruxelles," Acier-Stahl-Steel, No. 2, Feb., 1972, pp. 49–58.
9. "Manual On Uniform Traffic Control Devices for Streets and Highways," Federal Highway Administration, Washington, D.C., 1978, p. 3A-4.
10. Maring, G., "Highway Travel Forecasts," Federal Highway Administration, Washington, D.C., Nov., 1974, pp. 11–13.
11. Nobels-Kline, Ltd., "Traffic Problems That Have Been Building Up For Years Can Now Be Solved Over A Weekend," *Sales Brochure, by Nobels-Kline, Ltd.,* Columbia, S.C., 1980.
12. Pleasants, W. W., "The Fly-Over: It Unclogs Urban Traffic in a Hurry," *Civil Engineering,* Vol. 52, No. 5, May, 1980, pp. 71–75.
13. Strate, H. B., "An Evaluation of Federal Highway Safety Program Effectiveness," Federal Highway Administration, Washington, D.C., Aug., 1976, pp. 1–57.
14. Wagner, F. A., "Traffic Control System Improvements: Impacts and Costs," Federal Highway Administration, Washington, D.C., Mar., 1980, pp. 1–55.

SUBAREA FOCUSING WITH UTPS DISTRIBUTION-SPLIT MODEL

By Nancy L. Nihan[1]

(Reviewed by the Urban Transportation Division)

INTRODUCTION

In recent years, the emphasis of transportation planning has shifted from long-range planning for large metropolitan regions to short-range planning for small urban areas and subareas of large urban regions. This paper addresses some of the special needs of subarea planners and, specifically, considers the usefulness of one technique, subarea focusing, that has been developed to meet these needs.

Subarea planners have experienced difficulties in applying conventional forecasting techniques to the local planning process. (For a case study of some of these problems see Norris and Nihan (7).) Part of the problem is the lack of computer skills required to access conventional models. Even with such expertise, however, the subarea planner usually has too little time and money to conduct a full-scale forecast. Yet subarea planning requires a greater level of detail and accuracy than regional planning. Consequently, transportation planners are looking for ways to obtain quicker, cheaper, and more accurate forecasts at the short-range subarea level. Some are developing new quick-response techniques (4,1,2) which have not yet been properly verified. Others are attempting to make conventional packages easier and cheaper to use (5,3).

One of the latter approaches involves the simplification of model inputs through data aggregation. Subarea focusing is one such means of data aggregation. The effects of this type of aggregation on the accuracy of trip distribution forecasts has been explored in Miller and Nihan (6), and Nihan and Lasablierre (8). The purpose of this paper is to apply the same type of analysis to the distribution-split model which is a default option in the Urban Transportation Planning System (UTPS) developed by the Urban Mass Transportation Administration (UMTA).

[1]Assoc. Prof., Dept. of Civ. Engrg., Univ. of Washington, Seattle, Wash. 98195.

Note.—Discussion open until April 1, 1982. To extend the closing date one month, a written request must be filed with the Manager of Technical and Professional Publications, ASCE. Manuscript was submitted for review for possible publication on December 10, 1980. This paper is part of the Transportation Engineering Journal of ASCE, Proceedings of the American Society of Civil Engineers, ©ASCE, Vol. 107, No. TE6, November, 1981. ISSN 0569-7891/81/0006-0681/$01.00.

UTPS Distribution Split Model

The distribution-split model incorporated as a default option in UMTA's UTPS package is a share model which simultaneously forecasts trip distribution and modal split. The model equations are

$$T_{ijm} = \frac{P_i \alpha_j A_j e^{-\theta t_{ijm}}}{\sum_j \sum_m \alpha_j A_j e^{-\theta t_{ijm}}} \quad \ldots\ldots\ldots\ldots\ldots\ldots\ldots\ldots\ldots\ldots (1)$$

$$\sum_i \sum_m T_{ijm} = A_j \quad \ldots\ldots\ldots\ldots\ldots\ldots\ldots\ldots\ldots\ldots\ldots\ldots\ldots\ldots (2)$$

in which t_{ijm} = trips between i and j on mode m; i = "home" district; j = "nonhome" district; m = mode; P_i = productions, district i; A_j = attractions, district j; α_j = normalizing parameter, district j; t_{ijm} = impedance measure for trips between i and j on mode m; and θ = constant that may change with trip purpose or income level, or both.

The normalizing parameters, α_j, are obtained through an iterative process similar to that of the conventional gravity model with initial values $\alpha_j = 1$. The impedance measures are calculated as follows:

$$t_{ijm} = t_{ijm}(r) + 2.5t_{ijm}(e) + \frac{c_{ijm}(I)}{(0.33)(1{,}200)} \quad \ldots\ldots\ldots\ldots\ldots\ldots\ldots (3)$$

in which t_{ijm}(r) = running time (in-vehicle), in minutes; $t_{ijm}(e)$ = excess time (out-of-vehicle), in minutes; c_{ijm} = cost, in cents (includes fare, parking, auto running cost); and I = annual income in dollars. The model is stratified by purpose and income.

Subarea Focusing.—Subarea focusing is a means of data aggregation that allows a transportation planner to estimate trip demands within a subarea of an urban region at a fine level of detail. (We refer to the subarea of interest as the window.) In order to include trips to, from, and through the window, the surrounding region is also considered in the analysis, but at a coarser level of detail. This type of aggregation reduces the total number of zones or centroids in the regions that need to be analyzed. If sufficiently accurate, it therefore represents a potentially significant savings in the cost and time required to apply conventional travel forecasting techniques.

The subarea focusing approach used in the present study is an application of an algorithm developed by Miller and Nihan (6). The algorithm combines nearest-neighbor zone into districts based on their travel time to the window. As travel time to the window increases, more zones are combined, creating larger districts.

Study Scope.—The current study applied the subarea focusing technique previously described with the inputs of the UTPS distribution-split model for one window (Seattle CBD) and three levels of aggregation. The region containing the windowed area was the three county mainland portion of the Puget Sound region. The original number of centroids in the study region was 635, representing 597 traffic analysis zones and 38 external stations. A network with 9,495 one-way links and 3,186 nodes connected the centroids. The data base supplied by the

Puget Sound Council of Governments (PSCOG) included projected 1990 home-based person work-trip productions and attractions and time and cost data for work trips in the year 1990. The Seattle CBD, which was chosen as the windowed area, contained 42 traffic analysis zones. This remained constant for each level of aggregation.

To control for window size, the degree of aggregation was defined independently of the number of centroids inside the window. The degree of aggregation,

TABLE 1.—Aggregation Levels Achieved

Aggregation classification (1)	Reduction, as a percentage (2)	Total number of centroids (3)	Number of centroids inside window (4)	Number of centroids outside window (5)
Level I	55	302	42	260
Level II	79	165	42	123
Level III	90	103	42	61

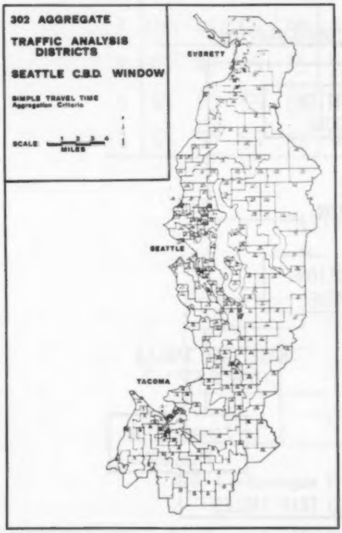

FIG. 1.—Districts, Level I Aggregation

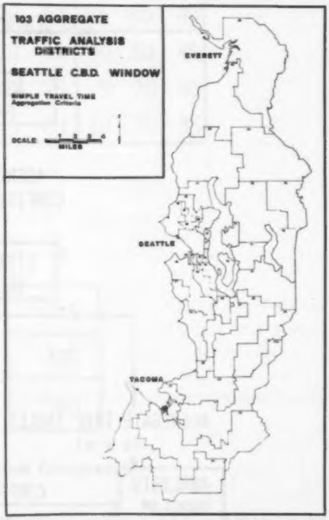

FIG. 2.—Districts, Level II Aggregation

therefore, was taken to be the percent reduction of centroids outside the window. This is given by

$$P = \frac{b - a}{b} \quad \ldots \quad (4)$$

in which P = percent reduction of centroids located outside the window; b = number of centroids outside the window in the base (635 centroid) configuration; and a = number of centroids outside the window in the aggregate configuration.

Three desired levels of aggregaton (50%, 75%, and 90% reduction) were initially chosen for analysis. These, however, were not precisely achieved. Table 1 shows the percent reductions obtained for each level of aggregation and the total number of centroids at each level. Figs. 1 and 2 show districts for the first and last levels of aggregation and location of the study window. The 42 zones representing the Seattle CBD window are represented by the blacked-out subarea in each figure.

Study Procedure

A general description of the experiment is given in Fig. 3. The aggregation algorithm was applied to the 635 centroid configuration to procude an aggregate configuration of n centroids at the desired level of aggregation. The UTPS distribution-split model was then applied to the aggregate data base to produce aggregate $n \times n$ trip tables for transit and highway. (The model is run precalibrated using cost and time data provided by PSCOG.) The distribution-split model

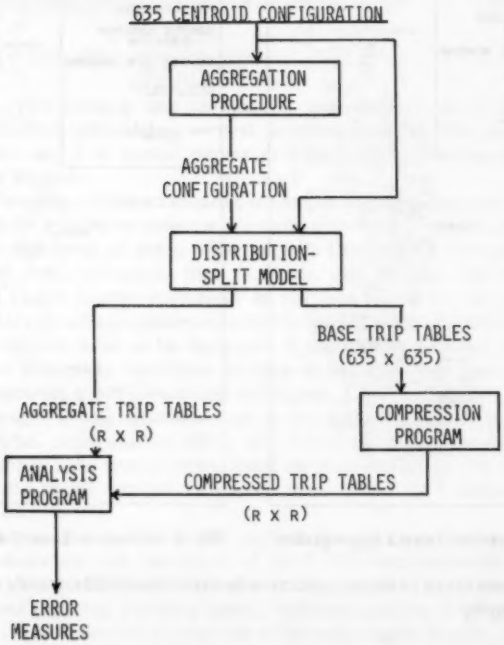

FIG. 3.—Experiment Description

was also applied to the 635 centroid configuration to produce the base forecast trip tables. Then, depending on the dimensions of the aggregate trip table being tested, the forecast matrix was compressed to a conformable ($n \times n$) size, yielding "true" trips for the appropriate set of centroid pairs. Fig. 4 illustrates this for a hypothetical 10×10 base trip table compressed to a 3×3 compressed trip table where aggregate District 1 contains Zones 1, 2, 3 and 4, District

ZONES

	1	2	3	4	5	6	7	8	9	10
1	10	20	35	40	5	15	10	20	55	30
2	25	10	35	55	40	5	30	15	45	35
3	30	35	75	95	30	10	85	50	40	25
4	80	40	65	80	70	20	70	20	50	60
5	40	20	40	100	50	30	65	10	45	40
6	35	25	50	60	25	10	35	30	75	30
7	100	45	60	90	35	25	40	25	65	45
8	95	45	45	75	50	10	45	40	60	45
9	45	30	55	85	30	15	75	5	70	40
10	55	50	65	90	40	5	60	10	75	35

DISTRICTS

	1	2	3
1	730	390	445
2	665	315	365
3	735	330	380

FIG. 4.—Example Trip Table Compression

2 contains Zones 5, 6 and 7, and District 3 contains Zones 8, 9 and 10. (Windowed zones are ignored for purposes of this illustration but are part of the compressed matrices in the study.) Thus, a distinct compressed matrix was produced for each level of aggregation tested and each mode. Compressed and aggregate matrices were then compared on a cell-by-cell basis to produce a set of matrix error measures.

Before comparisons of equally dimensioned compressed and aggregate matrices were made, the matrices were rearranged so that trips to, from, and within

the window could be isolated into quadrants. The quadrants are defined in Fig. 5. As shown in Fig. 5, the aggregate and compressed matrices were arranged so that the lowest numbered centroids were those contained within the window. All of the trips in Quadrants I, II, and III were of interest to the analysis, while only the trips in Quadrant IV that passed through the window were important. A complete cell-by-cell analysis was conducted for Quadrants I, II, and III, as explained in the next section. In addition, a sample of likely through-trip interchanges for Quadrant IV was analyzed.

Error Measures.—Two error measures, absolute deviation and absolute percent deviation, were calculated for each interchange in Quadrants I, II, and III.

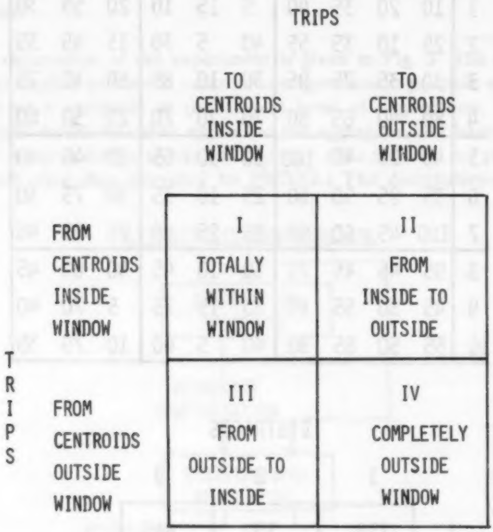

FIG. 5.—Quadrant Definition

These measures are defined in Eqs. 5 and 6:

$$E_{ij} = |\mathbf{C}_{ij} - \mathbf{A}_{ij}| \quad (5)$$

$$PE_{ij} = \frac{|\mathbf{C}_{ij} - \mathbf{A}_{ij}|}{\mathbf{C}_{ij}} \times 100 \quad (6)$$

in which **C** = compressed trip matrix, dimensions $r \times r$; **A** = aggregate trip matrix, dimensions $r \times r$; C_{ij} = trips predicted from i to j for Matrix **C**; A_{ij} = trips predicted from i to j for matrix **A**; r = total number of centroids; E_{ij} = absolute trip error for interchange i, j; and PE_{ij} = absolute percent trip error for interchange i, j. To eliminate undefined numbers, the absolute percent error measure was constrained to ignore interchanges having zero base (compressed) trips. Also, interchanges with $C_{ij} \leq 3$ trips were not analyzed unless

the absolute trip deviation was greater than 10. This was done to avoid very large percent errors associated with deviations of one or two trips.

Method of Summarizing Error Measures.—The mean and standard deviation of the two error measures were calculated for the first three matrix quadrants. In addition, error distributions were plotted for each quadrant. For the error distributions, the average values of each error measure for one minute trip time intervals were plotted. Although error distributions were plotted for both percent and absolute errors, the percent error distributions were consulted only for points where the absolute error was 10 or more trips. Again, this was done in an effort to avoid giving undue weight to large percentage errors associated with small numbers of actual trips.

A sampling of Quadrant IV for likely through trip interchanges was performed by hand. The resulting values of actual trips, C_{ij}'s, versus aggregate forecast trips, A_{ij}'s, were then plotted.

Analysis and Conclusion

Results.—The distribution-split model was applied to the data base with a value of $\theta = 0.035$ for all levels of aggregation. The total number of productions

TABLE 2.—Regional Mode Split

Aggregation level (1)	Total trips (2)	Total transit, as a percent (3)	Total highway, as a percent (4)	Number of trips transit (5)	Number of trips highway (6)
Level I	1,270,738	14.12	85.88	179,461	1,091,277
Level II	1,270,754	14.03	85.97	178,322	1,092,432
Level III	1,270,736	14.07	85.93	178,793	1,091,943

(or attractions) was 1,270,732. Due to a constraint on the number of iterations that was feasible for the study, the total person-trips for each run was close but not exactly the same as this value. Table 2 shows the regional mode split for each run. At the regional level, it appears that even the highest level of aggregation has no significant effect on mode split. At the subregional level, however, this is not always the case.

Figs. 6, 7, and 8 show the mean absolute error distributions for the highway mode. For all levels of aggregation, the absolute errors for trips within the window are minimal. For levels of Aggregation I and II, mean errors for Quadrants II and III are also within the range of acceptability. All fall within 10 or less person-trip deviations from the base values. For level of Aggregation III, however, this is not the case. In several instances, the mean deviation is between 10 and 20 trips, and in one case, the mean deviation is 51 trips (Quadrant II, time interval 52–53 minutes). This is associated with a mean percent error of 54. Thus, the average number of base trips for this time interval was 111, while the average absolute deviation was 51 trips. This is a significant error and casts doubt on the accuracy of the distribution-split model for subarea

focusing at aggregation levels as high as 90%.

The transit error distributions support the aforementioned conclusion. Figs. 9, 10, and 11 show the mean absolute error distributions for transit. As with the highway results, all three levels of aggregation produce minimal errors for

FIG. 6.—Trip Errors Highway, Level I Aggregation

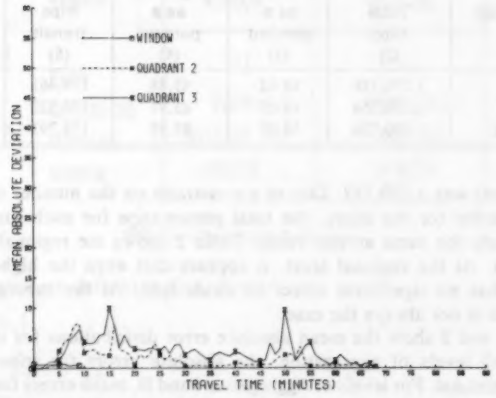

FIG. 7.—Trip Errors Highway, Level II Aggregation

the windowed area. At aggregation Level I, all errors are less than 10 person-trips and are therefore acceptable for the other two quadrants as well. For aggregation Level II, all but one time interval (8–9 mins., quadrant III) had errors less than 10 person-trips. The error in question was 17 trips; this represented a percent error of 290%, meaning that the base number of trips was 9 trips.

This is a significant error. However, since it was the only significant error for all three quadrants, a Level II type aggregation might still have adequate accuracy depending on the study requirements. The last aggregation level, however, exhibits several significant errors for Quadrant III. The significant

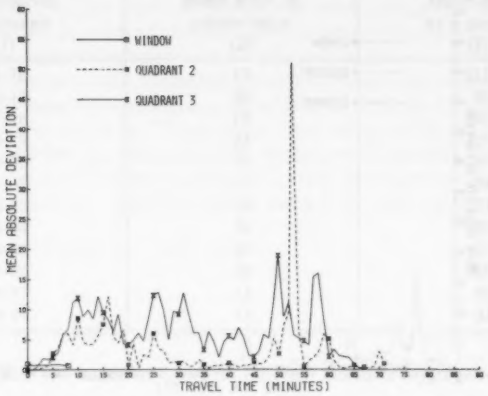

FIG. 8.—Trip Errors Highway, Level III Aggregation

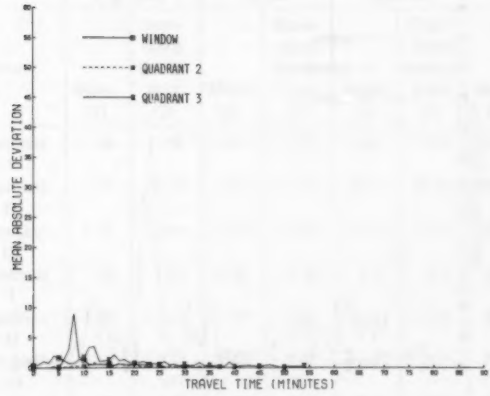

FIG. 9.—Trip Errors Transit, Level I Aggregation

deviations, their percent errors, and associated time intervals are shown in Table 3. The mean errors and their associated mean percent errors appear serious enough to reject or at least seriously question the accuracy of using subarea focusing with the UTPS distribution-split model at this highest level of aggregation.

Sometimes in planning forecasts we may be interested in only the aggregate

results. That is, if doing long-range sketch planning, we may only require accuracy at the level of total flows into, out of, and within the window. For purposes of sketch planning, therefore, all three levels of aggregation may be sufficiently accurate. Table 4 illustrates this possibility. At the quadrant level of error

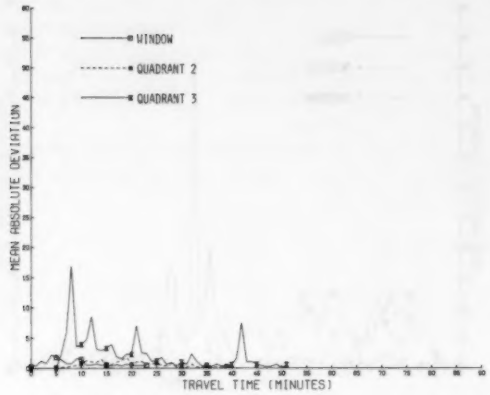

FIG. 10.—Trip Errors Transit, Level II Aggregation

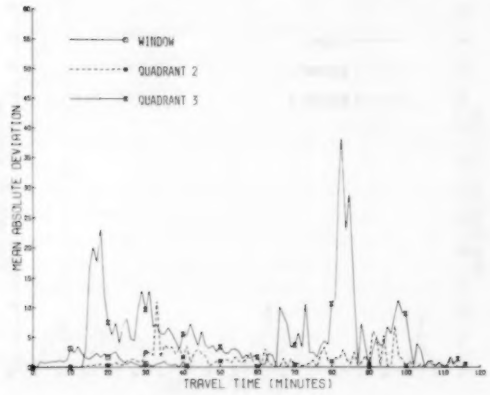

FIG. 11.—Trip Errors Transit, Level III Aggregation

summary, all quadrants have average absolute errors of less than 6 trips. The pecentage errors are reasonable with the higher percentages associated with low average trips.

The above results have, up to this point, concentrated on Quadrant I, II, and III errors. Quadrant IV errors were of no importance for distribution-split

TABLE 3.—Significant Errors—Transit, 103 Centroids

Time interval, in minutes (1)	Mean error, in person-trips (2)	Mean error, as a percent (3)
15–16	17	211
16–17	20	20
17–18	18	249
18–19	23	220
29–30	13	59
31–32	13	58
82–83	29	73
83–84	38	53
84–85	23	57
85–86	29	60
86–87	13	56
98–99	11	32

TABLE 4.—Quadrant Errors for Different Levels of Aggregation

Aggregation level (1)		ABSOLUTE ERROR				PERCENT ERROR			
		Highway		Transit		Highway		Transit	
		Mean (2)	Standard deviation (3)	Mean (4)	Standard deviation (5)	Mean (6)	Standard deviation (7)	Mean (8)	Standard deviation (9)
Level I	Quadrant I	.56	.92	.91	2.14	8.6	9.3	11.2	9.5
	Quadrant II	.73	5.74	.31	2.78	28.7	35.4	39.5	141.9
	Quadrant III	1.36	3.80	1.06	3.83	11.7	17.6	39.2	91.8
Level II	Quadrant I	.61	1.02	1.05	2.42	9.9	9.7	12.8	10.0
	Quadrant II	1.68	10.01	.73	4.44	33.1	37.9	49.6	155.7
	Quadrant III	3.01	7.41	2.62	7.87	14.4	21.7	53.4	116.5
Level III	Quadrant I	.82	1.43	1.46	3.58	13.4	11.1	17.5	10.9
	Quadrant II	3.31	13.45	1.42	6.32	31.8	32.3	45.7	73.3
	Quadrant III	6.87	13.03	5.60	16.10	18.6	25.0	56.9	118.5

trips affecting the window. So, if one were interested only in a distribution-split forecast, the error analysis would be complete with these three quadrants. However, if traffic assignment is also to be performed, certain Quadrant IV trips (namely, through-trips) become important. Thus, to get an idea of the effect of aggregation on through-trips, a random sample of such trips was taken. Since the 103 aggregation level was already in doubt in the previous analysis, the next highest level of aggregation was chosen for this analysis. Fig. 12 shows the results for the 165 centroid forecast. All of the errors fall within the acceptable range with the larger percentages associated again with low numbers of trips. Thus, at Level II aggregation and lower, all errors fall within the acceptable range.

Conclusions.—Due to time and money limitations, the present study was limited to the analysis of only one window, the Seattle CBD. Thus, although we can use a single test to find weaknesses in the technique, we cannot make strict

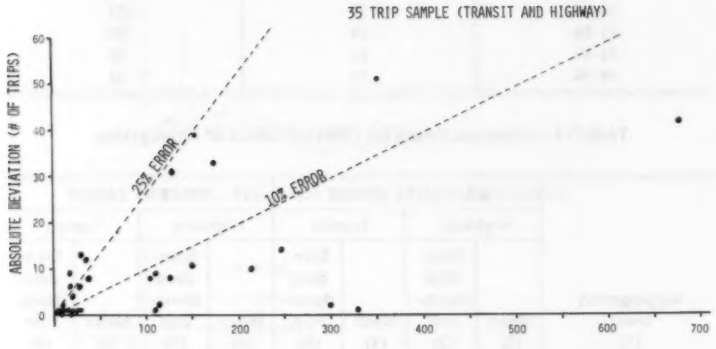

FIG. 12.—Through Trip Errors Highway and Transit, Level II Aggregation

conclusions about the accuracy of the technique. This experiment, coupled with the knowledge of the previous studies on trip distribution (6,8) does, however, give us strong indications about the accuracy that can be expected with the UTPS distribution-split model at various levels of aggregation.

These indications or preliminary conclusions are summarized as follows:

1. Errors for trips within a window are minimal regardless of their degree of aggregation or mode.
2. Errors for trips to, from, within, and through a window are acceptable for conventional subarea focusing at levels of Aggregation I and II for both modes.
3. Errors for trips to, from, within, and through a window are not acceptable for conventional forecasting at the 90% level of aggregation for either mode.
4. Errors at level of Aggregation III may, however, be within the acceptable range of accuracy for sketch planning forecasts for both modes.

Thus, it appears at first glance that the UTPS distribution-split model is not

unduly sensitive to subarea focusing, particularly at levels of aggregation of 75% or less. Even at the highest level of aggregation, the technique could give satisfactory results for sketch planning purposes. Again, these results are preliminary, and further tests for various metropolitan regions and subarea types are necessary to support the above indications.

Acknowledgment

A portion of the research described in this paper was conducted as part of a university research and training grant (UMTA-URT-WA-11-0005, 7/1/75–76/30/78) sponsored by the Urban Mass Transportation Administration of the U.S. Department of Transportation. The author would also like to acknowledge the contributions of Michael Fanning and Cheryl Galt of Boeing Computer Services.

Appendix I.—References

1. COSMIS Corp., "Travel Estimation Procedure for Quick Response to Urban Policy Issues," *Report No. 186,* National Cooperative Highway Research Program, 1978.
2. COSMIS Corp., "Travel Estimation Procedure for Quick Response to Urban Policy Issues," *Report No. 187,* National Cooperative Highway Research Program, 1978.
3. Dial, R. G., et al., "New Systems Requirements Analysis Program: A Procedure for Long-Range Transportation (Sketch) Planning," National Technical Information Service, *No. PB-233-344,* Springfield, Va., July, 1973.
4. Manheim, M. L., Furth, P., and Saloman, I., "Responsive Transportation Analysis: Pocket Calculator Methods," paper presented at the Fifty-Seventh Annual Meeting of the Transportation Research Board, Washington, D.C., Jan., 1978.
5. Mann, W. W., "T.R.I.M.S.—A Procedure for Quick Response Transportation Planning," paper presented at the Fifty-Fourth Annual Meeting of the Transportation Research Board, Washington, D.C., Jan., 1975.
6. Miller, Donald G., and Nihan, N. L., "Development and Demonstration of the Subarea Focusing Concept for Trip Distribution in the Puget Sound Area," *Transportation Research Record 610,* Washington, D.C., 1976, p. 37–43.
7. Norris, G., and Nihan, N. L., "Subarea Transportation Planning: A Case Study," *Traffic Quarterly,* Vol. 33, No. 4, 1979, pp. 589–605.
8. Nihan, N. L., and Lassabliere, J., "Sensitivity of Trip Distribution to Subarea Focusing," *Transportation Engineering Journal of ASCE,* Vol. 102, No. TE3, Aug., 1976, pp. 555–569.

Appendix II.—Notation

The following symbols are used in this paper:

$\mathbf{A}$ = aggregate trip matrix, dimensions $r \times r$;
$\mathbf{A}_{ij}$ = trips predicted from i to j for Matrix $\mathbf{A}$;
$\mathbf{A}_j$ = attractions, district j;
a = number of centroids outside the window in the aggregate configuration;
b = number of centroids outside the window in the base (635 centroid) configuration;
$\mathbf{C}$ = compressed trip matrix, dimensions $r \times r$;
$\mathbf{C}_{ij}$ = trips predicted from i to j for Matrix $\mathbf{C}$;
c_{ijm} = cost, in cents (includes fare, parking, auto running costs);

E_{ij} = absolute trip error for interchange i, j;
I = annual income, in dollars;
P = percent reduction of centroids located outside the window;
PE_{ij} = absolute percent trip error for interchange i, j;
P_i = productions, district i;
r = total number of centroids;
T_{ijm} = trips between i and j on mode m;
t_{ijm} = impedance measure for trips between i and j on mode m;
$t_{ijm}(e)$ = excess time (out-of-vehicle), in minutes;
$t_{ijm}(r)$ = running time (in vehicle);
α_{ijm} = normalizing parameter; and
θ = constant that may change with trip purpose or income level, or both.

Subscripts

i = "home" district;
j = "non-home" district; and
m = mode.

DISCUSSION

Note.—This paper is part of the Transportation Engineering Journal of ASCE, Proceedings of the American Society of Civil Engineers, ©ASCE, Vol. 107, No. TE6, November, 1981. ISSN 0569-7891/81/0006-0697/$01.00.

Discussions

Discussions may be submitted on any Proceedings paper or technical note published in any *Journal* or on any paper presented at any Specialty Conference or other meeting, the *Proceedings* of which have been published by ASCE. Discussion of a paper/technical note is open to anyone who has significant comments or questions regarding the content of the paper/technical note. Discussions are accepted for a period of 4 months following the date of publication of a paper/technical note and they should be sent to the Manager of Technical and Professional Publications, ASCE, 345 East 47th Street, New York, N.Y. 10017. The discussion period may be extended by a written request from a discusser.

The original and three copies of the Discussion should be submitted on 8-1/2-in. (220-mm) by 11-in. (280-mm) white bond paper, typed double-spaced with wide margins. The length of a Discussion is restricted to two *Journal* pages (about four typewritten double-spaced pages of manuscript including figures and tables); the editors will delete matter extraneous to the subject under discussion. If a Discussion is over two pages long it will be returned for shortening. All Discussions will be reviewed by the editors and the Division's or Council's Publications Committees. In some cases, Discussions will be returned to discussers for rewriting, or they may be encouraged to submit a paper or technical note rather than a Discussion.

Standards for Discussions are the same as those for Proceedings Papers. A Discussion is subject to rejection if it contains matter readily found elsewhere, advocates special interests, is carelessly prepared, controverts established fact, is purely speculative, introduces personalities, or is foreign to the purposes of the Society. All Discussions should be written in the third person, and the discusser should use the term "the writer" when referring to himself. The author of the original paper/technical note is referred to as "the author."

Discussions have a specific format. The title of the original paper/technical note appears at the top of the first page with a superscript that corresponds to a footnote indicating the month, year, author(s), and number of the original paper/technical note. The discusser's full name should be indicated below the title (see Discussions herein as an example) together with his ASCE membership grade (if applicable).

The discusser's title, company affiliation, and business address should appear on the first page of the manuscript, along with the *Proceedings* paper number of the original paper/technical note, the date and name of the *Journal* in which it appeared, and the original author's name.

Note that the discusser's identification footnote should follow consecutively from the original paper/technical note. If the paper/technical note under discussion contained footnote numbers 1 and 2, the first Discussion would begin with footnote 3, and subsequent Discussions would continue in sequence.

Figures supplied by the discusser should be designated by letters, starting with A. This also applies separately to tables and references. In referring to a figure, table, or reference that appeared in the original paper/technical note use the same number used in the original.

It is suggested that potential discussers request a copy of the *ASCE Authors' Guide to the Publications of ASCE* for more detailed information on preparation and submission of manuscripts.

Environmental Considerations in Highway Planning[a]

Closure by John J. Meersman,[4] A. M. ASCE,
and Leonard Ortolano,[5] M. ASCE

The writers would like to thank William R. Green for his interest in the paper and for his comments. His observations complement the research findings by providing the perspective of CALTRANS as a transportation planning agency.

As indicated by the discusser, consideration of environmental factors in highway projects has and will continue to evolve under the current CALTRANS Action Plan. The new generation of transportation projects will provide greater opportunity to consider environmental factors in the formulation of alternatives, as well as in the ranking and modification of alternatives. In the opinion of the writers, effectively utilized Project Development Teams may be the keystone of future highway planning studies. Indeed, to the extent that broad-based public participation in early planning stages is encouraged, the number of surprises at subsequent public hearings may be reduced and, more importantly, the outcome of the planning process will be significantly improved. The writers concur with the discusser that positive attitudes toward consideration of environmental factors on the part of planners and engineers will be promoted by a recognition of the desirability and advantages of such consideration.

---

[a]July, 1980, by John J. Meersman and Leonard Ortolano (Proc. Paper 15525).

[4]Engrg. Planner, Bechtel Group, Inc., San Francisco, Calif.; formerly Grad. Research Asst., Dept. of Civ. Engrg., Stanford Univ., Stanford, Calif.

[5]Prof., Dept. of Civ. Engrg., Stanford Univ., Stanford, Calif.

Technical Papers

Original papers should be submitted in triplicate to the Manager of Technical and Professional Publications, ASCE, 345 East 47th Street, New York, N.Y. 10017. Authors must indicate the Technical Division or Council, Technical Committee, Subcommittee, and Task Committee (if any) to which the paper should be referred. Those who are planning to submit material will expedite the review and publication procedures by complying with the following basic requirements:

1. Titles must have a length not exceeding 50 characters and spaces.

2. The manuscript (an original ribbon copy and two duplicate copies) should be double-spaced on one side of 8-1/2-in. (220-mm) by 11-in. (280-mm) paper. Three copies of all figures and tables must be included.

3. Generally, the maximum length of a paper is 10,000 word-equivalents. As an *approximation*, each full manuscript page of text, tables or figures is the equivalent of 300 words. If a particular subject cannot be adequately presented within the 10,000-word limit, the paper should be accompanied by a rationale for the overlength. This will permit rapid review and approval by the Division or Council Publications and Executive Committees and the Society's Committee on Publications. Valuable contributions to the Society's publications are not intended to be discouraged by this procedure.

4. The author's full name, Society membership grade, and a footnote stating present employment must appear on the first page of the paper. Authors need not be Society members.

5. All mathematics must be typewritten and special symbols must be identified properly. The letter symbols used should be defined where they first appear, in figures, tables, or text, and arranged alphabetically in an appendix at the end of the paper titled Appendix.—Notation.

6. Standard definitions and symbols should be used. Reference should be made to the lists published by the American National Standards Institute and to the *Authors' Guide to the Publications of ASCE*.

7. Figures should be drawn in black ink, at a size that, with a 50% reduction, would have a published width in the *Journals* of from 3 in. (76 mm) to 4-1/2 in. (110 mm). The lettering must be legible at the reduced size. Photographs should be submitted as glossy prints. Explanations and descriptions must be placed in text rather than within the figure.

8. Tables should be typed (an original ribbon copy and two duplicates) on one side of 8-1/2-in. (220-mm) by 11-in. (280-mm) paper. An explanation of each table must appear in the text.

9. References cited in text should be arranged in alphabetical order in an appendix at the end of the paper, or preceding the Appendix.—Notation, as an Appendix.—References.

10. A list of key words and an information retrieval abstract of 175 words should be provided with each paper.

11. A summary of approximately 40 words must accompany the paper.

12. A set of conclusions must end the paper.

13. Dual units, i.e., U.S. Customary followed by SI (International System) units in parentheses, should be used throughout the paper.

14. A practical applications section should be included also, if appropriate.